

HIGH POWER LASER DRIVEN TERAHERTZ GENERATION IN PLASMA

A Thesis

Submitted in partial fulfillment of the requirements for the
award of the degree of

DOCTOR OF PHILOSOPHY

in

(Physics)

By

Alka Mehta

(11617202)

Supervised by

Prof. Niti Kant



LOVELY
PROFESSIONAL
UNIVERSITY

Transforming Education Transforming India

**LOVELY PROFESSIONAL UNIVERSITY
PUNJAB
2020**

DECLARATION

I hereby declare that the thesis entitled, “High Power Laser Driven Terahertz Generation in Plasma” has been prepared by me under the guidance of Dr. Niti Kant, Professor of Department of Physics at Lovely Professional University. This work is entirely my original work and all the ideas and references have been duly acknowledged. It does not contain any work for the award of any other degree or fellowship previously at any University.

Alka Mehta

Reg. No. 11617202

Department of Physics,

Lovely Professional University,

Phagwara, Punjab.

Pin Code-144411

Date: May 10, 2020.

CERTIFICATE

This is to certify that Alka Mehta has completed her Ph.D. thesis entitled, “High Power Laser Driven Terahertz Generation in Plasma” for the award the degree of Doctor of Philosophy in Physics at Lovely Professional University under my guidance and supervision. To the best of my knowledge, the present work is the result of her original investigation and study. No part of the thesis has ever been submitted for any other degree or fellowship previously at any University.

Dr. Niti Kant

(Professor)

Lovely Professional University,

Phagwara, Punjab.

Pin Code-144411

Date: May 10, 2020.

ABSTRACT

Terahertz radiation can provide novel information in various fields of science for example, in manufacturing as quality control and monitoring. The main key performance factors are the peak THz energy (or electric field strength), conversion efficiency and the bandwidth of THz. In order to meet the demanding applications the areas such as, collimation (directionality) of radiation, radiation source tunability and proper power of the source, are where new concepts and efforts are needed. Therefore, in the present work, we have proposed some new schemes based on the interaction of high power lasers with plasmas by exploring the interesting physics involve in the process. On the basis of these schemes, we have been able to control the direction of emission and to tune the frequency as well as power of emitted terahertz radiation. Our main goal of the studies presented here is to explore the physics of laser plasma interaction up to terahertz frequency range by introducing some external parameters, on the way of using various exceptional capabilities of plasma, to understand new information about fundamental concept behind the physical processes. Four distinct objectives are depicted in this thesis, each underpinned by the laser plasma interaction using the technique of paraxial ray approximation. Methodology and basic formulation is given in Chapter-2. Present method is very powerful and adapted one to achieve efficient THz radiation and allows us to gauge the electric field and amplitude of the THz radiation in the form of coupled equation. Furthermore, the method of terahertz generation can be combined with different laser and plasma parameters which additionally make the process resonant and efficient one.

In the first objective (Chapter-3) a scheme is presented to produce THz radiation using intense electromagnetic beam having Gaussian profile. The beam is beating in a hot collision less plasma having surface density ripple, parallel to z-axis. These p-polarised lasers propagate in x-z plane, incident obliquely to the density ripple on plasma surface, and exert a ponderomotive force to the electrons. The plasma electrons start oscillating since; the neutrality of the plasma get disturbed by the nonlinearity arises due to the ponderomotive force. This oscillatory velocity beats with the density ripple; as a result an irrotational current density \vec{J}^{NL} arises at beating

frequency $\omega_1 - \omega_2$ (with $\vec{\nabla} \times \vec{J}^{NL} \neq 0$). This nonlinear current density urges a wave whose frequency is in THz range. Our results show that, for a set of laser and plasma parameters, the power of emitted THz radiation scales as the square of density ripple amplitude as well as the amplitude of emitted THz wave decreases with the THz frequency and increases with the incidence angle up to an optimum value. Our second and third research objectives are reported in Chapter-4, in part one a model described the combined influence of the chirp characteristics of the pump pulses and spatially periodic density (density ripple) plasma on terahertz (THz) radiation generation by beating of two chirped pulses has been investigated. The beating lasers exert a nonlinear ponderomotive force along the z-direction, transverse to the field's of incident lasers. A self consistent field is generated due to the nonlinear oscillations of plasma electrons, as a result of these linear and nonlinear forces the plasma electrons attain an oscillatory velocity that couples with the density ripple to generate a stronger transient transverse current, driving THz radiation. The importance of chirp parameter, amplitude and periodicity of density structure are discussed for emitted THz radiation. Our numerical simulations disclose that the variation of chirp frequency parameter and ripple amplitude has a considerable role in improving the nonlinear oscillating current. By optimizing the chirp parameter and amplitude of density ripple, a notable change in the magnitude of terahertz field amplitude is found. Present investigation maybe useful for broadband THz pulses and they can be used for plasma diagnostics and time-domain spectroscopy.

On the other hand, the second model explores the effect of frequency chirp on the generated terahertz (THz) wave produced by the interaction between intense laser pulses and under dense plasma in the presence of transverse magnetic field. An expression for the electron Lorentz factor coupling cyclotron motion nonlinearity is derived for static magnetic field perpendicular to the laser propagation axis. The influence of the external magnetic field on the optimization process of THz field amplitude is investigated numerically. A linear frequency chirp increases the duration of nonlinear interaction of laser pulse with plasma electrons and hence, enforces the interaction for longer duration. The presence of magnetic field further provides the additional momentum to the THz photon to obtain a significant gain in output yield.

Our numerical simulations reveal that there is a significant enhancement in the THz field strength for optimized value of chirp parameter and magnetic field. After describing first three schemes we move to our fourth objective (Chapter-5). Here, we generate terahertz wave by self-focusing of an intense amplitude modulated Super-Gaussian laser pulse propagating through a plasma. Further, we observe a novel proposal for THz generation by the self focusing of an amplitude-modulated super-Gaussian laser beam in the preformed rippled density plasma. The ripples of suitable wave number help to provide exact phase matching. As a result an enhancement in the THz field amplitude is observed also, we can tune the output radiation by varying modulation index.

The last chapter is devoted to the summary and future scope. In Chapter-6, several insights and inferences obtained from the above analysis discussed collectively.

ACKNOWLEDGEMENT

I express my deep gratitude & sincere thanks to my research supervisor Prof. Niti Kant for his invaluable guidance, inspiring discussions, critical review, care & encouragement throughout this work. His ideas, stimulating comments, interpretations & suggestions increased my cognitive awareness & have helped considerably in the fruition of my objectives. I remain obliged to him for his help & guidance through all stages of this. Their constant inspiration & encouragement towards my efforts shall always be acknowledged. I express my sincere thanks to Prof. Ramesh Thakur, Prof. Kailash Juglan, Department of Physics & Division of Research & Development, Lovely Professional University, Phagwara (Punjab) for general support & providing congenial working environment.

I want to convey my deepest thanks to Dr. Shivani Vij, DAVIET, Jalandhar, for her graciousness to give me a chance to work with her during various research papers. It is a memorable experience to interact & learn from her. I remain obliged for her inspiring discussions, constant inspiration and encouragement throughout the work. My sincere thanks are due to Dr. Jyoti Rajput for her support & encouragement throughout my research work. I am thankful to Prof. Dino, Prof. H. Suk, Prof. H.K. Malik, Prof. M. V. Takale, Dr. Harjit Ghotra & Mr. Keekon Kang for the fruitful discussions, support & their valuable suggestions at various stages during the work. Dr. Rajan Kumar, Dr. Kiran & Dr. Vishal Thakur deserves special mention for their support, guidance & consistent motivation at various stages. I take this opportunity to express my gratitude to my entire family of Lovely Professional University, our Laser Plasma Group & my Ph.D. colleague for their affection & support during my research work. I want to mention my high school & B.Sc. teachers for shaping my thoughts & post graduation professors Prof. Ramesh Chandra, Prof. Suchi Bisht, Prof. Sanjay Pant, whose kind personality made me deeply interested in Physics.

I pay my humble respect to my Grandma Late. Mrs. Kanta Rani & my granny Late. Mrs. Nirmla Bedi, their blessings are always with me. I further express my deep respect to my father Mr. Mahesh Chandra Mehta for raising me the way I am & by all means to my mother Mrs. Sona Mehta for her trust, unlimited affection & care. I pay

my hearty respect to my fiancé Mr. Rahul Arora & my brothers Mr. Sumit Mehta, Mr. Shubham Mehta & Mr. Mukul Mehta who always understand & support me. I remember & thank my sisters Mrs. Neha Kapoor & brother-in-law Mr. Lavi Kapoor & the lovely little Dhani Kapoor for their tremendous love, affection, moral support. I learn by heart to pay my regards to my Uncles Mr. Gyanendra Tripathi & Mr. L.S. Bedi, who always wish me success & support me to study more and more. I also wish to thank all my cousins, relatives & friends for their affection & support.

Author is grateful to the Council of Scientific & Industrial Research (CSIR), Government of India for providing financial support to carry out research program.

Debts being various, are not easy to remember, hence I convey my heartiest thanks to all those who helped me or blessed me in making this milestone.

May, 2020

Alka Mehta

CONTENTS

* Declaration	i
* Certificate	ii
* Abstract	iii
* Acknowledgements	vi
* Table of Contents	viii
* Definitions	xi
* List of Figures	xiii
<i>1. CHAPTER-1: Introduction and Overview</i>	1-12
1.1 Introduction & Prior Research	1
1.2 Schemes For THz Radiation Generation	9
1.3 Motivation of The Study	10
1.4 Research Objectives	11
1.5 Thesis Contribution	12
1.6 Thesis Outline	12
<i>2. CHAPTER-2: Methodology</i>	13-25
2.1 Research Hypothesis	13
2.2 Theoretical Formalism: Paraxial Ray Approximation	13
2.3 Origin of Ponderomotive Force	14
2.4 Analysis For Wave Governing Equation	15
2.5 Role of Different Laser & Plasma Parameters	16
2.5.1 Laser Polarization	17
2.5.1.1 Linear Polarization	18
2.5.1.2 Circular Polarization	18
2.5.1.3 Elliptical Polarization	18
2.5.1.4 s- and p-Polarization	19
2.5.2 Self-Focusing of Laser	19

2.5.3 Ripple Density Plasma	20
2.5.4 Applied Magnetic Field	21
2.5.5 Frequency Chirp	21
2.5.5.1. Linear Positive Frequency Chirp	23
2.5.5.2. Linear Negative Frequency Chirp	23
2.5.6. Laser Profile	23
2.5.7. Intensity of Incident Laser	23
2.5.8. Amplitude Modulated Laser Wave	24
2.5.9. Plasma Frequency	25
2.6 Research Design & Tools	25
2.7. Sources of Data	25
3. CHAPTER-3: Terahertz Generation by Beating of Obliquely Incident Lasers	26-39
3.1. Introduction	26
3.2 Proposed Model	27
3.2.1 Generation of THz Radiation by p-Polarised Lasers Beating in Hot Plasma	27
3.3 Analysis and Observations	33
3.4 Conclusion	38
4. CHAPTER-4: Effect of Frequency Chirp on Generated THz Wave in Plasma	40-55
4.1. Introduction	40
4.2 Proposed Model For Rippled Density Plasma	41
4.2.1 THz Generation by Beating of Two Chirped Pulse Lasers in Spatially Periodic Density Plasma	41
4.2.2 Analysis & Observations	44
4.3 Proposed Model For Magnetized Plasma	48
4.3.1 Effect of frequency chirped laser pulses on Terahertz generation in magnetized plasma	48
4.3.2 Analysis & Observations	50

4.4 Conclusion	55
5. CHAPTER-5: Self-Focusing & Numerical Formalism of THz Radiation Field in Plasma	56-64
5.1 Introduction	56
5.2 Proposed Model	58
5.2.1 Self Focusing & THz Generation by Amplitude Modulated Pulse	58
5.2.2 Ponderomotive Nonlinearity	58
5.2.3 Self Focusing	59
5.2.4 Amplitude Modulated Wave Assisted THz Field	60
5.3 Analysis & Observations	63
5.4 Conclusion	64
6. CHAPTER-6: Summary and Future Scope	65-68
6.1 Summary	65
6.1.1 THz Community	66
6.1.2 Plasma & High Energy Density Physics	66
6.1.3 Condensed Matter Physics	66
6.1.4. Other Research	66
6.2. Future Scope	66
* References	69-77
* List of Publications	78
* Authors' Bio-Data	79-84
* Copy of Published Work	-

DEFINITIONS

Abbreviations

- EM wave: Electromagnetic wave
- THz: Terahertz
- GHz: Gigahertz
- TDS: Time-Domain Spectroscopy
- fs: Femtosecond
- ps: Picoseconds
- μm : Micrometer
- CPA: Chirp Pulse Amplification
- PRA: Paraxial Ray Approximation

Symbols

Other symbols are used in the text, but following are assumed throughout.

- E: Electric field
- H: Magnetic field
- c: Speed of light in vacuum
- k: Wave-vector
- m: Mass of electrons
- v_{th} : Thermal velocity of electrons
- ω : Angular frequency
- ω_p : Angular plasma frequency
- μ : Permeability
- ε : Permittivity
- $\bar{\varepsilon}$: Permittivity tensor
- n_0 : Ripple Amplitude
- ∇ : Operator
- λ : Wavelength
- ρ : Density or Volume mass density
- σ : conductivity
- φ : Potential

- χ : Susceptibility
- \cdot : Dot Product
- $*$: Complex Conjugate

LIST OF FIGURES

Chapter 1

Fig. 1.1 Electromagnetic spectrum and its range

Fig. 1.2 THz gap in the electromagnetic radiation spectrum © Martin Saraceno

Fig. 1.3 THz generation using nonlinear optics

Fig. 1.4 THz generation using electronics

Chapter 2

Fig. 2.5.1 Different Laser Polarizations

Fig. 2.5.2 Diagram for s- and p-polarized light

Fig. 2.5.3 Diagram for self focusing of laser in nonlinear medium

Fig. 2.5.4 Schematic for linear Frequency Chirp

Fig. 2.5.5 Schematic for Amplitude modulated wave generation

Chapter 3

Fig. 3.1 Schematic for THz wave generation in rippled density hot plasma

Fig. 3.2 Variation of normalised terahertz amplitude ($eA_{THz}/m\omega_{THz}c$) with normalised THz frequency (ω_{THz}/ω_p) for different values of θ at $T_e = 0.5\text{keV}$, $\omega_1 = 1.973 \times 10^{14}$, $\omega_2 = 1.783 \times 10^{14}$ and $n_q = 0.2n_0$.

Fig. 3.3 Variation of normalised THz amplitude with normalised THz frequency for different values of density ripple, at constant angle of incidence $\theta = 30^\circ$ at $T_e = 5\text{keV}$ Frequency of incidence laser beams are same as that of fig.3.2.

Fig. 3.4 Spectrum of the normalised amplitude of emitted THz wave versus normalised amplitude of incident laser beams at $v_{th}=0.1c$ corresponding to $T_e = 5\text{keV}$,

$\omega_{THz} / \omega_p = 1.08$, $n_q = 0.3n_0$ and $\theta = 30^\circ$. All other parameters are same as that of fig.3.2.

Fig. 3.5 Variation of normalised amplitude of terahertz yield ($eA_{THz} / m\omega_{THz}c$) with normalised velocity (v_{th}/c) for different values of density ripple at $\theta = 30^\circ$ and $\omega_n = 1.08$.

Fig. 3.6 Variation of normalised terahertz amplitude ($eA_{THz} / m\omega_{THz}c$) with the specular angle θ for different values of density ripple at $\omega_n = 1.08$.

Chapter 4

Fig. 4.2.1 Schematic of THz generation via frequency chirped laser pulses in rippled density plasma.

Fig. 4.2.2 Variation of normalised THz amplitude as function of normalised THz frequency for different values of density ripple at fixed value of chirp parameter $b=0.0099$.

Fig. 4.2.3 Plot of normalised THz amplitude versus frequency chirp parameter (b). Rest of the parameters are similar as that of fig.4.2.2.

Fig. 4.2.4 Spectrum of normalised THz amplitude corresponding to the incident lasers amplitude at $b=0.0099$ for different value of ripple density.

Fig. 4.3.1 Schematic for frequency chirp driven THz generation.

Fig. 4.3.2 Plot of the normalised amplitude of THz wave (A_{ω}) with normalised frequency (ω / ω_p) for frequency of incident laser $\omega_o = 2.3545 \times 10^{15}$ rad/sec at normalised laser intensity 0.1 corresponding to the laser intensity $I \approx 3 \times 10^{14}$ W/cm².

Inset graph: Plot similar to fig.4.3.2, at different chirp parameter without magnetic field.

Fig. 4.3.3 Plot of the normalised THz amplitude (A_{ω}) as a function of the frequency chirp parameter (b). Rest of the parameters are same as those in fig.4.3.2.

Fig. 4.3.4 Plot of the normalised THz amplitude (A_{thz}) as a function of the normalised intensity of incident lasers (A_0) at $b=0.0099$ for different values of normalised cyclotron frequency (ω_c / ω_p).

Fig. 4.3.5 Plot of the normalised amplitude (A_{thz}) of THz wave with normalised cyclotron frequency (ω_c / ω_p) corresponding to static magnetic field 54 kG to 322 kG for different values of frequency chirp parameter (b).

Chapter 5

Fig. 5.1 Self-focusing of laser beam

Fig. 5.2 Schematic for THz generation via amplitude modulate wave in pre formed rippled density plasma

Fig. 5.3 Plot of normalized propagation distance ξ versus beam with parameter f .

CHAPTER-1

INTRODUCTION & OVERVIEW

1.1. INTRODUCTION & PERIOR RESEARCH

The universe is bathed in terahertz energy; most of it going unnoticed and undetected due to lack of suitable sources and detectors. Terahertz frequency is sandwiched between highly investigated, infra-red (photonics) and traditional microwave (electronics), regions of electromagnetic spectrum. It was difficult to approach THz radiations directly by using microwave engineering because frequencies are too high to approach while too low to be generated by any laser until 1990s. Therefore, this spectral range is known as the terahertz gap [1-3].

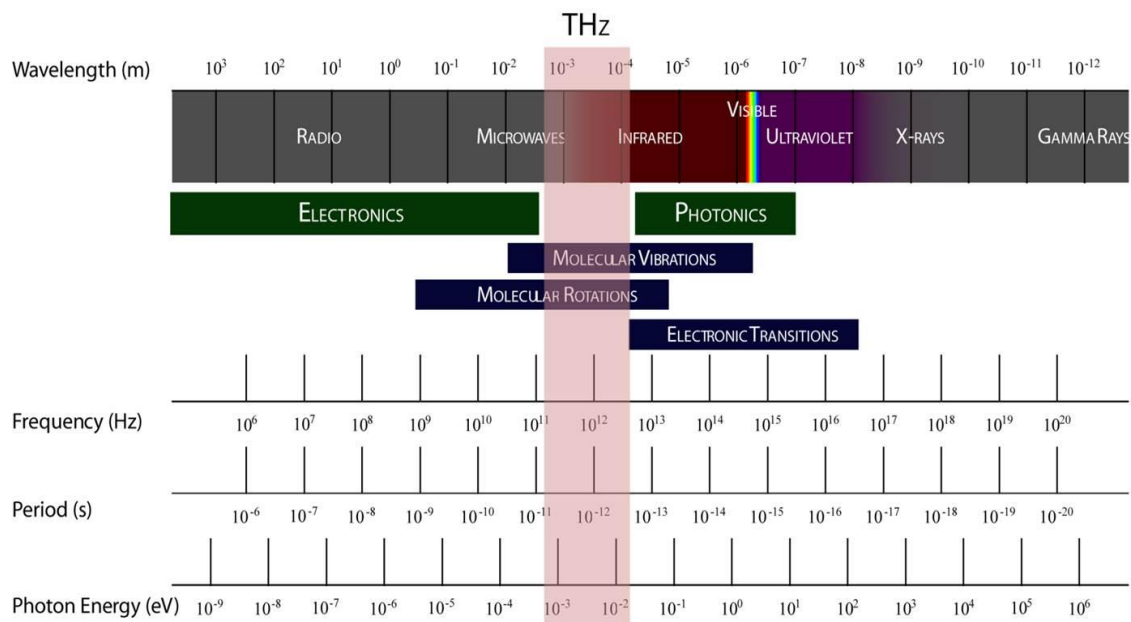


Fig.1.1. Electromagnetic spectrum and its range

(URL: <http://www.iiserpune.ac.in/~pankaj/> Dated 04/05/2020)

THz radiation is a part of electromagnetic spectrum, generally refers to far-infrared or submillimeter radiations also known as sub metric linear unit radiation, T-lux, T-light, T-waves, rate waves, high frequency T-rays or terahertz. The frequency range of 0.1-10 THz usually represents the terahertz wave, whereas, in terms of wavelength,

1THz=10¹²Hz=1000GHz corresponding to 0.3 mm in free space or the photon energy corresponding to 1THz is 4.1 milli-electron-volt and temperature, T= 4.8 to 478K. Crystalline phonon vibrations, molecular rotations, rotations of low frequency bond, H-bond stretches and torsions are the main sources of THz radiation [4-11].

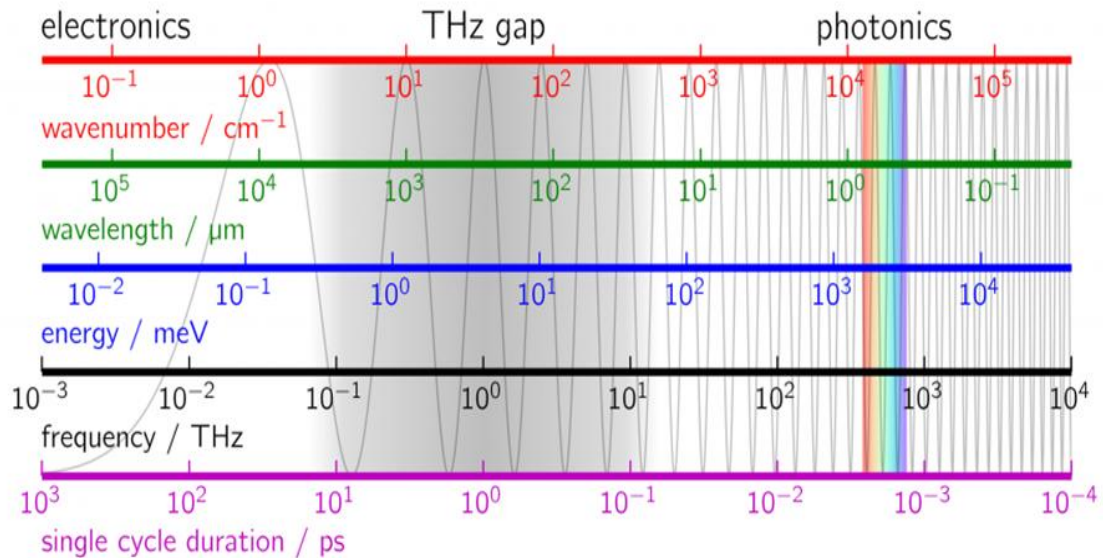


Fig.1.2. THz gap in the electromagnetic radiation spectrum © Martin Saraceno
 (URL: <http://resolv-blog.de/tag/thz/> Dated: 04/05/2020)

Since, T-rays have too low photon energy for the ionization of materials as compared to X-rays. Therefore, they do not produce harmful free radicals for living cells which means much less likely to cause cancer and genetic mutations. Thus it has an advantage over most other ionising imaging modalities that are commonly used today such as MRI, PET, planar X-rays and X-ray CT-scans due to its non ionising property [6]. Also, terahertz has the ability to penetrate many millimetres therefore it is appropriate for diagnosis of burn and cancerous cells. T-rays can also penetrate non-conducting materials (such as plastic, papers, textiles and foams) so can be used in material characterization, security screening purpose, non-destructive industrial quality checks, and for the identification of concealed explosives, weapons and drugs [3, 4, 7]. However, molecules of air (including water vapour) strongly absorb T-waves at various frequencies but fast data transmission is still possible at least over short distances like couple of meters. On the other hand, T-waves can be useful for

communication at high altitude such as satellite to satellite, aircraft to satellite etc because it has line of sight propagation [8].

THz frequencies are useful for spectroscopy in various areas such as the investigation of rotational state of molecules, superconductor's investigation, plasmonic effects in conducting materials. This is because the rotational and vibrational spectra of many fundamental molecules (such as: H₂O, O₂ and CO) and chemical substances falls under THz region [3, 8-10]. It is clear, that THz radiations can be utilized in many fields such as remote sensing, communication technology [12, 13], Spectroscopy, environmental monitoring, and biological imaging etc [14, 15]. Previously, complications in efficiently producing and controlling THz waves served as an obstruction for the region. However, due to continuous development in this area, from the past two decades, terahertz portion of the electromagnetic spectrum surfaces out as a resourceful tool owing to its versatile and wide range of applications in different aspect of science and technology [11-19].

The primary challenges in the progress of THz generation till date are ascertaining high conversion efficiencies with their scaling to achieve higher energies. Various schemes and methods have been devised for the improvement in the quality as well as efficiency of THz radiation [20-23]. One of which is the application of external magnetic field and suitable frequency chirp. Hamazaki *et al.* [23] have investigated the influence of frequency chirp on THz pulse spectra generated due to optical rectification. They observed that to ensure the smooth and single peaked THz spectra, the pre compensation for dispersion of GaP is required. Also, the excessive amount of frequency chirp causes distortions in the THz spectra. Frederike *et al.* [24] have experimentally generated THz wave generation employing periodically poled lithium niobate (PPLN) using dual frequency chirped, moderately delayed laser pulses from Ti: sapphire laser and the internal conversion efficiencies up to 0.13% with a multi-cycle THz energy of 40μJ have been reported. They further concluded that frequency chirp with delay pumping of PPLN is highly crucial to establish narrowband THz (~mJ level) for future applications. On the similar lines, a noteworthy efficiency of $> 10^{-4}$ and a remarkable bandwidth in excess of 75 THz has been realized by Kim *et al.* [25] , in which they have explained the THz generation mechanism due to transient

nonlinear electron current produced by two-colour photo-ionization in gases. Wang *et al.* [26] have analysed that chirped laser pulses facilitates the generation of strong THz pulses having amplitudes varying linearly with laser amplitude. These THz pulses have amplitude 10–100 times greater than that from the well-known two-color laser scheme, hence, facilitating one to achieve THz field up to 10MV/cm with initial laser intensity of about 10^{16} W/cm².

Furthermore, a range of solid state materials like lithium tantalite, lithium niobate, gallium arsenide and zinc telluride have been employed in order to produce THz radiations by nonlinear phenomenon [27]. The breakdown and damage threshold of these optical crystals due to short pulse laser limits the reliability of these materials for THz generation. Recently, an experiment was conducted at FLASH, the Free-electron LASer in Hamburg, at Deutsches Elektronen-SYNchrotron (DESY) utilizing the THz radiation, where; Azima *et al.* [28] employed a single-shot THz streak-camera for measuring the duration and spectral phase of the intense XUV pulses. Although, for THz applications in case of photoconductive antennas and semiconductors etc, low conversion efficiency and the material breakdown efficiency serves as major shortcoming. Hence, the alternative to avoid this issue is to employ a non linear medium which can endure high peak ultra-short laser powers. In order to overcome these concerns, plasma acts as an appropriate medium which overcomes the material damage related problems in case of THz generation. Also, one of the promising techniques for generating terahertz radiation is utilizing a short laser pulse. In contrast with photoconductive antennas or optical rectification, laser coupling with the plasma gives an intense and broadband THz pulse. Researchers experimentally as well as theoretically proposed several techniques [29-72] for efficient THz generation by considering plasma as a medium.

At first, Hamster *et al.* [29] demonstrated that the main source of THz radiation is the self consistent current driven by ponderomotive force of a short pulse laser in plasma. Plasma waves driven by the ponderomotive force of the laser have been extensively employed for frequency up conversion, particle and photon acceleration etc. For these applications, the typical plasma oscillation frequency lies is in the terahertz (THz) scale. Sheng *et al.* [30] have revealed that THz waves (GV/m) can be produced

around the plasma oscillation frequency due to linear mode conversion of the laser wake field. Although, THz frequency pulses produced due to accelerator-based sources are limited by the bandwidth and laser peak intensity. Liu *et al.* [31] have simulated THz generation in the two-color laser field based on the transient photocurrent model along with the physical mechanisms of THz generation at low and high laser intensities via THz spectrum investigation.

Kwon *et al.* [32] have reported highly energetic, short duration bursts of coherent THz radiation from an embedded plasma dipole. Plasma dipole oscillations are produced due to trapping of electrons in the potential wells generated due to ponderomotive force arising from two laser pulses (moderately detuned), due to which a quasi-monochromatic radiation is produced. Tripathi *et al.* [33] have investigated the THz radiation generation due to an amplitude modulated laser beam in the presence of density ripple. They concluded that the THz amplitude varies linearly with the modulation index and square of laser amplitude and inversely varies with electron collision frequency. The density ripple provides the phase matching-condition and give rise to high power efficiency. Also a scheme to generate terahertz (THz) radiation by electromagnetic Gaussian beams beating in hot collision less density rippled plasma has been investigated [34]. It has been concluded that the power of emitted THz radiation is proportional to the square of the density ripple amplitude. The THz wave amplitude decreases with the THz frequency and increases with the incidence angle up to an optimum value. Recently, Mehta *et al.* [35] have investigated the effect of frequency-chirped laser pulses on terahertz radiation generation in magnetized plasma. A suitable frequency chirp enhances the laser and electron interaction duration and applied magnetic field further imparts a significant momentum to THz photon. Hence, the combined effect of the frequency chirp and applied magnetic field results in a significant enhancement in the THz field strength.

On the basis of fluid model, the coherent terahertz radiations generated by the interaction of bunched relativistic electron beam with helical wiggler pump [36]. By numerical analysis they showed that the presence of the ion-channel can play a vital role for the THz power enhancement and the maximum power can be tune with ion channel density. Malik *et al.* [37] proposed a mechanism to tune the frequency and

power of THz radiation. They applied an external DC magnetic field and fixed the focus of emitted radiation by employing triangular lasers for the space-periodically beating in modulated plasma density. Bakhtiari *et al.* [38] analytically investigated the effects of laser and plasma parameters on THz generation by beating two dark hollow laser beams in collisional plasma. Kumar and Tripathi [39] put forward a numerical scheme of terahertz generation by optical mixing of two collinear laser pulses in rippled density plasma. The linearly polarised lasers propagate through plasma having density ripple at an angle to the direction of propagation of laser beam. As a result the phase matched THz wave generation rises for a density ripple of suitable wave number. By increasing the ripple angle the phase matching condition also obtained, so that the required ripple wave number produce more resonant THz wave.

A resonant THz generation observed by Bhasin and Tripathi [40] by optical rectification of picoseconds laser in a rippled density magneto-plasma. They showed in their results that the magnetic field enhances the power of emitted THz wave. Tyagi *et al.* [41] recently investigated the generation of THz radiation field inside the plasma channel assisted by an ion acoustic wave. The involvement of the ion acoustic wave is to provide proper phase matching for the momentum conservation. Kumar *et al.* [42] suggested an analytical formalism of generating THz radiation in hot plasma having step density profile. Resonant terahertz radiation achieved due to coupling between Langmuir wave and electromagnetic wave. Recently they also proposed a mathematical model for efficient power conversion of radiated THz wave (about 0.15GW) by nonlinear mixing of two p-polarised lasers in plasma with density hill [43].

A scheme was proposed to employ a laser spark produced under Axicon focusing of an optical radiation in order to generate terahertz radiation. Axicon is a conical shaped optical lens which is employed to generate efficient Bessel beams. Axicon optical elements are employed to generate radially polarized beams, and the generated the fields are referred as Axicon fields. Axicon optical lens is a conical shaped lens and can be employed in atomic traps and for generating plasma in wake-field accelerators and direction acceleration [44, 45] in laser-plasma interactions. By regulating the apex

angle of the Axicon lens and the diameter of the incident Gaussian beam; a focused Bessel beam can be generated, which is striking for THz imaging based applications. Recently, terahertz Bessel beams has attracted attention from researchers and scientists because of their attractive properties. Beams having Bessel-like profile employed in terahertz imaging applications, as a result the focus depth is improved considerably.

Akhmedzhanov *et al.* [46] have experimentally generated terahertz radiation in the gas breakdown due to high power Axicon-focused quasi-monochromatic laser pulses. The generation of THz radiation is a characteristic of oscillations produced in excited plasma column. The angular pattern in case of generated terahertz wave has been observed of a pronounced conical shape with an angle equal to the focusing angle of Axicon optical element. Wei *et al.* [47] have also experimental demonstrated the generation of an arbitrary order Bessel beams due to 3D printed helical Axicon optical elements at THz frequency range. These helical Axicon elements contain thickness gradients in both radial and azimuthal direction and transform an incident Gaussian beam into a higher order tightly focused Bessel beam. Semenova *et al.* [48] have shown a simulation-based study of the broadband terahertz Gauss-Bessel beams produced due to the Axicon lens. Their results reveal that for an optimum set of the Axicon lens parameters, the Gauss-Bessel beam of frequency range from 0.1 to 3 THz can be achieved. Recently, Kulya *et al.* [49] have studied the spatio-temporal and the spatio-spectral evolution of THz Gauss-Bessel beam. The temporal and spectral structure of the beam's profile depicts the scheme that the wave front of the Gauss-Bessel beam from the Axicon can be defragmented into radial segments for which the wave vectors cross during propagation, demonstrating a strong spatio-temporal coupling. Bystrov *et al.*[50] have investigated THz radiation from excited plasma oscillations due to optical (Axicon) breakdown of a gas in the presence of external fields. They analyzed that the intensity and spectra of plasma oscillations and generated THz radiation strongly relies on the characteristic of the spatiotemporal evolved plasma. Busch *et al.* [51] have utilized Axicon to generate broadband "focus-free" imaging in case of transmission and reflection in the terahertz range.

Sprangle *et al.* [52] have presented their theoretical and simulation based observations for Terahertz wave generation. They presented that the plasma current (with Fourier components) in a density modulated filament can emit a THz wave similar to Cherenkov radiation. In the presence of transverse electric field, due to filamentation of a femtosecond laser in air, orders of magnitude enhancement of THz energy has been achieved [53]. Malik *et al.* [54] have explored a scheme for generating terahertz wave due to the relativistic density modulated beam of electron utilizing density ripples in plasma, at an optimum angle. The dispersion relation of the wave radiation is modified by the non-linear interaction of the beam to the plasma. They have also investigated that, the requisite wavelength of ripple decreases with increasing the value of ripple angle and grow to be steeper for resonant terahertz emission. On the pathway of ripped density plasma, Kumar *et al.* [55] have scrutinized the THz radiation due to amplitude-modulated self-focused Gaussian laser in plasma. In the presence of density ripple, they have observed a strong transient current due to transverse component of ponderomotive force; which is responsible for the radiation at the modulated frequency (THz range). They have reported a significant enhancement in the THz yield due to self-focusing effect as compared to in its absence. Singh and Sharma [56] have presented theoretical analysis of efficient terahertz generation by self-focusing of amplitude modulated Gaussian x-mode laser in magnetized ripple density plasma. Here, they have analyzed that resonant enhancement in the THz yield can be accomplished by the help of externally applied magnetic field.

Mehta *et al.* [57] have also investigated the combined influence of the frequency chirp pulses and spatially periodic density plasma, on THz radiation generation, due to beating of two chirped pulses. It was reported that application of frequency chirp and ripple plays a vital role in progressing the nonlinear oscillating current. Kumar *et al.* [58] have investigated a strong terahertz generation by optical rectification of a super-Gaussian laser beam. They have observed a stronger THz generation due to super-Gaussian intensity profile than that of Gaussian intensity profile. They have also reported the enhancement in the intensity of terahertz as the value of collision frequency parameter decreases. On the similar lines, Singh *et al.* [59] have observed a

novel proposal for THz generation by the optical rectification of the super-Gaussian amplitude-modulated beam in the preformed magnetized plasma. Their findings include enhancement in the THz field amplitude due to index of modulation as well as order of super-Gaussian laser.

1.2. SCHEMES FOR THz RADIATION GENERATION

Researchers from all over the world are working in to produce efficient THz sources from the past three decades. A number of methods are proposed to achieve high power THz sources. Basically it is generated by lasers, non-linear optics (Fig.1.3) and electronics (Fig.1.4). These methods are further divided into some other sub-schemes such as quantum cascade or semiconductor laser, gas lasers, high frequency oscillators, sources based on accelerators, laser-matter interaction, optical rectification, optical terahertz generation and solid state electronic devices (see section 1.1). The radiation produced using these techniques are of various wavelengths either pulsed or continuous wave (CW). A range of solid state materials like lithium tantalite, lithium niobate, gallium arsenide and zinc telluride have been employed in order to produce THz radiations by nonlinear phenomenon [27]. The breakdown and damage threshold of these optical crystals due to short pulse laser limits the reliability of these materials for THz generation. However, the efficiency of THz pulses produced by most of the above methods is not enough due to their lower damage limit.

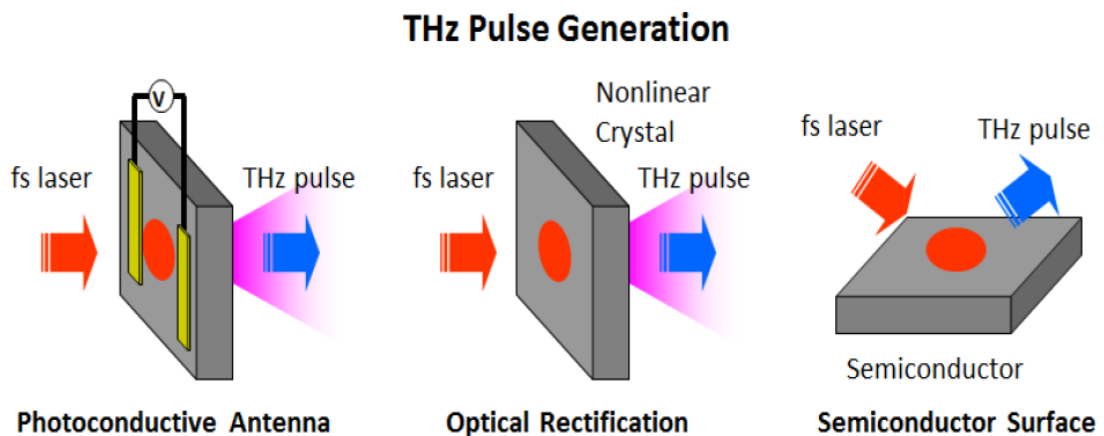


Fig.1.3. THz generation using nonlinear optics

(URL: <http://phome.postech.ac.kr/user/indexSub.action?codyMenuSeq=2853646&siteId=nbtp&menuU>

[IType=top](#) Dated: 07/08/2020

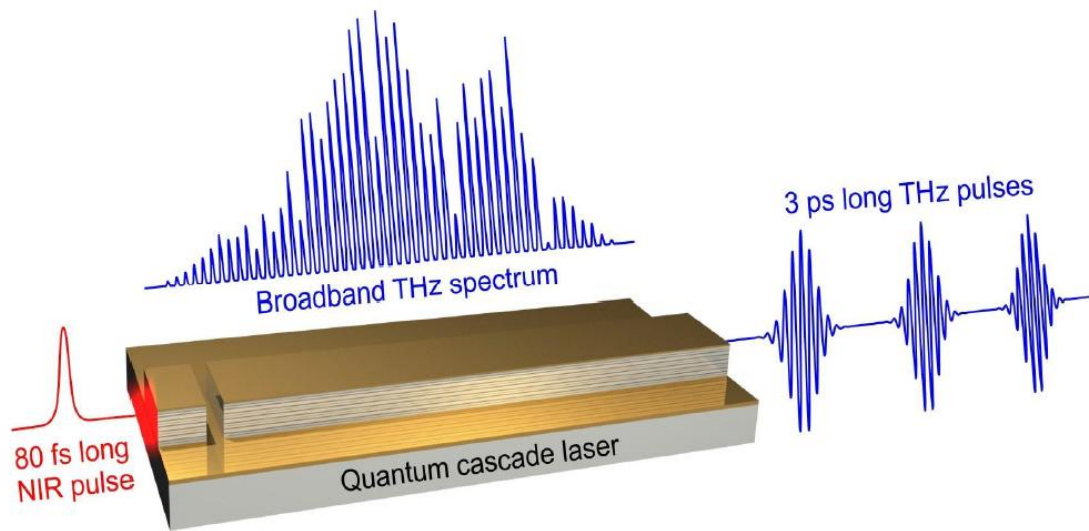


Fig.1.4. THz generation using electronics
 (URL: https://www.opli.net/opli_magazine/eo/2017/new-record-achieved-in-terahertz-pulse-generation-feb-news/ Dated: 07/08/2020)

Although, for THz applications in case of photoconductive antennas and semiconductors etc, low conversion efficiency and the material breakdown efficiency serves as major shortcoming. Thus the interaction of energetic electron beam and strong laser pulse with plasma is the key to overcome this limitation. In contrast with photoconductive antennas or optical rectification, laser coupling with the plasma gives an intense and broadband THz pulse [60-66]. Due to the incessant development in the field of ultra intense lasers, tuneable terahertz sources with high efficiency can be produced with the help of laser plasma interaction. Since plasma can easily handle very high power radiation and provide a very high dipole moment which added an advantage of not having damage limit. There are two routes to generate the T-waves by laser plasma interaction named as; Laser beat-wave (LBW) and Laser wake-field (LWF) schemes. Both the above mentioned schemes take place via the excitation of plasma wave, in which a large phase velocity plasma wave is excited by the laser.

1.3. MOTIVATION OF THE STUDY

The interest of researchers in THz technology is strongly motivated by a burgeoning range of promising applications in science and industry [18]. For example, given the fact that the THz waves can stimulate molecular and electronic motions in many materials and yet be non-ionizing, THz radiation can be used to not only identify

hidden explosives and screen for skin cancer, but also engineer transient states of matter like superconductivity [20]. High-power THz sources are highly desired for the development of THz science. Thanks to advances in ultrafast techniques particularly the laser technology, THz sources have witnessed a tremendous development in recent decades. Currently, the two most prominent THz sources, based upon large-scale accelerators or high-power laser-pumped crystals, can produce hundreds-of-micro-joules THz pulses [11]. Work presented in here further greatly advanced the relevant research of high power laser-driven THz radiation. In terms of THz generation, laser-solid interaction shows an apparent advantage over other approaches in the THz yield. On one hand, using plasma as the THz generation medium circumvents the limitation of optical damage that is confronted by the crystal-based sources. On the other hand, unlike larger conventional accelerators, a laser plasma source can achieve ultra-short electron bunches of high charge within millimetre-scale distances. However, considerable deficiency exists in terms of energy efficiency compared to crystal-based sources. In addition, due to the THz radiation generated having a large divergence angle the actual THz energy readily collected with a finite-size lens is only a few millijoules. Hence, our primary goal is to achieve a step change in the laser-to-THz generation efficiency and then push the practically available THz energy to its extreme.

1.4. RESEARCH OBJECTIVES

The overall aim of the proposed thesis is to significantly increase our understanding and control of laser plasma based THz sources to enable new and novel high-field studies utilizing these unique ultra-bright pulses. This will be achieved through the following objectives:

- Resonant THz generation in plasma by obliquely incident lasers.
- Investigate the effect of frequency chirp pulses on THz radiation in ripple-density plasma.
- Terahertz generation by chirped pulse laser in magnetised plasma.
- Effect of self-focusing of lasers on THz radiation in plasma.

1.5 THESIS CONTRIBUTION

The work presented in this thesis is based on theoretical approach to deal with the generation of THz radiation by the interaction of lasers with under-dense plasmas. As per our first approach in rippled density hot collision less plasma, the nonlinear mixing of lasers plays an important role when the incident lasers travel at an angle normal to the plasma surface. The transverse intensity gradient of the electromagnetic wave contributes significantly to the plasma wave generation. The generated plasma wave interacts with the electromagnetic wave and leads to the generation of a radiation whose frequency lies in THz range. Furthermore, the density ripple of suitable wave number provides the phase matching which further helps in the efficiency enhancement. Here, we choose hot plasma for the propagation of electromagnetic wave because in the cold plasma only damped oscillations exist.

The investigation, given in our second model, deals with the influence of frequency chirp on the generated terahertz (THz) wave due to interaction between intense laser pulses and rippled density plasma in part one and further, in magnetized plasma in second part. For achieving a significant enhancement in THz efficiency and field strength, the frequency chirped laser, density ripple wave number and magnetic field parameters are optimized. A significant increment in THz efficiency is obtained due with the help of density ripple of suitable wave number. The external magnetic field also plays a crucial role in enhancing the efficiency of THz wave. Tuneable and coherent THz radiation through electrostatic to electromagnetic field conversion due to an ionization front can be produced in a uniform electrostatic field. Our third approach is based on the self focusing of amplitude modulated super-Gaussian wave propagating in plasma. We consider rippled density plasma to satisfy the exact phase matching.

1.6 THESIS OUTLINES

The thesis is organised as follows: the methodology is given in Chapter-2, along with the hypothesis and the theoretical consideration of basic equations used in our analysis. The models with the detailed numerical analysis and observation of our results are discussed in Chapter-3, 4 and 5. Summary and future scope of the work accomplished in this thesis is discussed in the Chapter-6.

CHAPTER-2

RESEARCH METHODOLOGY

2.1. RESEARCH HYPOTHESIS

The long-term goal of our research is to develop ultra-intense THz sources and advancing the field of extreme THz science. To achieve this goal, the objective of the present work is to significantly improve the performance of laser-driven THz sources. Our specific hypothesis is that high power laser-plasma interactions provide an ideal platform to deliver an intense THz source. This hypothesis is based on the previous results of different experimental, theoretical as well as simulation work carried out by researchers in the field of electromagnetic radiation and high harmonic generation (see section 1.1).

2.2. THEORETICAL FORMALISM: PARAXIAL RAY APPROXIMATION

There are various methods to study the nonlinear phenomena occurs during the laser plasma interaction for example: Paraxial Ray Approximation (PRA), Variational Method and Moment Theory. It is clear from the literature survey that in 1968 the Paraxial Ray Approximation (near axis) method, suggested by Akhmanov *et al.* [46] is not only the simplest one but also qualitatively agrees well with experimental results. According to this approach the one will only consider the behaviour of rays close to the axis (or say paraxial). To study the electromagnetic wave propagation in semiconductors, dielectrics as well as gaseous plasmas Sodha *et al.* [75] employed the PRA approach. Also in the years 1974 and 1976, to describe the phenomena of self focusing using PRA approach, an elementary monograph and a review article had been published, respectively [76,77]. Therefore, on the basis of above theory we have considered the PRA approach throughout the thesis. Out of the a variety of schemes, on the basis of interaction of laser to the plasma, for the T-wave generation caused by lasers beating in plasma demonstrated remarkable potential in the field of amplitude, tunability, efficiency and directionality. The high peak power can also be scaled by

sources of THz based on beating scheme. The basic mechanism of electrostatic-electromagnetic wave coupling along with ponderomotive force and wave governing equation are given in the following sections of this chapter.

2.3. ORIGIN OF PONDEROMOTIVE FORCE

When high power electromagnetic wave interacts with plasma; the electrons of plasma starts oscillating due to a nonlinear ponderomotive force. The drift velocity of plasma electrons, in collision less plasma, can be calculated using equation given as follows [78];

$$\left(m \frac{\partial}{\partial t} + m \vec{v} \cdot \vec{\nabla} \right) \vec{v} = -e\vec{E} - e(\vec{v} \times \vec{B})/c - N_e^{-1} \vec{\nabla}(N_e k_0 T_0), \quad (2.3.1)$$

The expression on right hand side corresponds to the force on an electron. Here, 1st and 2nd term denotes the force on the account of electric and magnetic fields, respectively, whereas the third term signifies the force attributable to the gradient of partial pressure. Rewriting Eq. (2.3.1), we have

$$m \frac{\partial \vec{v}}{\partial t} = \vec{F}_p - e\vec{E} - N_e^{-1} \vec{\nabla}(N_e k_0 T_0), \quad (2.3.2)$$

here, $\vec{F}_p = -e(\vec{v} \times \vec{B})/c - m(\vec{v} \cdot \vec{\nabla})\vec{v}$, is usually termed as the ponderomotive force. It may be readily seen that this force arises on the account of the interaction of drift velocity of electrons (which is due to electric vector of the wave) with the magnetic vector \vec{B} of the wave and from the gradient of the drift velocity. The magnitude of \vec{F}_p and the last term in Eq. (2.3.2) is very small as compared to the force $(-e\vec{E})$ on the account of the electric field. Thus to the 0th order of approximation the steady state solution of the Eq. (2.3.1) calculated as;

$$\vec{v} = -\frac{e\vec{E}}{mi\omega}. \quad (2.3.3)$$

The magnetic induction vector B of the wave may be evaluated using Maxwell's 3rd equation as

$$\vec{B} = -\frac{c}{i\omega} \text{Curl}\vec{E}. \quad (2.3.4)$$

Using Eq. (2.3.3) & (2.3.4) the time independent part of \vec{F}_p (Which is relevant to self focusing) can be written as

$$\vec{F}_p = -\frac{e^2}{4m\omega^2} \nabla(\vec{E} \cdot \vec{E}^*). \quad (2.3.5)$$

The same expression for the ponderomotive force has been derived by many researchers [79-81] using different approach. Hence from Eq. (2.3.5) the ponderomotive force can be defined as a non linear force experienced by an electrically charged particle in an oscillating inhomogeneous electromagnetic field that pushes the particles toward the area having weaker field strength.

2.4. ANALYSIS FOR WAVE GOVERNING EQUATION

For a discussion of propagation of electromagnetic waves in conducting media it is very helpful to introduce the concept of effective dielectric constant from consideration of Maxwell's equations and other auxiliary relations, valid for conducting media. Maxwell's equations are [82]

$$\vec{\nabla} \cdot \vec{D} = 4\pi\rho, \quad (2.4.1)$$

$$\vec{\nabla} \cdot \vec{B} = 0, \quad (2.4.2)$$

$$\vec{\nabla} \times \vec{E} = -\frac{1}{c} \frac{\partial \vec{B}}{\partial t}, \quad (2.4.3)$$

$$\vec{\nabla} \times \vec{H} = \frac{4\pi}{c} \vec{J} + \frac{1}{c} \frac{\partial \vec{D}}{\partial t}, \quad (2.4.4)$$

here, \vec{E} and \vec{D} are the electric and displacement vectors ($\vec{D} = \epsilon_L \vec{E}$, for conducting media), \vec{H} and \vec{B} are the magnetic and magnetic induction vectors ($\vec{B} = \mu \vec{H}$), \vec{J} and ρ represents the current density and the charge density free carrier charge, respectively and are related through the equation of continuity. Also, ϵ_L stand as the

lattice dielectric constant in the case of semiconductors and the dielectric constant of the gas in the case of gaseous plasmas. μ , the magnetic permeability, is approximately equal to unity for plasmas and nonmagnetic media. By taking curl of the Eq. (2.4.3), we have

$$\text{Curl}(\vec{\nabla} \times \vec{E}) = \text{Curl}\left(-\frac{1}{c} \frac{\partial \vec{B}}{\partial t}\right), \quad (2.4.5)$$

Using vector identity for Eq. (2.4.5) as; $\text{Curl}(\vec{a} \times \vec{b}) = \vec{\nabla} \times (\vec{a} \times \vec{b}) = \vec{a}(\vec{\nabla} \cdot \vec{b}) - (\vec{\nabla} \cdot \vec{a})\vec{b}$, Left Hand Side (LHS) of above equation takes the form $\text{Curl}(\vec{\nabla} \times \vec{E}) = \vec{\nabla} \times (\vec{\nabla} \times \vec{E}) = \vec{\nabla}(\vec{\nabla} \cdot \vec{E}) - \nabla^2 \vec{E}$, where as the Right Hand Side (RHS) gives;

$$\text{Curl}\left(-\frac{1}{c} \frac{\partial \vec{B}}{\partial t}\right) = -\frac{1}{c} \frac{\partial}{\partial t}(\vec{\nabla} \times \vec{B}), \quad (2.4.6)$$

Now substituting the value of from Eq. (2.4.4) in Eq. (2.4.6) and putting the values of LHS and RHS of Eq.(2.4.5), we obtain

$$\vec{\nabla}(\vec{\nabla} \cdot \vec{E}) - \nabla^2 \vec{E} = -\frac{1}{c} \frac{\partial}{\partial t} \left(\frac{4\pi}{c} \vec{J} + \frac{\epsilon}{c} \frac{\partial \vec{E}}{\partial t} \right), \quad (2.4.7)$$

$$\nabla^2 \vec{E} - \vec{\nabla}(\vec{\nabla} \cdot \vec{E}) = \frac{4\pi}{c^2} \frac{\partial \vec{J}}{\partial t} + \frac{4\pi\epsilon_L}{c^2} \frac{\partial^2 \vec{E}}{\partial t^2}, \quad (2.4.8)$$

The above Eq. (2.4.8) is the wave governing equation. In the case of non-conducting medium $\vec{J} = 0$.

2.5. ROLE OF DIFFERENT LASER & PLASMA PARAMETERS

During our analysis we see the effect of following laser and plasma parameters on Terahertz radiation generation:

2.5.1. LASER POLARIZATION

The optical parameters of a medium were supposed to be independent of the propagating lights' intensity before the invention of lasers. The reason behind this is that the electric field strength of such light sources is of the order of 10^3 V/cm , which is too small to affect the mediums' interatomic fields (around $\approx 10^7 \text{ to } 10^{10} \text{ V/cm}$). At these low fields, the perturbation of the medium is not sufficient to generate a measurable nonlinear effect and the electric polarization is simply assumed to vary linearly with the electric field strength \vec{E} as; $P = \epsilon_0 \chi E$; where ϵ_0 is free space permittivity, χ is the susceptibility of the medium. The behaviour of atoms in the presence of intense laser fields is very different. Intensities of the order of 10^{12} W/cm^2 correspond to electric field strengths which is sufficient to perturb electrons of the interacting medium and cause a nonlinear response. So the interesting nonlinear effects are observed once the perturbation to the interatomic field becomes significant. With sufficiently intense laser radiation the induced electric polarization becomes [83]

$$P = \epsilon_0 \left(\chi^{(1)} E + \chi^{(2)} E^2 + \chi^{(3)} E^3 + \dots \right) \quad (2.5.1)$$

Where, $\chi^{(1)}, \chi^{(2)}, \chi^{(3)} \dots$ are first, second and third order non-linear susceptibilities. At low fields, as in the case of ordinary light sources, only first term of Eq. (2.5.1) can be retained, which corresponds to linear optics. Higher the value of electric field, more significant becomes the higher order terms. Also, the other optical characteristics of a medium such as refractive index and dielectric permittivity etc. become functions of the field strength \vec{E} . Hence it is clear that the laser polarization plays an important role during laser plasma interaction and hence we have considered different laser polarisation in our analysis, discussed Chapter-wise. In general, an electromagnetic wave consists of mutually perpendicular electric and magnetic fields; so that the polarization can be refers to the direction of electric field. This can be further categorised into three categories (fig.2.5.1.) and described as follows:

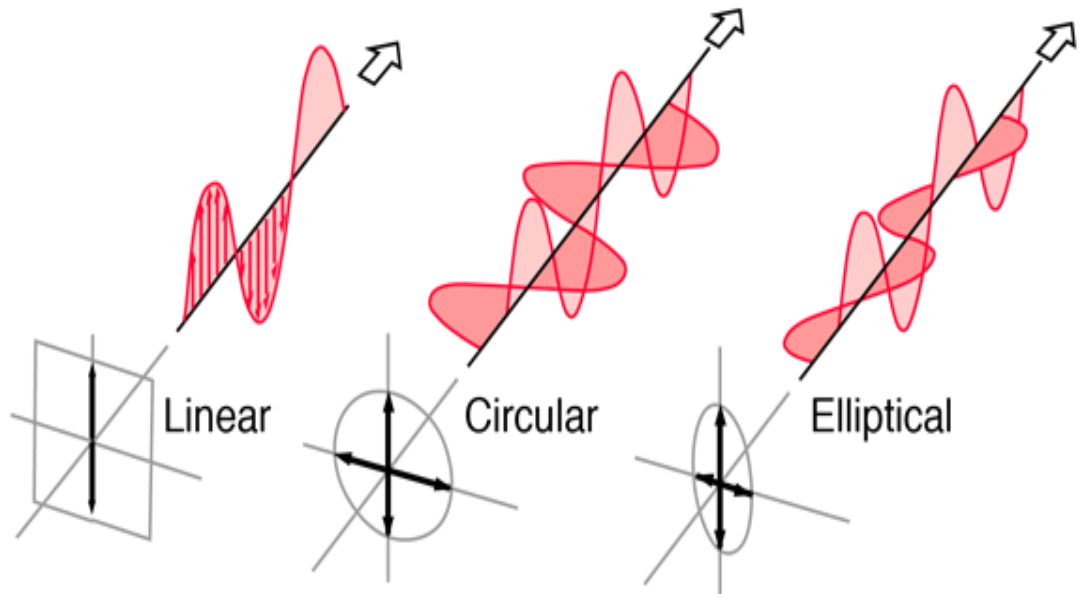


Fig.2.5.1. Different Laser Polarizations

(URL: <http://hyperphysics.phy-astr.gsu.edu/hbase/phyopt/polclas.html>, Dated: 04/05/2020)

2.5.1.1 Linear Polarization

The light is said to be linearly polarised if the fields oscillate in a single direction, i.e., (plane wave in space) is said to be linearly polarized. This is further divided into two sub categories s- and p-polarization, defined in section 2.5.1.4.

2.5.1.2 Circular Polarization

Two mutually perpendicular plane waves having same amplitude and differ by 90° phase angle, are called circular polarized. The circular polarized light is further categorised as left and right handed on the basis of the direction of the rotation of their electric field vector, i.e., clockwise for the former and counter clockwise for the later. One can also convert a linearly polarised light into circular by using the quarter-wave plate. The plates should be at the angle of 45° to the plates' optic axis.

2.5.1.3 Elliptical Polarization

Two mutually perpendicular plane waves having unequal amplitude and are differ in phase by 90° are called elliptically polarised.

2.5.1.4 s- and p-Polarization

This is also known as parallel polarized light both are basically linearly polarised. The axis of the propagation of light and the line normal of a sample surface creates a plane, so, a linearly polarized light that runs perpendicularly to the plane is known as s-polarized however, the light that runs in this plane is called p-polarized (Fig. 2.5.2.).

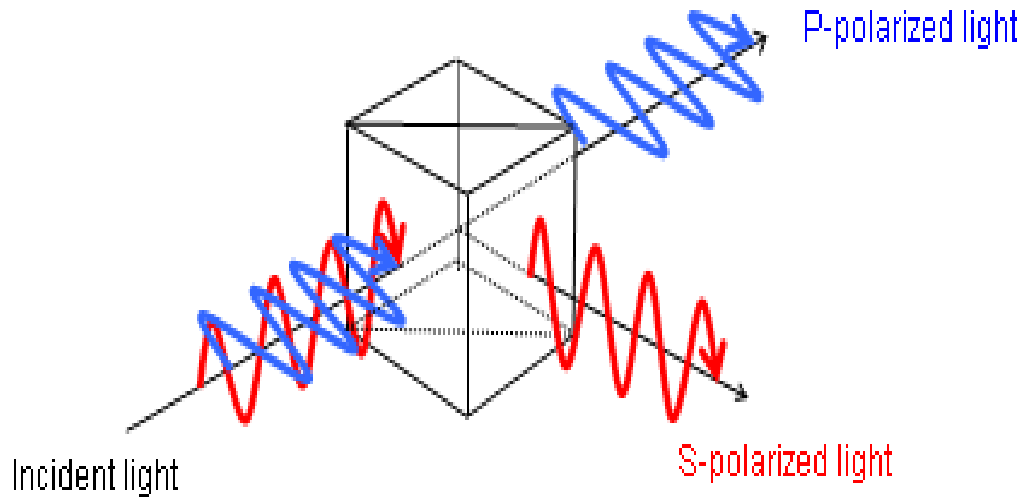


Fig.2.5.2. Diagram for s- and p-polarized light

(URL: https://www5.epsondevice.com/en/information/technical_info/glossary/alpha_p.html,

Dated:04/05/2020)

2.5.2. SELF-FOCUSING OF LASER

The nonlinearities responsible for focusing in plasmas are: collisional, relativistic and ponderomotive. We also considered the self focusing effect when ponderomotive nonlinearity is operative. When a highly intense beam of laser propagates through the plasma, the plasma electrons are pushed out from the strong power region due to the ponderomotive force. Further, the plasma dielectric function shows a growth due to the decrement of the density of local electrons. As a result, self focusing of laser takes place, whereas, the laser diverges due to the diffraction (Fig.2.5.3). Under the competition among ponderomotive nonlinearity and diffraction, periodic self-focusing and defocusing arises and the density-modulated filament is produced. The detailed study of the self focusing due to ponderomotive nonlinearity is discussed in Chapter-5.

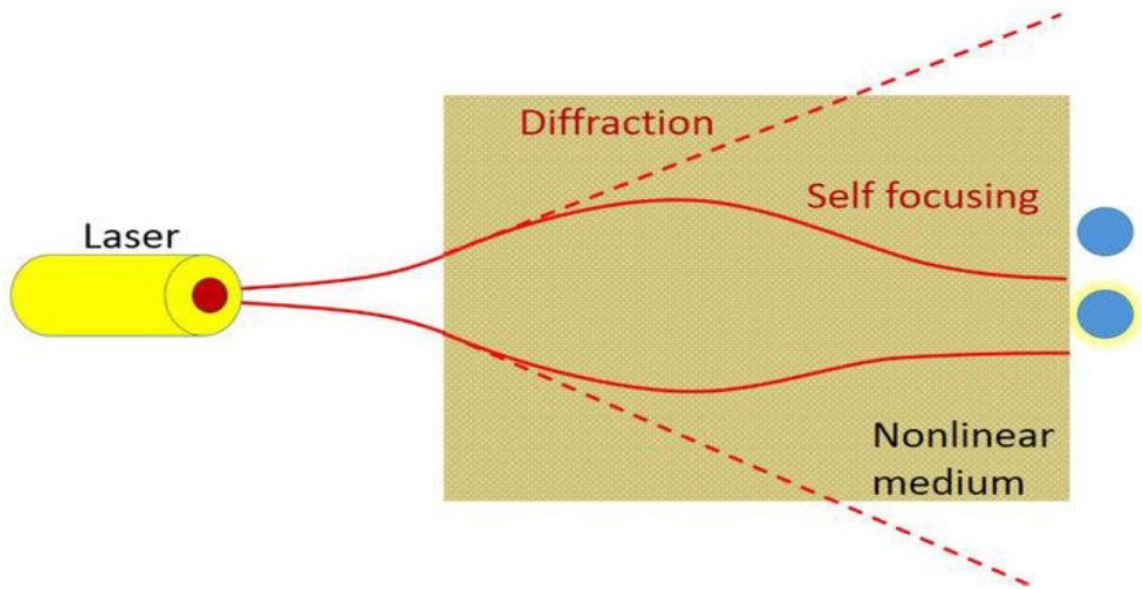


Fig.2.5.3. Diagram for self focusing of laser in nonlinear medium

[URL:https://www.researchgate.net/publication/306008209](https://www.researchgate.net/publication/306008209) The quest for ultimate super resolution/figures?lo=1

(Dated: 07/05/2020)

2.5.3. RIPPLE DENSITY PLASMA

We have considered the effect density ripples in our analysis. The plasma density ripple can be produced by using various schemes involving machining beam, Axicon grating, patterned mask and transmission ring grating. Where by adjusting the period and the mask size and by changing groove structure, groove period and the duty cycle of such grating one can control the ripple parameters [33, 34, 40]. The resonance condition is satisfied with the help of density ripple of appropriate wave number. The proper matching of the ripple wave number with the beat wave number provides the maximum transfer of energy and momentum under the resonance condition. The ripple helps THz generation in following two ways: first it makes the nonlinear current irrotational and second by providing the phase matching. So, it is clear from the analysis given in all the chapters that the maximum momentum is transfer to the electrons at resonace condition. On the other hand, the role of amplitude of density ripple is to enhance the THz wave field. Since, higher the amplitude of density ripple, more the number of electrons take part in the excitation of radiation. Therefore, one can tune the frequency of the emitted resonant signal [67] with the help of appropriate value of ripple amplitude.

2.4.4. APPLIED MAGNETIC FIELD

Plasma's dielectric function displays the anisotropic behaviour in the presence of externally applied magnetic field and so, takes the tensor form [35-37]. Further, leads to two discrete modes of the propagation, namely the extraordinary and the ordinary modes. A number of methods to study the nonlinear processes have been made in the context of magnetized plasma (see section 1.1). A charged particle undergoes a circular orbit in the plane perpendicular to the direction of the field when placed in a magnetic field. due to the combined influence of magnetic field and ponderomotive force, charged particle executes the spiral trajectory. The externally applied magnetic field not only enhance the strength of ponderomotive force, but also provide an additional momentum to the plasma electrons and retains the energy to longer distance. One can use either static magnetic field, azimuthal magnetic field or wiggler magnetic field.

The effect of static magnetic field has also been considered in objective 3 and 4. In the presence of external magnetic field the electrons starts moving in a circle due to the Lorentz force. This circular motion is superimposed with the electric field of laser pulse results a cycloid of angular frequency ω_c . Further, the main role of externally applied magnetic field is to provide the additional momentum to the THz photon get the resonant THz-wave. The external applied static magnetic field enhances the strength of $(\vec{v} \times \vec{B})$ force, creates the bending effect on the plasma electron. As the static magnetic field also introduces an additional motion to the electrons; this gives an extra nonlinear current term which can be seen from current density equation. Also the applied magnetic field provides the additional transverse component of nonlinear current density, results the significant gain in amplitude of THz wave.

2.5.5. FREQUENCY CHIRP

A frequency chirp is defined as the frequency increases or decreases with time. Chirped Pulse Amplification (CPA) is a remarkable procedure to amplify an ultrashort pulse into a higher energy level. This method enables the construction of table top amplifiers, which can generate femtosecond pulses of peak powers upto several terawatts. This method was introduced in 1960 in order to amplify existing

power in RADAR. CPA has bridge the gap between multi terawatt and petawatt systems in research facilities. An expanded pulse has its frequency changing with time is referred as a chirped pulse. Researchers used different type of chirp as per their requirements. We have considered the effect of linear frequency chirp in Chapter-4 and it shows that a linear frequency chirp increases the duration of nonlinear interaction of laser pulse with plasma electrons and hence, enforces the interaction for longer duration. One can generate highly efficient chirped laser pulse by using two counter propagating lasers induced plasma Braggs grating (PBG) [74]. To control femtosecond laser pulses the plasma grating can be a novel because it has a much higher damage threshold than ordinary dielectric/ metal optical elements.

Let, ω_0 & $\omega(z,t)$ represented the fundamental frequency and chirped frequency of laser pulse, t and z stands for time and propagation distance, respectively. Speed of light denoted by c in vacuum and b represents chirp parameter. Since the chirp parameter b is inversely proportional to Group Delay Dispersion (GDD) so that the increase of b naturally implies the decreased GDD. Obviously, the decreased GDD means less-chirp. Hence, by choosing a suitable value of chirp parameter one can tune the output radiation. In the work presented in this thesis, we only considered a linear frequency chirp. A linear chirp is further divided into two sub categories such as;

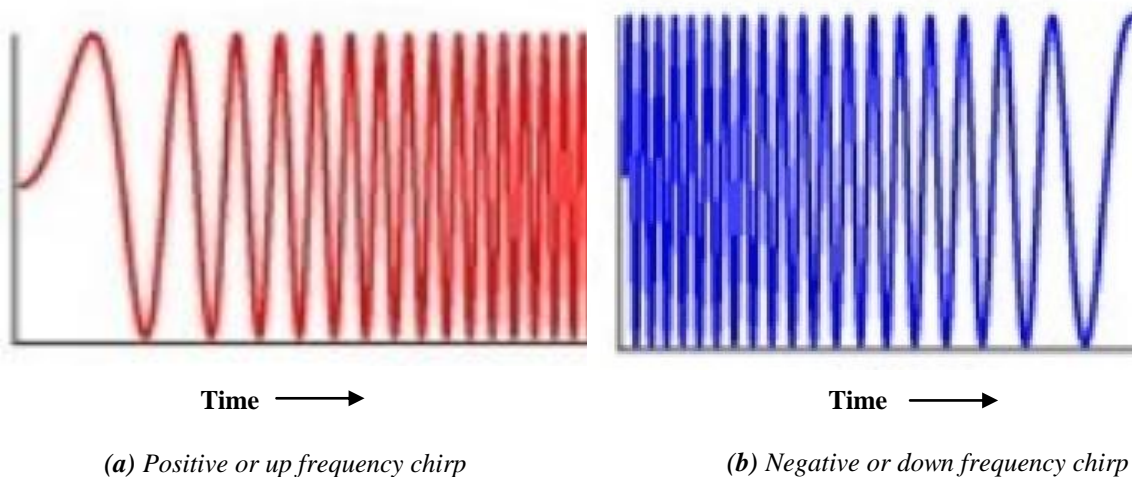


Fig. 2.5.3 Schematic for linear Frequency Chirp

2.5.5.1. Linear Positive Frequency Chirp

In the case of positive frequency chirp the frequency of the laser pulse increases with time linearly (Fig.2.5.3 (a)). The angular frequency of a positive chirp is as follows;

$$\omega(z, t) = \omega_0 + b\omega_0^2(t - z/c).$$

2.5.5.2. Linear Negative Frequency Chirp

In the case of negative frequency chirp the frequency of the laser pulse decreases with time linearly (Fig.2.5.3 (b)). The angular frequency of a negative chirp can be written as;

$$\omega(z, t) = \omega_0 - b\omega_0^2(t - z/c).$$

2.5.6. LASER PROFILE

An electromagnetic monochromatic beam having an amplitude envelope in a plane (transverse) denoted with a Gaussian function is known as Gaussian beam. Many different profiles can be generated from this Gaussian beam by using appropriate lenses to refocus and alter the dependence of beams' transverse phase. There are various laser profiles such as, Cosh-Gaussian, Hermite-Cosh-Gaussian, Super Gaussian, Hollow-Gaussian and many more [35-38, 55-59]. They all have their own characteristics and used by various researchers to study nonlinear physics. Since, the detail study of plasma physics and nonlinear phenomena are difficult to compile in a single document. In this thesis, we study a small portion of electromagnetic wave. Thus, we have used only Gaussian and super Gaussian profile to accomplish our objectives. In the presence of a Gaussian laser beam, the plasma gets depleted from the high field region to the low field region on account of the ponderomotive force. Due to which plasma electrons starts oscillating with a nonlinear velocity that drives resultant nonlinear current for generating terahertz radiation.

2.5.7. INTENSITY OF INCIDENT LASER

The intensity of incident laser has an important role in the laser plasma processes (see section 2.5.1). The increment in the incident beam intensity results the enhancement in the initial ionization of plasma and nonlinearity in the system due to the strength of ponderomotive force. As a result, greater will be the free electron density which produces more intense THz wave. Thus, strength of output wave can be controlled by

overseeing the intensity of incident laser pulses. We have shown the relationship between lasers intensity versus output yield in the work presented in this thesis. There is a direct relationship between THz amplitude and incident lasers' intensity. The physical reason behind this is that with the enrichment of the intensity of laser, the strength of ponderomotive force and therefore, the initial ionization of the plasma enhanced. Consequently, with the increase of free electron density, the nonlinearity increases. As THz generation is a nonlinear phenomenon, it enhances more and more.

2.5.8. AMPLITUDE MODULATION WAVE

Basically, in communication electronics the information signals are transmitted via carrier wave of radio frequency using a scheme of amplitude modulation (AM). In this technique, the information signal can be send to the observer by varying the transmitted signal strength as per the requirement. With the help of this technique the information can be send to the receiver more precisely. Further, pulse can be amplitude modulated with the help of terahertz signal by means of electro-optic modulator technique (Fig.5.5.4). In this process, one EM signal to be propagates through the electro optic modulator is identical in phase to the other EM signal. In Chapter-5, we proposed a model to generate THz wave using amplitude modulated super Gaussian pulse. The effect of self focusing is also considered.

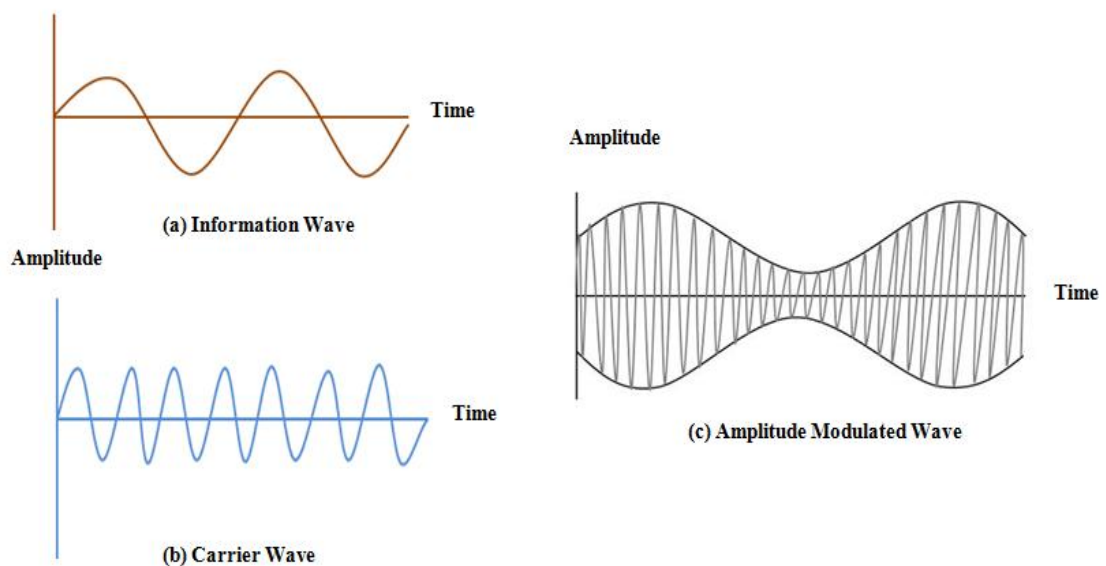


Fig.2.5.4 Schematic for Amplitude modulated wave generation

2.5.9. PLASMA FREQUENCY

As we are well aware of the electron density that it is the density of electrons in the plasma. There is one more type of density, called the critical density of the plasma. The value of this critical density distinguishes the regime of underdense as well as overdense plasma. The idea behind the theory, the laser frequency should be greater than the frequency of plasma to propagate a laser through the plasma. Hence, in the case of underdense plasma the electron density is less than the critical density. Whereas, in the case of overdense plasma the incident beam is prevented to propagate through the plasma by the high density of electrons as the frequency of incident laser is less than the frequency of plasma wave. In our analysis we have considered the under dense plasma. As mention above, it should be noted that the frequency of incident lasers should be much greater than the plasma frequency (ω_p) for efficient THz generation because in this limit ions are treated as stationary. The formula for the plasma density is given as $\omega_p = \sqrt{4\pi n e^2 / m}$, here, n represents the density of electron.

2.6. RESEARCH DESIGN & TOOLS

We have solved the coupled equations numerically and further analysed our results using Mathematica software. ORIGIN software can be used to plot the observed results.

2.7. SOURCES OF DATA

Finally, the analytical & theoretical results are compared with experimental as well as simulations work to justify the present work.

CHAPTER-3

TERAHERTZ GENERATION BY BEATING OF OBLIQUELY INCIDENT LASERS

3.1. INTRODUCTION

Undoubtedly, the investigation of nonlinear phenomena in plasma has demonstrated as complicated as well as demanding area of research in the course of the last few decades. The contributions in the areas of formation of coherent structures, plasma science, cosmology, solar plasma and astrophysics not only advanced our prospective of plasma behaviour but also helped us in making more development in laser plasma based terahertz sources. The interaction of an intense laser beam with plasma offers various wide ranging prospective applications of THz in science and technology. These potential outcomes of utilizing THz radiation in environmental monitoring, security, communications technology, food and material sciences, THz imaging and spectroscopy, remote identification of explosive and dangerous chemicals, etc. are actively studied by various researchers [1-8]. The non ionizing THz radiation can be broadly used in biological and medical applications. Radiation reflected and transmitted through biological objects carries important information for analysis [6, 15]. The main aim of the researchers nowadays is to develop efficient and tuneable terahertz sources. Thus, the purpose of our first theoretical approach is to generate efficient THz radiation by the interaction of lasers with the rippled density hot collision less plasma. The nonlinear mixing of lasers plays an important role when the incident lasers travel at an angle normal to the plasma surface. When the intense laser beam interacts with plasma the plasma the electrons of plasma starts oscillating due to which nonlinearity is generated in the plasma; results a non linear ponderomotive force. This force exerts a nonlinear velocity to the plasma electrons. This velocity

beats with the density ripple to generate the current density; responsible for THz generation. The transverse intensity gradient of the electromagnetic wave contributes significantly to the plasma wave generation. The generated plasma wave interacts with the electromagnetic wave and leads to the generation of a radiation whose frequency lies in THz range. Furthermore, the density ripple of suitable wave number provides the phase matching which further helps in the efficiency enhancement. Here, we choose hot plasma for the propagation of electromagnetic wave because in the cold plasma only damped oscillations exist. The paper is organised as follows: the theoretical considerations of linear and nonlinear current density in this work are presented in Sec. 3.2. The THz radiation generation formalism is given in Sec. 3.3. Observations are discussed in the 3.4 section and the last section is devoted to the conclusion of present analysis.

3.2. PROPOSED MODEL

3.2.1. Generation of THz Radiation by p-Polarised Lasers Beating in Hot Plasma

Consider the propagation of two p-polarised laser beams, having two different frequencies (ω_1 and ω_2), in a hot plasma of electron temperature T_e having density ripple on its surface. The plasma density ripple can be produced by using various schemes involving machining beam, patterned mask and transmission ring grating. Where by adjusting the period and the mask size, and by changing groove structure, groove period and the duty cycle of such grating one can control the ripple parameters [34, 40]. It should be noted that the frequency of incident lasers should be much greater than the plasma frequency (ω_p) for efficient THz generation because in this limit ions are treated as stationary. These lasers are incident obliquely at an angle θ (angle of incidence) on the plasma surface (at $x=0$). The rippled density profile of plasma electrons can be written as,

$$n = n_0 + n_q, \quad (3.1)$$

where, n_0 is electron plasma density, $n_q (= n_q^0 e^{iqz})$ is the amplitude or periodicity of density ripple, $q = 2\pi / \lambda$, is the ripple wave vector in z-direction and λ is the wavelength of ripple (fig.3.1).

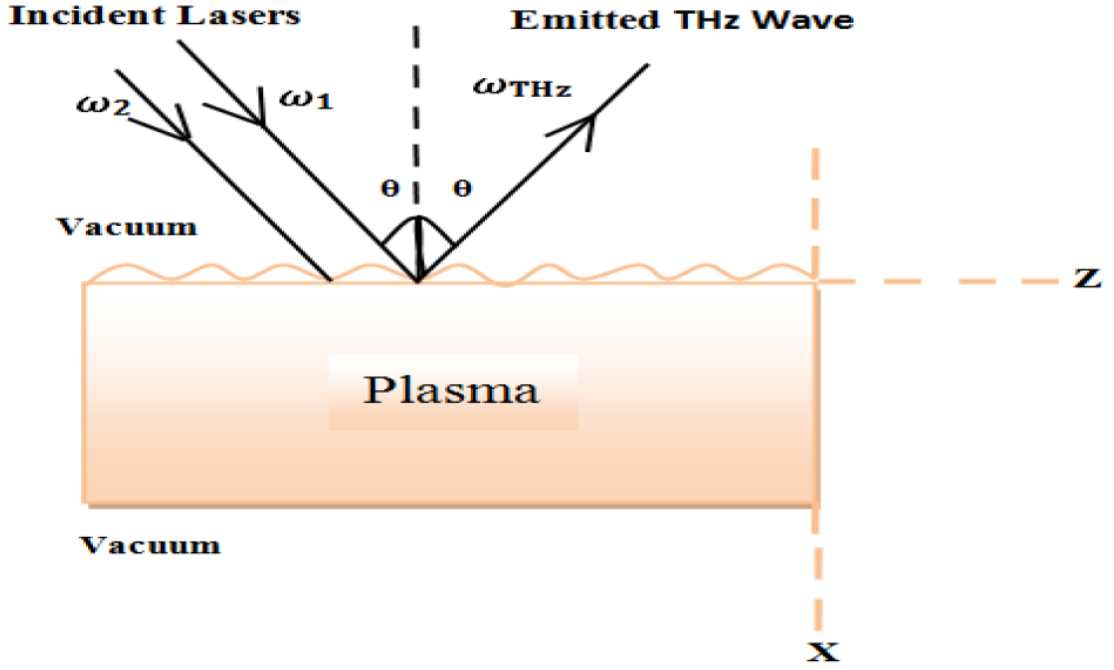


Fig.3.1. Schematic for THz wave generation in rippled density hot plasma

The electric and magnetic components associated with the laser field within the plasma are:

$$\left. \begin{aligned} \vec{E}_j &= (\hat{z} \cos \theta - \hat{x} \sin \theta) A_j e^{-i(\omega_j t - k_j(z \sin \theta + x \cos \theta))} \\ \vec{B}_j &= (\vec{k}_j \times \vec{E}_j) / \omega_j \end{aligned} \right\}, \quad (3.2)$$

where, $j = 1, 2$, $k_j = (\omega_j / c) \sqrt{1 - \omega_p^2 / \omega_j^2}$, $\omega_p^2 = 4\pi n_0 e^2 / m$. Under the influence of these fields, plasma electrons start oscillating. The oscillatory velocity of plasma electrons due to these fields is $\vec{v}_j = e\vec{E}_j / mi\omega_j$. Beating lasers couple nonlinearly at difference frequency $(\omega_1 - \omega_2)$ with wave vector $(\vec{k}_1 - \vec{k}_2)$, which exert a nonlinear ponderomotive force on plasma electrons given as, $\vec{F}_{p(\omega_1 - \omega_2)} = -\frac{1}{2} (e(\vec{v}_j \times \vec{B}_j^* - \vec{v}_j^* \times \vec{B}_j) + m(\vec{v}_j \cdot \nabla \vec{v}_j^*))$. On substituting the values of \vec{B}_j and \vec{v}_j in the above expression, the second part on the right hand side becomes zero. Hence, the ponderomotive force comes out

$$\vec{F}_{p(\omega_1 - \omega_2)} = \frac{e^2 (\vec{k}_1 - \vec{k}_2) \vec{E}_1 \cdot \vec{E}_2^*}{2mi\omega_1\omega_2}. \quad (3.3)$$

Where frequency $(\omega_1 - \omega_2)$ lies in the range of THz, e and m are the electronic charge and mass respectively and $*$ represents the complex conjugate. This nonlinear ponderomotive force disturbs the plasma neutrality as a result plasma electrons start oscillating in x-z plane inside the plasma to produce a nonlinear velocity. The nonlinear velocity due to this ponderomotive force can be written as,

$$\vec{v}_{(\omega_1 - \omega_2)}^{NL} = -\frac{\vec{F}_{p(\omega_1 - \omega_2)}}{mi(\omega_1 - \omega_2)} = \frac{e^2}{2m^2\omega_1\omega_2} \frac{\vec{k}_1 - \vec{k}_2}{(\omega_1 - \omega_2)} \vec{E}_1 \cdot \vec{E}_2^*. \quad (3.4)$$

The divergence of this velocity is finite, i.e., $\vec{\nabla} \cdot \vec{v}_{\omega_1 - \omega_2}^{NL} \neq 0$, hence, it gives rise to nonlinear density perturbation $n_{\omega_1 - \omega_2}^{NL}$ at $(\omega_1 - \omega_2)$ and $(\vec{k}_1 - \vec{k}_2)$. By solving the equation of continuity, $\partial n_{\omega_1 - \omega_2}^{NL} / \partial t + \vec{\nabla} \cdot (n_0 \vec{v}_{\omega_1 - \omega_2}^{NL}) = 0$, we obtain,

$$n_{\omega_1 - \omega_2}^{NL} = \frac{n_0(k_1 - k_2)(\hat{z} \sin \theta + \hat{x} \cos \theta) \cdot \vec{v}_{\omega_1 - \omega_2}^{NL}}{(\omega_1 - \omega_2)} = \frac{\omega_p^2}{(\omega_1 - \omega_2)^2} \frac{(k_1 - k_2)^2}{8\pi m \omega_1 \omega_2} \vec{E}_1 \cdot \vec{E}_2^*. \quad (3.5)$$

This density perturbation produces a self-consistent space charge field $\vec{E}_s = -\vec{\nabla} \phi_s$ which also causes a density perturbation as, $n_{\omega_1 - \omega_2}^L = (k_1 - k_2)^2 \chi_e \phi_s / 4\pi e$. Here, $\chi_e = -\omega_p^2 / (\omega_1 - \omega_2)^2$ is the free electron plasma susceptibility. Now using the Poisson's equation, $\nabla^2 \phi_s = 4\pi e (n_{\omega_1 - \omega_2}^L + n_{\omega_1 - \omega_2}^{NL})$, we obtain the self-consistent space charge potential,

$$\phi_s = -\frac{e\omega_p^2 (\vec{E}_1 \cdot \vec{E}_2^*)}{2m\omega_1\omega_2 ((\omega_1 - \omega_2)^2 - \omega_p^2)}. \quad (3.6)$$

Hence, the net electron velocity due to the ponderomotive force and the self-consistent field is written as,

$$\vec{v}_{\omega_1 - \omega_2} = \vec{v}_{\omega_1 - \omega_2}^{NL} + \frac{e\vec{E}_s}{mi(\omega_1 - \omega_2)} = \frac{e^2(\hat{x}k_x + \hat{z}k_z)}{2m^2\omega_1\omega_2} \frac{(\omega_1 - \omega_2)}{((\omega_1 - \omega_2)^2 - \omega_p^2)} \vec{E}_1 \cdot \vec{E}_2^*, \quad (3.7)$$

where $\vec{\nabla} = i(k_1 - k_2)(\hat{z} \sin\theta + \hat{x} \cos\theta)$. The net velocity $\vec{v}_{\omega_1 - \omega_2}$ is large, when $(\omega_1 - \omega_2)$ is near to ω_p . Velocity $\vec{v}_{\omega_1 - \omega_2}$ and density ripple beats together to generate a nonlinear current-density at $(\omega_1 - \omega_2, \vec{k}$; here $\vec{k} = \vec{k}_1 - \vec{k}_2 + \vec{q}$, which is responsible for the generation of terahertz radiation. The nonlinear current density in $x - z$ plane is as follows,

$$\vec{J}_{(\omega_1 - \omega_2)}^{NL} = -\frac{e}{2} n_q \vec{v}_{\omega_1 - \omega_2} = -\frac{e^3 n_q^0 e^{iqz} (\omega_1 - \omega_2)}{4m^2 \omega_1 \omega_2} \frac{(\hat{x}k_x + \hat{z}k_z)}{((\omega_1 - \omega_2)^2 - \omega_p^2)} (\vec{E}_1 \cdot \vec{E}_2^*). \quad (3.8)$$

If one includes collisions, $((\omega_1 - \omega_2)^2 - \omega_p^2)$ in equation (3.8) is replaced by $[(\omega_1 - \omega_2)(\omega_1 - \omega_2 + i\nu) - \omega_p^2]$, where ν is the frequency of electron collision. Since it does not much alter our result so here we are not taking it into consideration. This nonlinear current density would excite p-polarised T-wave and couples to a wave associated with space-charge field. Suppose this composite wave has a self-consistent electric field as:

$$\vec{E}_{(\omega_1 - \omega_2)} = \vec{A}(x) e^{-i[(\omega_1 - \omega_2)t - k_z z]}. \quad (3.9)$$

where, $k_z = k_{1z} - k_{2z}$. The plasma electrons start oscillating under the influence of this self-consistent field. The drift velocity of plasma electrons at THz wave frequency ($\omega_{THz} = \omega_1 - \omega_2$) due to this self-consistent field can be derived by solving equation of motion and Poisson's equations simultaneously as;

$$\vec{v}_{\omega_1 - \omega_2}^L = \frac{e\vec{E}_{(\omega_1 - \omega_2)}}{mi(\omega_1 - \omega_2)} - \frac{v_{th}^2 \epsilon_0}{n_0 ie(\omega_1 - \omega_2)} \vec{\nabla} (\vec{\nabla} \cdot \vec{E}_{(\omega_1 - \omega_2)}), \quad (3.10)$$

where, $v_{th} = (T_e / m)^{1/2}$ is the thermal velocity of electron. Here, $v_{th} \ll \omega_{THz} / k$, so we ignore the kinetic effect. The linear current density due to oscillatory motion of plasma electrons is,

$$\vec{J}_{(\omega_1-\omega_2)}^L = -n_0 e \vec{v}_{(\omega_1-\omega_2)}^L = -\frac{n_0 e^2 \vec{E}_{(\omega_1-\omega_2)}}{m i (\omega_1 - \omega_2)} + \frac{v_{th}^2 \epsilon_0}{i (\omega_1 - \omega_2)} \vec{\nabla} \left(\vec{\nabla} \cdot \vec{E}_{(\omega_1-\omega_2)} \right). \quad (3.11)$$

The wave equation for THz generation, using Maxwell's equations can be written as:

$$\nabla^2 \vec{E} - \vec{\nabla} (\vec{\nabla} \cdot \vec{E}) \left(1 - \frac{v_{th}^2}{c^2} \right) + \frac{1}{c^2} \left((\omega_1 - \omega_2)^2 - \omega_p^2 \right) \vec{E} = -\frac{i(\omega_1 - \omega_2)}{c^2 \epsilon_0} \vec{J}_{\omega_1-\omega_2}^{NL}. \quad (3.12)$$

This equation provides two well defined solutions in the absence of nonlinear sources: first with $\vec{\nabla} \cdot \vec{E} = 0$, is an electromagnetic wave and the second with $\vec{\nabla} \times \vec{E} = 0$, is a Langmuir wave, with corresponding dispersion relations $k_{mx} = \left((\omega_1 - \omega_2)^2 - \omega_p^2 - k_z^2 c^2 \right)^{1/2} / c$ and $k_{sx} = \left((\omega_1 - \omega_2)^2 - \omega_p^2 - k_z^2 v_{th}^2 \right)^{1/2} / v_{th}$, are given in equation (3.13) and (3.14) respectively:

$$\vec{E}_m = A_m \left(\hat{x} - \frac{k_{mx}}{k_z} \hat{z} \right) e^{i k_{mx} x} e^{-i [(\omega_1 - \omega_2) t - k_z z]}, \quad (3.13)$$

$$\vec{E}_s = A_s \left(\hat{x} + \frac{k_z}{k_{sx}} \hat{z} \right) e^{i k_{sx} x} e^{-i [(\omega_1 - \omega_2) t - k_z z]}. \quad (3.14)$$

The isothermal approximation is inferred for the electron response in this deduction. One can have it valid in the adiabatic approximation by suitably multiplying the electron temperature by the ratio of specific heat at constant pressure and volume. In the presence of nonlinear source, a particular solution obtained from the wave equation (3.12) by putting $\vec{\nabla} \times \vec{E} = 0$:

$$\vec{E}_p = -\frac{i(\omega_1 - \omega_2)}{\epsilon_0 [(\omega_1 - \omega_2)^2 - \omega_p^2 - k^2 v_{th}^2]} \vec{J}_{\omega_1-\omega_2}^{NL}. \quad (3.15)$$

Here, we have $\vec{\nabla} \times \vec{E}_p = 0$ and $\vec{\nabla} \times \vec{E}_s = 0$, therefore, no magnetic field is associated with both these components. Hence, the only electromagnetic wave field \vec{E}_m is responsible for the associated magnetic field \vec{H}_m . Therefore,

$$\vec{H}_m = \frac{\vec{k}_m \times \vec{E}_m}{\mu_0(\omega_1 - \omega_2)} = \hat{y} A_m \frac{k_{mx}^2 + k_z^2}{\mu_0 k_z (\omega_1 - \omega_2)} e^{ik_{mx}x} e^{-i[(\omega_1 - \omega_2)t - k_z z]}. \quad (3.16)$$

Only outgoing part of electromagnetic wave exists for $x < 0$ (in vacuum region), so that

$$\begin{aligned} \vec{E}_r &= A_r \left(\hat{x} + \frac{k_x}{k_z} \hat{z} \right) e^{-ik_x x} e^{-i[(\omega_1 - \omega_2)t - k_z z]}, \\ \vec{H}_r &= \hat{y} A_r \frac{k_x^2 + k_z^2}{\mu_0 k_z (\omega_1 - \omega_2)} e^{-ik_x x} e^{-i[(\omega_1 - \omega_2)t - k_z z]}. \end{aligned} \quad (3.17)$$

At $x=0$, three boundary conditions can be obtained. For first and second boundary conditions E_z and H_y must be continuous at $x=0$, therefore, the first boundary condition ($E_{mz} + E_{sz} + E_{pz} = E_{rz}$) and the second boundary condition ($H_{my} = H_{ry}$), simultaneously give:

$$A_s \frac{k_z^2}{k_{sx}} = A_r k_x + A_m k_{mx} + \frac{i(\omega_1 - \omega_2) k_z J_{z(\omega_1 - \omega_2)}^{NL}}{\epsilon_0 [(\omega_1 - \omega_2)^2 - \omega_p^2 - k^2 v_{th}^2]}. \quad (3.18)$$

$$A_m = A_r \frac{k_x^2 + k_z^2}{k_{mx}^2 + k_z^2}. \quad (3.19)$$

Now taking the z-component of wave equation (3.12) and integrating it over x between the limits 0^- to 0^+ , to deduce the third boundary condition as;

$$A_r (k_x^2 + k_z^2)^2 = A_m [k_{mx}^2 + k_z^2] - \frac{v_{th}^2}{c^2} (A_m k_z^2 + A_s k_z^2) + \frac{i(\omega_1 - \omega_2) k_x k_z J_{z(\omega_1 - \omega_2)}^{NL} v_{th}^2 / c^2}{\epsilon_0 [(\omega_1 - \omega_2)^2 - \omega_p^2 - k^2 v_{th}^2]}. \quad (3.20)$$

By solving equation (3.18), (3.19) and (3.20) we get;

$$A_{THz} = \frac{i}{\epsilon_0} \frac{k_x k_z (1 + k_{sx} / k_x)}{(k_x k_{sx} + k_z^2 + k_{mx} k_{sx})} \frac{(\omega_1 - \omega_2) J_{z(\omega_1 - \omega_2)}^{NL}}{[(\omega_1 - \omega_2)^2 - \omega_p^2 - k^2 v_{th}^2]}. \quad (3.21)$$

This is the expression for amplitude of the reflected terahertz wave (here A_r is replaced by A_{THz}).

3.3. ANALYSIS & OBSERVATIONS

Equation (3.21) is solved numerically for a set of suitable laser and plasma parameters. The values of the chosen parameters for computation are as follows: the normalised laser intensities, $a_1 = eA_0 / m\omega_1 c = 0.22$, $a_2 = eA_0 / m\omega_2 c = 0.24$ (A_0 is the amplitude of incident laser beam corresponding to laser intensity, $I \sim 7 \times 10^{14} \text{W/cm}^2$), two different wavelengths, $\lambda_1 = 9.57 \mu\text{m}$, $\lambda_2 = 10.57 \mu\text{m}$ (for CO_2 laser), $\omega_1 = 1.973 \times 10^{14}$, $\omega_2 = 1.783 \times 10^{14}$, electron thermal velocity $v_{th} = 0.03c$ and $0.1c - 0.18c$ corresponding to electron temperature $T_e = 0.5 \text{keV}, 5 \text{keV}$ ($0.2c$ corresponds to 20keV) for $\theta = 15^\circ - 55^\circ$.

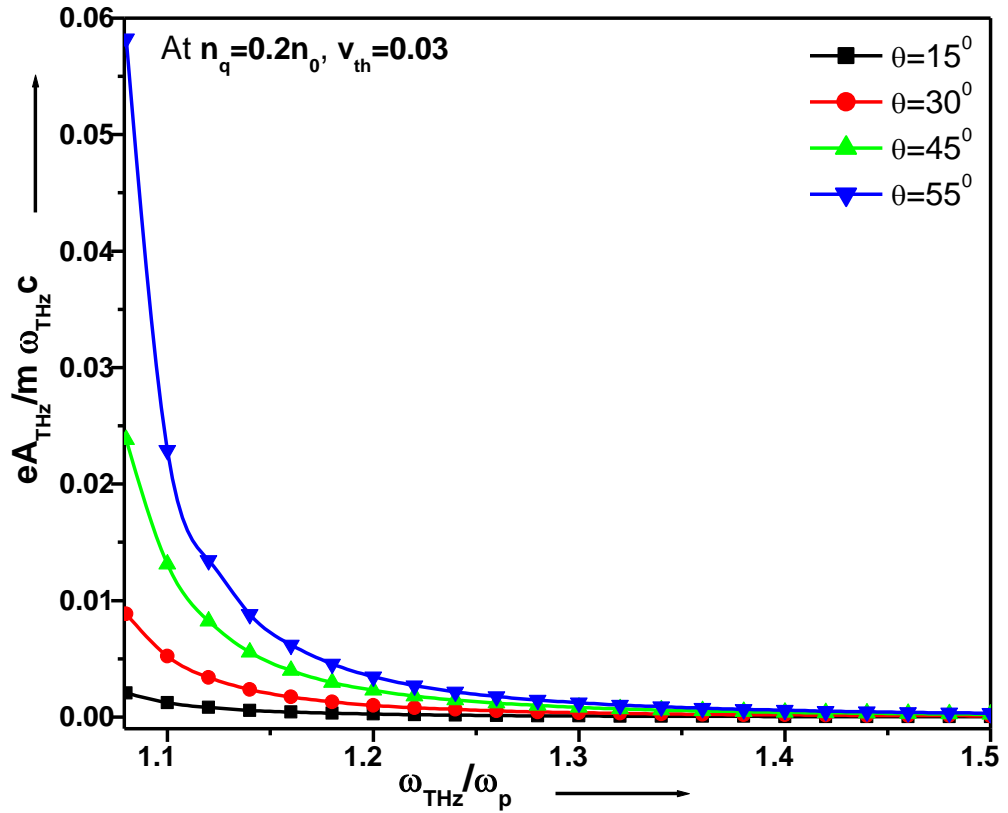


Fig.3.2. Variation of normalised terahertz amplitude ($eA_{\text{THz}} / m\omega_{\text{THz}}c$) with normalised THz frequency ($\omega_{\text{THz}} / \omega_p$) for different values of θ at $T_e = 0.5 \text{keV}$, $\omega_1 = 1.973 \times 10^{14}$, $\omega_2 = 1.783 \times 10^{14}$ and $n_q = 0.2n_0$.

In fig.3.2, we have plotted normalised THz amplitude $eA_{THz}/m\omega c$ with normalised THz frequency ω_{THz}/ω_p (where $\omega_{THz} = \omega_1 - \omega_2$) of THz wave for different values of incidence angle θ . It can be observed from this figure that the amplitude decreases with increasing THz frequency. This amplitude is maximum when ω_{THz} is comparable with ω_p (due to resonance). It also observed that with increasing the value of θ from $15^\circ - 55^\circ$ the normalised amplitude increases from 0.002–0.058 at $n_q = 0.2n_0$. We obtained the highest values at $n_q = 0.3n_0$ but it is difficult to create 30% ripple experimentally so we plotted our results corresponds to 20% density ripple.

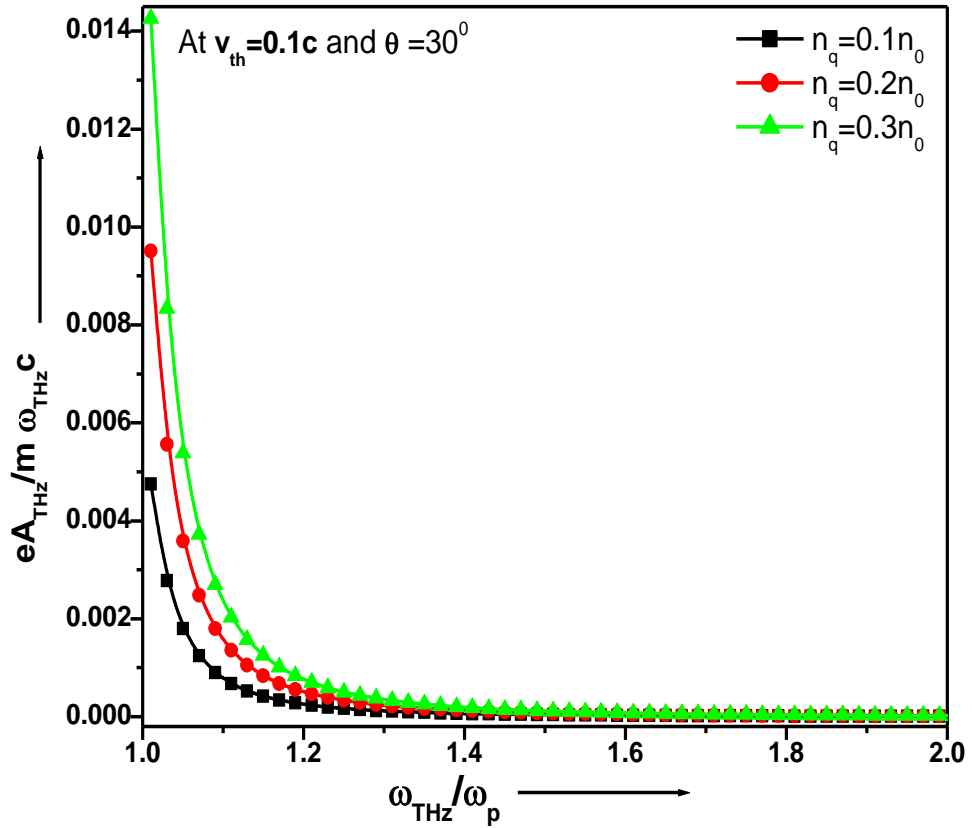


Fig.3.3. Variation of normalised THz amplitude with normalised THz frequency for different values of density ripple, at constant angle of incidence $\theta = 30^\circ$ at $T_e = 5\text{keV}$ Frequency of incidence laser beams are same as that of fig.3.2.

The variation of normalised THz amplitude is plotted with the increasing value of THz normalised frequency for different values of density ripple ($n_q = 0.1n_0, 0.2n_0, 0.3n_0$) shown in Fig.3.3, at $\theta = 30^\circ$. The ripple helps THz generation in following two ways: first it makes the nonlinear current irrotational, and second by providing the phase matching (when ripple wave vector \vec{q} equals $\vec{k}_{THz} - \vec{k}_1 + \vec{k}_2$, where \vec{k}_1 and \vec{k}_2 are the laser wave vector and \vec{k}_{THz} is THz wave vector). So, it is clear from this graph that the maximum momentum is transfer to the electrons at resonance condition. On the other hand, the effect of amplitude of density ripple n_q is to enhance the THz wave field. Since, higher the amplitude of density ripple, more the number of electrons take part in the excitation of radiation. Fig. 3.3, also infers that frequency distribution of reflected THz wave is closely related to the incidence angle and coupling. Therefore, it could play an important role in the generation of THz wave of higher intensity.

For fig.3.4, we calculate the normalised amplitude for different intensity range and finally plotted the graph between normalised amplitude of emitted terahertz wave and amplitude of incident laser (A_0) at $\theta = 30^\circ$, $n_q = 0.3n_0, 0.2n_0, 0.1n_0$, and $\omega_{THz} / \omega_p = 1.08$. For fig.3.4, we calculate the normalised amplitude for different intensity range and finally plotted the graph between normalised amplitude of emitted terahertz wave and amplitude of incident laser (A_0) at $\theta = 30^\circ$, $n_q = 0.3n_0, 0.2n_0, 0.1n_0$, and $\omega_{THz} / \omega_p = 1.08$. This exhibits a variation, which displays the linear relationship of THz amplitude with the intensity of incident lasers. The physical reason is that, with the enhancement of the laser intensity, the strength of ponderomotive force and hence the initial ionization of the plasma increases. Thus with the increase of free electron density, the nonlinearity increases. As THz generation is a nonlinear phenomenon, it enhances more and more. The highest value of the normalised amplitude corresponding to incident laser beam intensity $\sim 7 \times 10^{14} W / cm^2$ achieved is 0.038 in our scheme. We neglect the effect of collisions in our analysis.

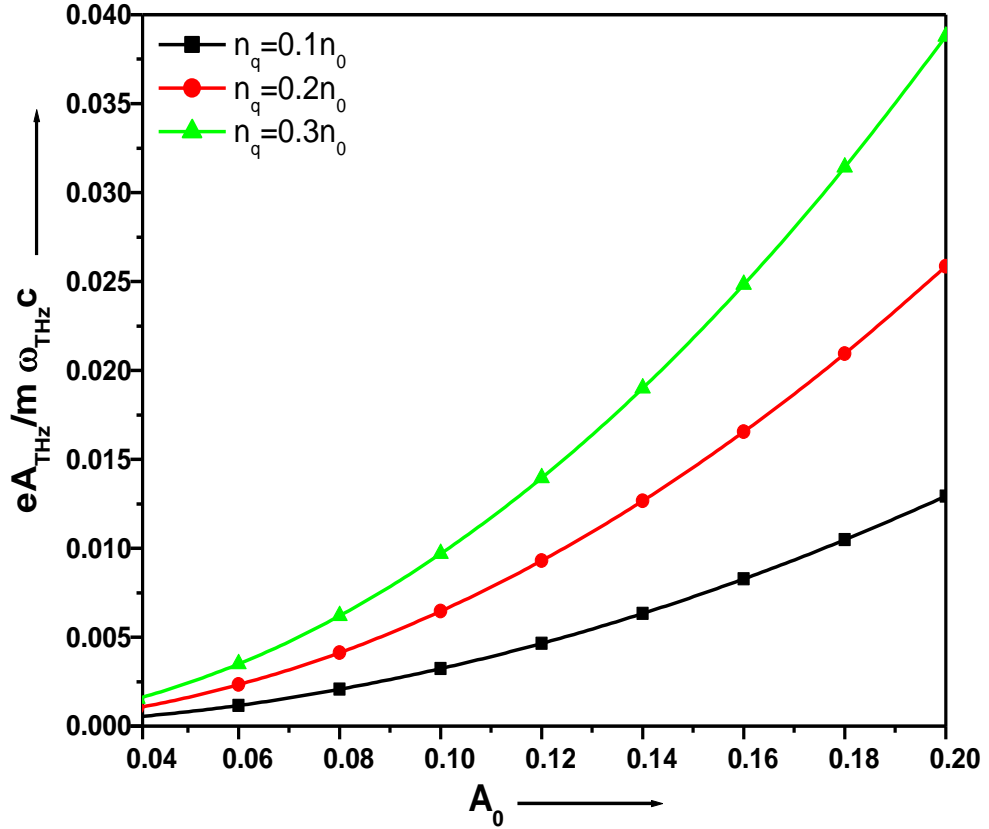


Fig.3.4. Spectrum of the normalised amplitude of emitted THz wave versus normalised amplitude of incident laser beams at $v_{th}=0.1c$ corresponding to $T_e = 5\text{keV}$, $\omega_{THz} / \omega_p = 1.08$, $n_q = 0.3n_0$ and $\theta = 30^\circ$. All other parameters are same as that of fig.3.2.

It can be seen [37] that in the presence of collisions, the term ω^2 is replaced by $\omega(\omega + i\nu)$ in equation (7). Since the imaginary term leads to resistivity and extracts energy from the electrons in collisions, consequently the efficiency decreases.

Fig.3.5 shows the variation of normalized amplitude of the THz wave with normalized velocity for different values of ripple density $n_q = 0.1, 0.2$ and 0.3 at $\theta = 30^\circ$, together with numerical calculations. It is clear from Fig.3.5 that initially at $n_q = 0.1n_0$, the THz wave of small amplitude is generated, it starts increasing up to 0.16 , as ripple increases to 30% , similar results were observed by Kumar *et al.* [42]. We observe that the normalised THz amplitude peaks at around 0.016 at thermal velocity

$\sim 0.19c$ corresponding to electron temperature $\sim 20\text{keV}$. It is very high electron temperature, so in our analysis the thermal velocity is valid up to $0.19c$ beyond which it will not be valid.

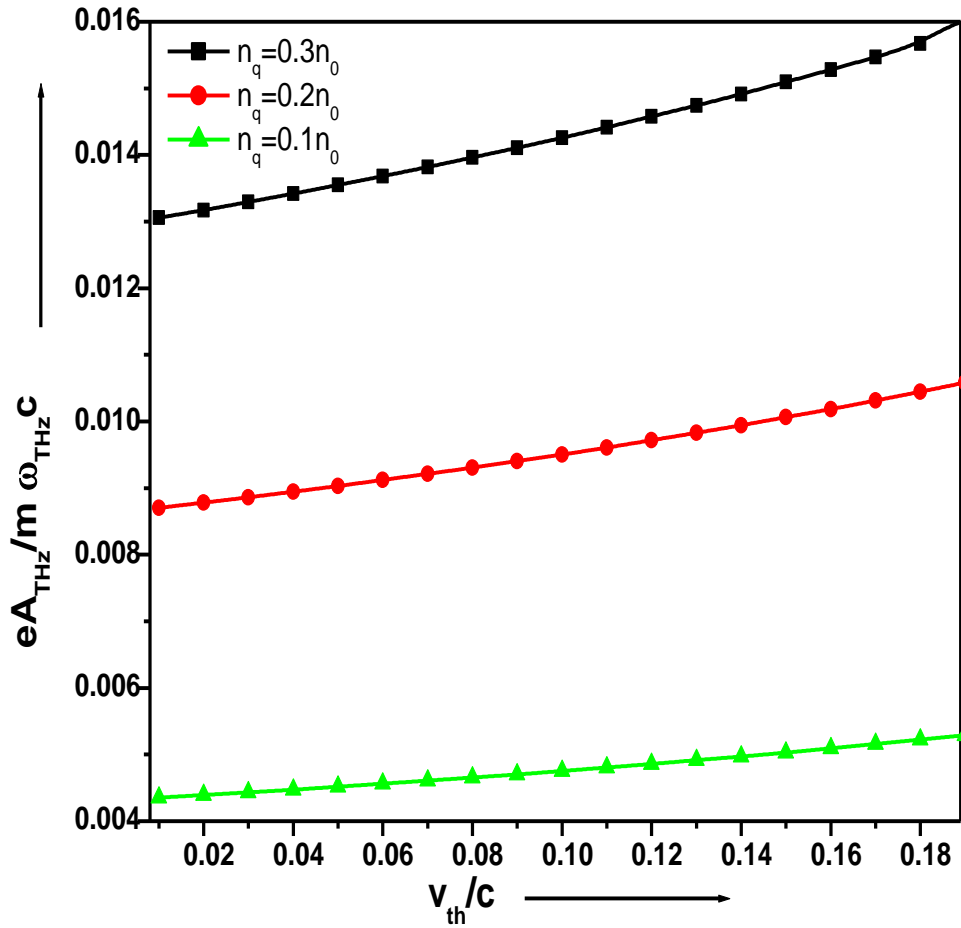


Fig.3.5. Variation of normalised amplitude of terahertz yield ($eA_{THz}/m\omega_{THz}c$) with normalised velocity (v_{th}/c) for different values of density ripple at $\theta = 30^\circ$ and $\omega_n = 1.08$.

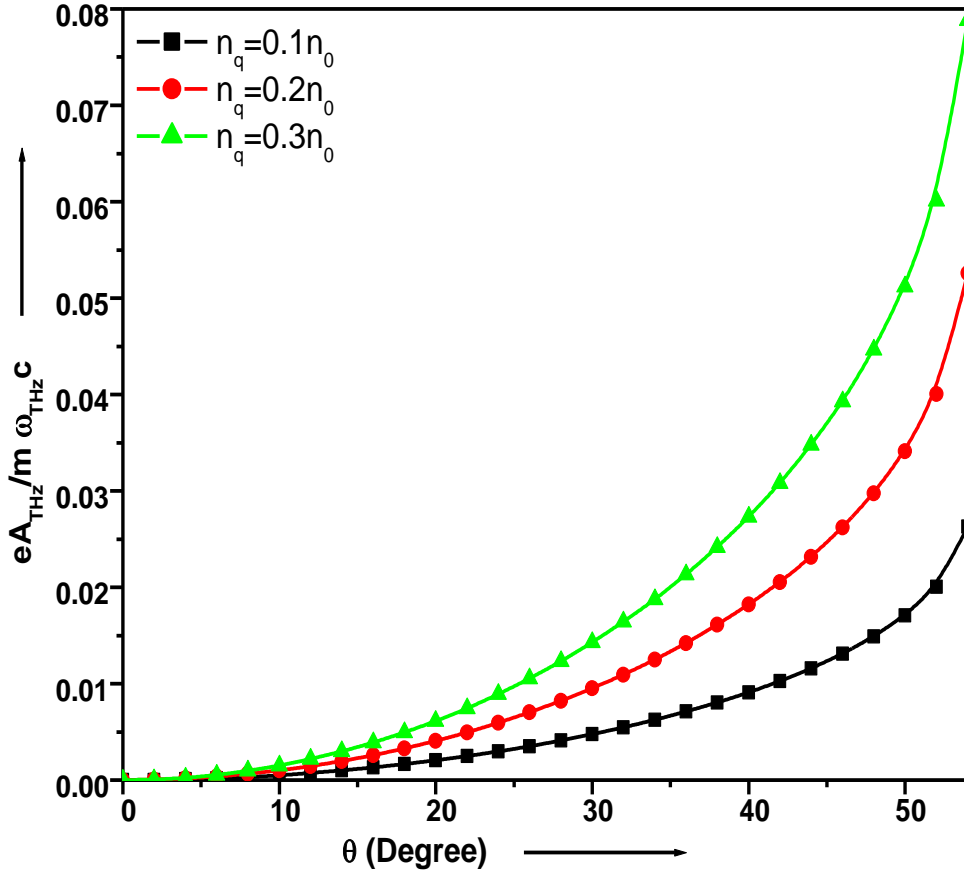


Fig.3.6. Variation of normalised terahertz amplitude ($eA_{THz} / m\omega_{THz}c$) with the specular angle θ for different values of density ripple at $\omega_n = 1.08$

Fig.3.6 shows the variation of normalised amplitude of THz wave with the specular angle at different values of ripple density. The THz wave amplitude increases linearly with density ripple and specular angle from 0 to 55° and shows a maximum at 55° .

3.4 CONCLUSION

The generation of THz radiation via nonlinear mixing of two laser pulses in hot plasma is a fetching alternative. We have mathematically investigated the laser beat wave excitation of the terahertz radiation in hot collision less plasma with density ripple on its surface. In the presence of a Gaussian laser beam, the plasma gets depleted from the high field region to the low field region on account of the ponderomotive force. From the above analysis it can be concluded that, the efficiency

and the amplitude of reflected THz field are sensitive not only to the density ripple but to the angle of incidence and the frequency of beating lasers. It increases with the plasma density and angle of incidence θ . Frequency of the emission of the resonant signal is tunable with the ripple density amplitude [67]. Here, we ignored the kinetic damping which is justified when $v_{th} \ll \omega_{THz} / k_{THz}$. We have also not considered the Landau damping of the electrostatic part of the ω_{THz} frequency wave associated with the electromagnetic THz wave. For the THz frequency substantially greater than the maximum plasma frequency ($\omega_{THz} - \omega_p$) greater than the Landau damping rate), this effect may not alter the results significantly. Also we have neglected the effect of beam size, so the terahertz emission occurs if and only if $\theta \neq 0$. On the other hand, at $\theta = 0$ the nonlinear current density has no transverse component as a result electromagnetic radiation does not take place [68,69]. Therefore, the laser spot size must be bigger than the THz wavelength is the necessary condition for the validation of present scheme. On account of nonlinear coupling between the electromagnetic wave and plasma wave, the power associated with the plasma wave and generated THz yield are also accordingly modified. Wu *et al.* [70] examined a strong THz emission from the non-uniform plasma slab in contrast to the uniform one, and the numerically evaluated conversion efficiency is fairly good agreement with their PIC simulation results. This shows a great plausibility of developing a tunable THz source having power to use in medical applications.

CHAPTER-4

EFFECT OF FREQUENCY CHIRP ON GENERATED THz WAVE IN PLASMA

4.1. INTRODUCTION

THz radiation generation has currently captured huge interest in the present era due to its diverse and vast applications in various fields; few of them are THz spectroscopy and THz imaging, medical imaging, environmental monitoring, remote identification of explosive and dangerous chemicals and food and material technology etc [1-8]. In order to produce an efficient THz radiation for communications and other applications, the diffraction angle in the propagation channel must be minimized so as to avoid the frequency shift from THz range. This study becomes crucial in case of broadband-based THz applications [23-25], as here a wide range of different wavelengths persists. To understand the theory behind the origin of terahertz (THz) field caused by beating of two lasers in a nonlinear medium (plasma for present scheme) we provide two analytical models here.

In this chapter, we develop an analytical formalism for terahertz generation from chirped lasers beating in the rippled density plasma. The density ripple is applied on the chirped laser pulses in order to adjust and control the yield of the THz wave. The density ripple plays a vital role in establishing the phase-matching condition. The resonance condition results a resonant excitation of THz radiation [34, 57]. The THz amplitude enhances considerably in the presence of density ripple. Further, in the second model we studied the influence of frequency chirp on the generated terahertz (THz) wave due to interaction between intense laser pulses and under dense plasma in the presence of transverse magnetic field. For achieving a significant enhancement in THz efficiency and field strength, the frequency chirped laser and magnetic field parameters are optimized. The external magnetic field also plays a crucial role in

enhancing the efficiency of THz wave. Tuneable and coherent THz radiation through electrostatic to electromagnetic field conversion due to an ionization front can be produced in a uniform electrostatic field. The application of frequency chirp extends the laser-plasma interaction time and thus facilitates the resonance condition for longer duration, which can be useful in the broadband THz radiation generation.

Recently, Hamazaki *et al.* [23] have experimentally investigated the impact of the frequency chirp of the laser pump pulse in broadband terahertz (THz) pulse generation by optical rectification (OR) in Gallium Phosphate (GaP) by measuring the TDS (Time Domain Spectroscopy) signals. They also reported the significance of accurate control over the frequency chirp of the laser pulse for producing the broadband THz pulses by optical rectification. The chapter is organised as follows: Section 4.2 & 4.3 formulates the problem for THz wave excitation due to frequency chirped laser with the expressions of ponderomotive force and nonlinear current density in rippled density & magneto-plasma respectively. A brief discussion & observations are given in the sub-sections of 4.2 & 4.3. Finally the conclusion is presented in section 4.4.

4.2. PROPOSED MODEL FOR RIPPLE DENSITY PLASMA

4.2.1. THz Generation by Beating of Two Chirped Pulse Lasers in Spatially Periodic Density Plasma

The mechanism of THz generation is as follows: we consider two Gaussian lasers with electric fields $\vec{E}_1(\vec{k}_1, \omega_1)$ and $\vec{E}_2(\vec{k}_2, \omega_2)$, polarized along \hat{y} , propagating in \hat{z} direction (fig.4.2.1). The lasers have a linear frequency chirp and the frequency $\omega_1 = \omega_0(1 + b\omega_0(t - z/c))$ and $\omega_2 = \omega_0(1 + b\omega_0(t - z/c) - \omega_r/\omega_0)$ can be chosen as the difference $(\omega_1 - \omega_2 = \omega_r)$ lies in THz range. The theory of generation of THz radiation due to the beating of two chirped laser pulses in plasma is explained and the analytical calculations are presented below. We consider plasma of electron density n_0 . The electric field profile of laser pulses (with two slightly different frequencies ω_1 and ω_2) is considered as; $\vec{E}_j = \hat{y}A_j e^{i(k_j z - \omega_j t)}$, here, $j = 1, 2$.

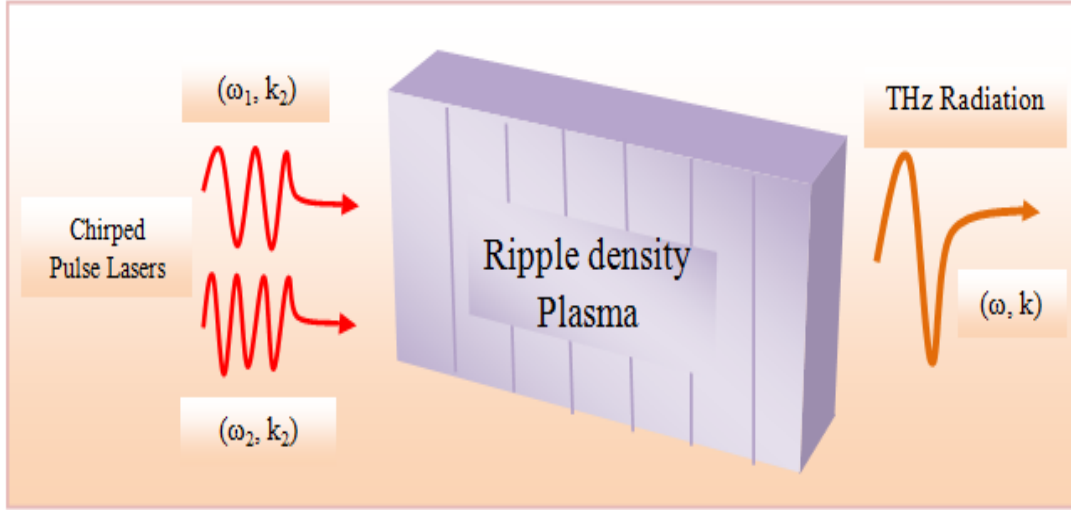


Fig.4.2.1. Schematic of THz generation via frequency chirped laser pulses in rippled density plasma

The laser imparts oscillatory velocity to the plasma electrons: $\vec{v}_j = e\vec{E}_j / mi\omega_0\alpha_j$, where, $\alpha_1 = 1 + b\omega_0(2t - z/c)$ and $\alpha_2 = \alpha_1 - ((\omega_1 - \omega_2) / \omega_0)$. A nonlinear ponderomotive force exerted due to the variation of amplitude of the laser's field beating at $(\omega_1 - \omega_2)$ written as:

$$\vec{F}_p = \hat{z}e^2 \frac{\alpha_1\beta_1 + \beta_2}{2mi\omega_0c\alpha_1\alpha_2} (\vec{E}_1 \cdot \vec{E}_2^*), \quad (4.2.1)$$

where, $\beta_1 = [ck_1 / \omega_1 - ck_2 / \omega_2 - 2ib / \alpha_1\alpha_2]$,

$\beta_2 = (\omega_1 - \omega_2) / \omega_0 [c(k_1 - k_2) / (\omega_1 - \omega_2) + ck_2 / \omega_2 + ib / \alpha_1\alpha_2]$ and e , m , c and $*$ represent the electronic charge, mass, speed of light in vacuum and complex conjugate respectively.

Here it is clear that the variables $\alpha_1, \alpha_2, \beta_1$ and β_2 are the function of chirp parameter b . Due to the nonlinear motion of plasma electrons a linear (n_ω^l) and

nonlinear (n_ω^{nl}) density perturbation is also observed which can be calculated by

solving the equation of motion such as: $n_\omega^{nl} = n_0(k_1 - k_2)F_p / m(\omega_1 - \omega_2)^2$ and

$n_\omega^l = (k_1 - k_2)^2 \chi_e \phi_s / 4\pi e$, where, $\chi_e = -\omega_p^2 / (\omega_1 - \omega_2)^2$ is the free electron plasma

susceptibility. The refractive index (μ) of a material is related to the susceptibility by

the relation; $\chi_e = \mu^2 - 1$; and for plasma medium in present case;

$\mu = \varepsilon^{1/2} = (1 - \omega_p^2 / \omega_T^2)^{1/2}$, here, ε is the permittivity of the medium and we choose $\omega_1, \omega_2 \gg \omega_p$ where, $\omega_p = (4\pi n_0 e^2 / m)^{1/2}$ is the plasma frequency. Now by employing Poisson's equation, $\nabla^2 \phi = 4\pi e(n_\omega^{nl} + n_\omega^l)$, the electrostatic potential ϕ , of this self-consistent space charge field can be written as: $\phi = -4\pi e n_\omega^{nl} / (1 + \chi_e)(k_1 - k_2)^2$. Thus, the nonlinear velocity under the influence of the ponderomotive force along with self consistent field is;

$$\vec{v}_\omega^{nl} = -\frac{\vec{F}_p + e\vec{\nabla}\phi}{mi(\omega_1 - \omega_2)} = -\frac{\vec{F}_p}{mi(\omega_1 - \omega_2)} \left(1 - \frac{i\omega_p^2}{(\omega_1 - \omega_2)^2 - \omega_p^2} \right). \quad (4.2.2)$$

Here, we introduce a density perturbation $n = n_0 + n_q e^{iqz}$ where, n_q represents the ripple amplitude and \bar{q} is density ripple wave number. This nonlinear velocity beats with the density ripple to drive a nonlinear current density in the transverse direction:

$$\vec{J}_\omega^{NL} = -\frac{e}{2} n_q \vec{v}_\omega^{nl} = -\hat{z} \frac{e\omega_p^2 n_q (\vec{E}_1 \cdot \vec{E}_2^*) (\alpha_1 \beta_1 + \beta_2) ((\omega_1 - \omega_2)^2 - \omega_p^2 (1+i))}{16\pi n_0 \omega_0 m c \alpha_1 \alpha_2 (\omega_1 - \omega_2) ((\omega_1 - \omega_2)^2 - \omega_p^2)}. \quad (4.2.3)$$

This non-linear current further couple to the wave associated to the self consistent space charge field and drives a THz wave. Now employing Maxwell's III and IV equations, we have derived the wave equation depending on the non-linear current density term. This wave equation can be given as:

$$\nabla^2 \vec{E}_\omega - \vec{\nabla}(\vec{\nabla} \cdot \vec{E}) - \frac{\omega_T^2}{c^2} \left(1 - \frac{\omega_p^2}{\omega_T^2} \right) \vec{E}_\omega = -\frac{4\pi i \omega_T}{c^2} \vec{J}_\omega^{NL}. \quad (4.2.4)$$

The exact phase matching condition and resonant excitation of THz generation can be achieved by introducing the suitable value of density ripple wave number \bar{q} . Hence $\vec{k}_T = \vec{k}_1 - \vec{k}_2 + \vec{q}$, and $k_T^2 - \omega_T^2 \varepsilon / c^2 = 0$, where \vec{k}_T is the THz wave vector and $q \approx \omega / c (\sqrt{\varepsilon} - 1)$. The electric field of THz varies as, $\vec{E}_\omega = \hat{y} A_\omega(z, t) e^{-i(\omega_T t - k_T z)}$. By assuming the fast variation of the THz field in order to neglect the higher order derivatives and using the phase matching condition, the z-component of above equation gives the

required THz field, $\partial E_{\omega_z} / \partial z = 2\pi\omega J_{\omega_z}^{NL} / c^2 k$. Now by putting the value of nonlinear current from Eq. (4.2.3), we obtain the final equation for the field of THz radiation:

$$\frac{\partial}{\partial z} \left(\frac{E_{\omega_z}}{E_1} \right) = - \frac{en_{q0} \omega_p^2 E_2^* (\alpha_1 \beta_1 + \beta_2) (\omega_T^2 - \omega_p^2 (1+i))}{8n_0 m \omega_0 c^3 k_T (\omega_T^2 - \omega_p^2)}, \quad (4.2.5)$$

where, E_{ω_z} / E_1 is the normalised field of THz wave. The efficiency of generated THz radiation is the ratio of the energy per unit area of the THz wave to the energy per unit area of the pump lasers, i.e., $\eta = W_{THz} / W_{pump}$, where the average electromagnetic energy stored per unit volume is given by the formula;

$$W_{Ei} = \frac{\epsilon}{8\pi} \frac{\partial}{\partial \omega_i} \left[\omega_i \left(1 - \frac{\omega_p^2}{\omega_i^2} \right) \right] \langle |E_i|^2 \rangle. \quad (4.2.6)$$

Thus using Eq. (4.2.6), one can obtain the efficiency of generated THz radiation. The features of THz electric field's amplitude have been studied by solving Eq. (4.2.5) for an optimised set of laser and plasma parameters.

4.2.2. ANALYSIS & OBSERVATIONS

The proper matching of the ripple wave number with the beat wave number provides the maximum transfer of energy and momentum under the resonance condition. In the present scheme, we consider a non-relativistic regime to see the combined effect of chirp characteristics and density ripple on the THz emission due to frequency chirped pulse lasers.

Since the chirp parameter b is inversely proportional to Group Delay Dispersion (GDD) so that the increase of b naturally implies the decreased GDD. Obviously, the decreased GDD means less-chirp. For a suitable choice of the pulse intensity, density ripple amplitude and chirp parameter, a significant gain in THz amplitude is observed. The following set of laser and plasma parameters throughout the manuscript are considered: The incident laser pulse of intensity $I \approx 3 \times 10^{14}$ W/cm² (femtosecond laser), angular frequency $\omega_0 = 2.355 \times 10^{15}$ rad/sec. The plasma frequency, $\omega_p = 3\pi$ THz corresponding to electron density $n_0 = 2.8 \times 10^{16}$ cm⁻³.

The variation of normalised THz amplitude as a function of normalised frequency of THz wave for different values of density ripple amplitude ($n_q = 0.1n_0, 0.2n_0, 0.3n_0$), at fixed value of frequency chirp parameter $b=0.0099$ is plotted in fig.4.2.2. From this graph, it is analysed that the higher values of the THz amplitude is obtained near the resonance condition $\omega \approx \omega_p$ and decreases as ω departs from ω_p . So we analysed from fig.4.2.2 that there is an enhancement in the THz amplitude by increasing the value of n_q and the effect of n_q on THz amplitude remains much significant near the resonance condition.

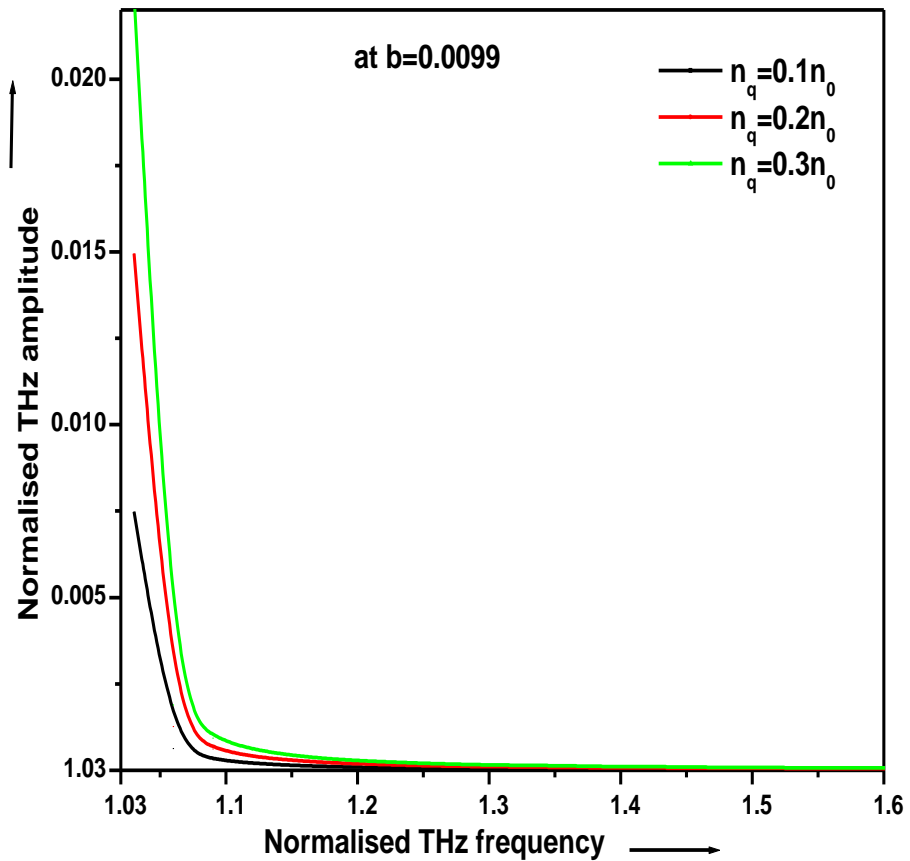


Fig.4.2.2. Variation of normalised THz amplitude as function of normalised THz frequency for different values of density ripple at fixed value of chirp parameter $b=0.0099$.

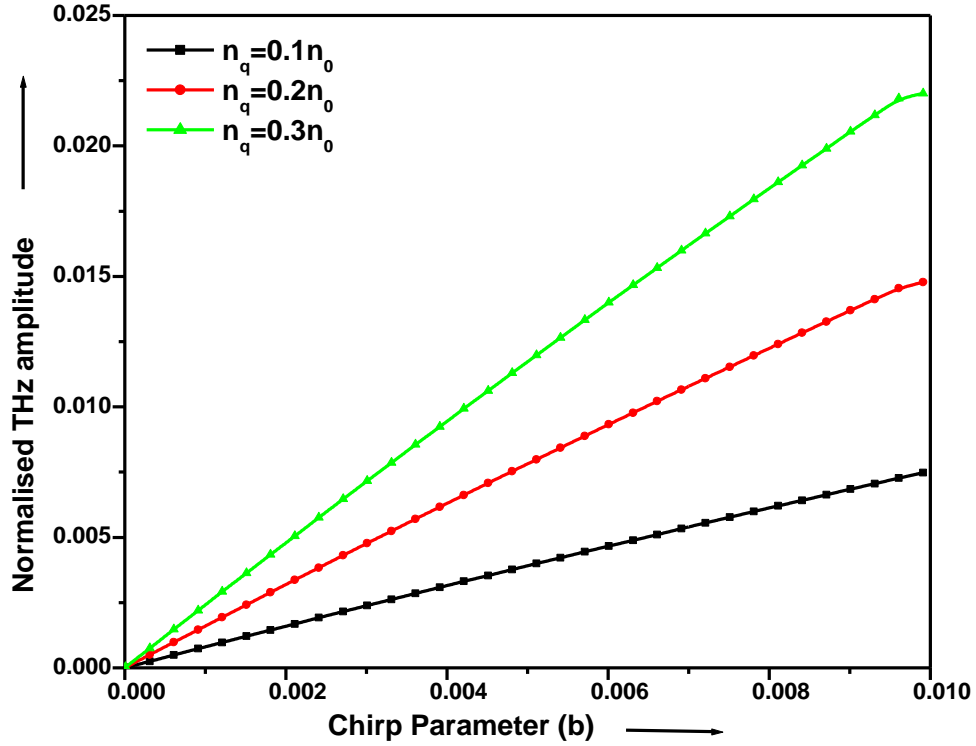


Fig.4.2.3. Plot of normalised THz amplitude versus frequency chirp parameter (b). Rest of the parameters are similar as that of fig.4.2.2.

Fig.4.2.3, displays the variation of normalised THz amplitude with frequency chirp parameter (b) ranges 0.00003 to 0.0099, for varying density ripple amplitude (n_q). It is clear from the graph the amplitude of THz wave gradually increases with increasing the value of chirp parameter. As seen from the graph the amplitude shows a sharp increase upto $b = 0.0099$. The present scheme is only valid for maximum chirp parameter 0.0099, beyond this value a negligible chirp appears and hard to see chirp effect. Therefore, we choose it as the optimized value of chirp parameter for present scheme. It is further observed, from the above figure, that the THz field amplitude varies with the chirp parameter. Also the higher value of density ripple enhances the effect of chirp on the output yield. This also infers that the output gain is closely related to the amplitude of ripples for different values of chirp parameter. So, the output of THz wave can be tuned by choosing suitable values of chirp parameter and

density ripple of suitable wave number. Thus it can be concluded from the graph that both ripple and frequency chirp together play a vital role in high intensity THz generation.

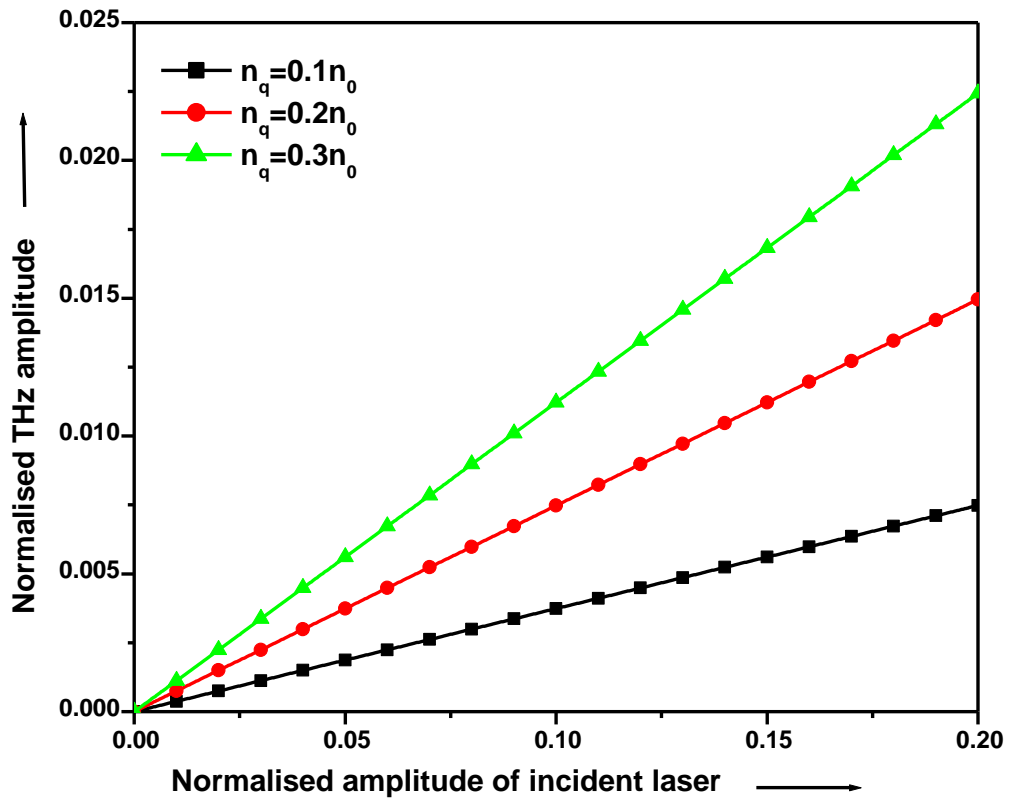


Fig.4.2.4. Spectrum of normalised THz amplitude corresponding to the incident lasers amplitude at $b=0.0099$ for different value of ripple density.

Fig.4.2.4. shows the spectrum of normalised THz corresponding to the amplitude of incident lasers for distinct values of density ripple at fixed $b=0.0099$. It can be concluded from the graph that the amplitude the laser and THz wave, are connected by a linear relationship. The increment in the incident pulse intensity results the enhancement in the initial ionization of plasma and nonlinearity in the system due to the strength of ponderomotive force. As a result, greater will be the free electron density which produces more intense THz wave. Thus, strength of output wave can be controlled by overseeing the intensity of incident laser pulses.

4.3. PROPOSED MODEL FOR MAGNETIZED PLASMA

4.3.1. Effect of Frequency Chirped Laser Pulses on THz Radiation Generation in Magnetized Plasma

To validate the theory behind the generation of THz radiation caused by beating of two laser pulses in plasma we provide the analytical calculations. We consider plasma of electron density n_0 . The electric field for laser pulses is assumed to be polarised in x-direction as $\vec{E}_j = \hat{x}A_j e^{-i(\omega_j t - k_j z)}$; where, $j = 1, 2$, $k_j \approx (\omega_j / c)$, external magnetic field is applied perpendicular to it, i.e., in the y-direction as $\vec{B}_s = B_0 \hat{y}$. Two lasers of slightly different frequencies ω_1 and ω_2 propagate through the plasma.

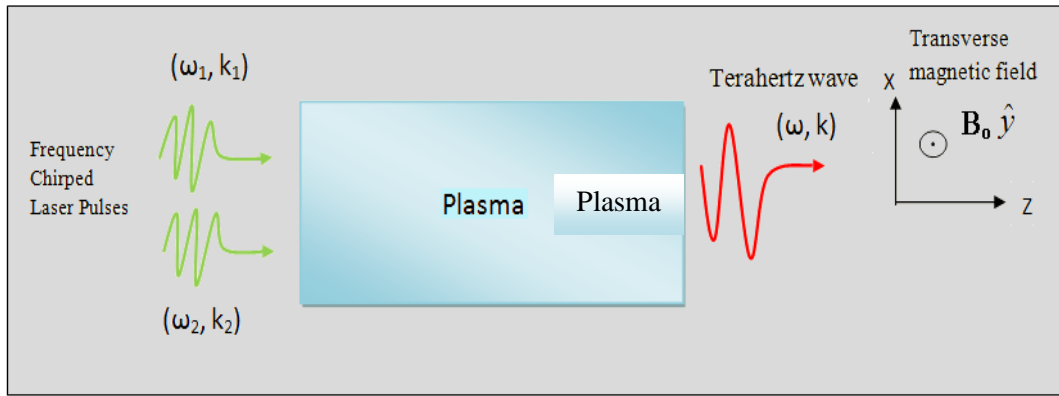


Fig.4.3.1. Schematic for frequency chirp driven THz generation

Let us suppose the frequency of incident laser is positively chirped [Fig.4.3.1] as follows; $\omega_1 = [\omega_0 + b\omega_0^2(t - z/c)]$, where ω_0 is the frequency of incident laser beam in the absence of chirp, b is the frequency chirp parameter, c is the velocity of light, and the frequency ω_2 is chosen as the difference, $\omega_1 - \omega_2 = \omega$, lies in the range of THz. One can generate highly efficient chirped laser pulse by using two counter propagating lasers induced plasma Bragg's grating (PBG) [26]. To control femtosecond laser pulses the plasma grating can be a novel because it has a much higher damage threshold than ordinary dielectric/metal optical elements. Thus the electric field of these two waves can be represented as,

$$\left. \begin{aligned} \vec{E}_1 &= \hat{x}A_1 e^{-i(\omega_1 t - \omega_1 z/c)} \\ \vec{E}_2 &= \hat{x}A_2 e^{-i(\omega_2 t - \omega_2 z/c)} \end{aligned} \right\} \quad (4.3.1)$$

and the magnetic field of incident lasers inside the plasma can be expressed as:

$$\vec{B}_j = \frac{c(\vec{k}_j \times \vec{E}_j)}{\omega_j} \quad (4.3.2)$$

here, $j=1,2$. The lasers impart an oscillatory velocity to the plasma electrons,

$\vec{v}_1 = e\vec{E}_1 / mi\omega_0[1+b\omega_0(2t-z/c)]$ and $\vec{v}_2 = e\vec{E}_2 / mi\omega_0[1+b\omega_0(2t-z/c)-\omega/\omega_0]$ along with the nonlinear terahertz ponderomotive force as,

$$\vec{F}_\omega^p = \hat{z} \frac{e^2 \omega (\vec{E}_1 \cdot \vec{E}_2^*) [(1+b\omega_0(2t-z/c))(1+b\omega_0(2t-z/c)-\omega/\omega_0) + ib\omega_0(1+b\omega_0(2t-z/c)-\omega/2\omega_0)/\omega]}{mi\omega_0^2 c (1+b\omega_0(2t-z/c))^2 (1+b\omega_0(2t-z/c)-\omega/\omega_0)^2}, \quad (4.3.3)$$

where, $-e$ and m are the electronic charge and mass respectively and $*$ represents the complex conjugate. In the presence of external magnetic field the electrons starts moving in a circle due to the Lorentz force. This circular motion is superimposed with the electric field of laser pulse results a cycloid of angular frequency ω_c . The response of electrons to the ponderomotive force along with the cyclotron motion can be obtained by solving the equation of motion, $\partial \vec{v}_\omega^{nl} / \partial t = -\vec{F}_\omega^p / m - \vec{v}_\omega^{nl} \times \vec{\omega}_c$ as;

$$\vec{v}_\omega^{nl} = \frac{\omega_c F_\omega^p \hat{x} - i\omega F_\omega^p \hat{z}}{m(\omega^2 - \omega_c^2)} \quad (4.3.4)$$

We choose $\omega_1, \omega_2 \gg \omega_p, \omega_c$ where, $\omega_p = \sqrt{4\pi n_0 e^2 / m}$ is the plasma frequency and $\omega_c = eB_0 / mc$ is the cyclotron frequency. The nonlinear current density can be calculated by solving the equation;

$\vec{J}_\omega^{NL} = -en_0 \vec{v}_\omega^{nl} / 2 = -\omega_p^2 (\omega_c \hat{x} - i\omega \hat{z}) F_\omega^p / 8\pi e (\omega^2 - \omega_c^2)$. This nonlinear current drives a wave whose frequency lies in THz range. Now using Maxwell's III and IV equations the wave equation governing the propagation of THz wave, with the inclusion of nonlinear current density given as,

$$-\nabla^2 \vec{E}_\omega + \vec{\nabla}(\vec{\nabla} \cdot \vec{E}_\omega) = \frac{\omega^2}{c^2} \vec{\epsilon} \cdot \vec{E}_\omega + \frac{4i\pi\omega}{c^2} \vec{J}_\omega^{nl}, \quad (4.3.5)$$

where, $\bar{\epsilon}$ is the permittivity tensor at the THz frequency, one may write the solution of above equation as $\vec{E}_\omega = \vec{A}_\omega(x)e^{-i(\omega t - kz)}$, and taking the divergence of Eq. (4.3.5), the z component

$$E_{\omega z} = -\frac{\epsilon_{zx}}{\epsilon_{xx}}E_{\omega x} - \frac{4\pi}{\omega k_z \epsilon_{zz}} \frac{\partial J_{\omega z}^{nl}}{\partial z}, \quad (4.3.6)$$

where, $\epsilon_{xx} = \epsilon_{zz} = 1 - \omega_p^2 / (\omega^2 - \omega_c^2)$ and $\epsilon_{xz} = -\epsilon_{zx} = -i\omega_c \omega_p^2 / \omega(\omega^2 - \omega_c^2)$. Now put the value of $E_{\omega z}$ from Eq. (4.3.6) into the wave equation, we obtain the equation governing $E_{\omega x}$ of the THz wave,

$$-k^2 E_{\omega x} + \frac{\omega^2}{c^2} \left(\epsilon_{xx} + \frac{\epsilon_{zx}^2}{\epsilon_{zz}} \right) E_{\omega x} = -\frac{4\pi i \omega}{c^2} \left(J_{\omega x}^{nl} + \frac{\epsilon_{xz}}{\epsilon_{zz}} J_{\omega z}^{nl} \right). \quad (4.3.7)$$

Solving Eq. (4.3.7) by substituting the values of nonlinear current density, we obtain the final amplitude of THz wave such as:

$$A_{\omega x} = -\frac{a_1 a_2 m c \omega^2 \omega_p^2 (\omega_c + i\omega \epsilon_{xz} / \epsilon_{zz}) [i\omega G + b\omega_0 (1 + b\omega_0 (2t - z/c) - \omega / 2\omega_0)]}{2i\omega e G^2 (\omega^2 - \omega_c^2) [k^2 c^2 - \omega^2 (\epsilon_{xx} + \epsilon_{zx}^2 / \epsilon_{zz})]}, \quad (4.3.8)$$

Here, $a_1 = eA_1 / m\omega_0 c$, $a_2 = eA_2^* / m\omega_0 c$ and $G = (1 + b\omega_0 (2t - z/c))(1 + b\omega_0 (2t - z/c) - \omega / \omega_0)$.

4.3.2. ANALYSIS & OBSERVATIONS

As the static magnetic field also introduces an additional motion to the electrons, this gives an extra nonlinear current term which can be seen from current density equation. In non relativistic regime the effect of the external magnetic field strength in the presence of chirped laser beams shows that for a suitable choice of the pulse intensity and external magnetic field strength, chirp parameter has the significant gain in THz amplitude. A suitable set of laser and plasma parameters is chosen for computations such as: femtosecond laser pulses having wavelength 800nm (Ti-Sapphire Laser), angular frequency $\omega_0 = 2.3545 \times 10^{15}$ rad/sec. Here, $\omega_p = 3\pi$ THz corresponding to electron density $n_0 = 2.8 \times 10^{16} \text{ cm}^{-3}$. For our numerical simulation we consider the normalised amplitude of incident lasers as:

$a_1 = a_2 = eA_0 / m\omega_0 c = 0.1$, where A_0 is the amplitude of the incident laser beam corresponding to the laser intensity $I \approx 3 \times 10^{14} \text{ W/cm}^2$.

The graph between normalised THz amplitude ($A_{\omega x}$) versus normalised frequency of terahertz wave (ω / ω_p) plotted in fig.4.3.2 for different values of magnetic field (54 kG-322 kG), corresponds to normalised value of cyclotron frequency, $\omega_c / \omega_p = 0.1 - 0.6$, at fixed value of frequency chirp parameter $b=0.0099$. From this graph, it can be analysed that the THz amplitude decreases with increasing THz frequency and amplitude is maximum when the ratio of the frequency of THz to the plasma wave tends to unity.

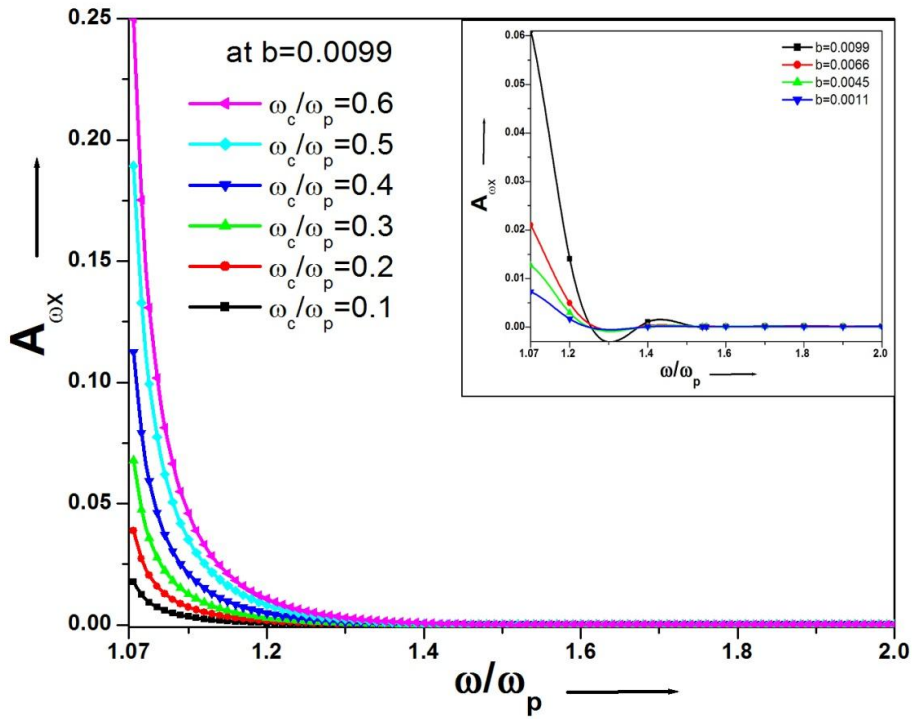


Fig.4.3.2. Plot of the normalised amplitude of THz wave ($A_{\omega x}$) with normalised frequency (ω / ω_p) for frequency of incident laser $\omega_0 = 2.3545 \times 10^{15} \text{ rad/sec}$ at normalised laser intensity 0.1 corresponding to the laser intensity $I \approx 3 \times 10^{14} \text{ W/cm}^2$.
Inset graph: Plot similar to fig.4.3.2, at different chirp parameter without magnetic field.

The physical reason behind this is that at this particular point, $\omega/\omega_p \sim 1.07$ is in proximity to the normalised value of upper hybrid frequency ω_{UH}/ω_p ; in the present analysis $\omega_{UH} = \sqrt{\omega_c^2 + \omega_p^2} = 1.077\omega_p$. This is the upper hybrid resonance condition. So when the beating frequency is close to the upper hybrid frequency, an efficient increase in terahertz amplitude is observed as the region near resonance frequency excites the THz radiation by achieving resonance condition. The resonance condition in collision less unmagnetized plasma is $\omega = \omega_p$. Also the applied magnetic field provides the additional transverse component of nonlinear current density, results the significant gain in amplitude of THz wave. The inset figure in fig.4.3.2 is plotted for different values of chirp parameter in the absence of magnetic field; other parameters are same as in fig.4.3.2. We observe a dip in normalised frequency at ~ 1.36 due to destructive interference. As we apply the external magnetic field this dip disappears due to resonance.

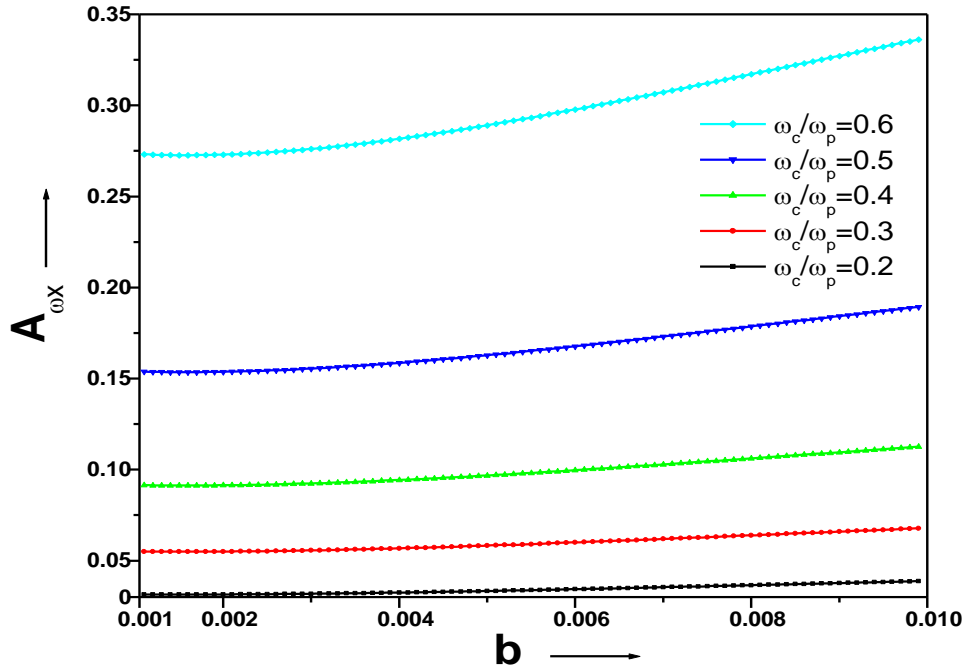


Fig.4.3.3. Plot of the normalised THz amplitude ($A_{\omega X}$) as a function of the frequency chirp parameter (b). Rest of the parameters are same as those in fig.4.3.2.

Fig.4.3.3, displays the variation of normalised THz amplitude (A_{ω_x}) with frequency chirp parameter (b) for varying electron cyclotron frequency $\omega_c / \omega_p = 0.1-0.6$, corresponds to magnetic field strength 54 kG to 322 kG. It can be clear from the graph the amplitude of THz wave gradually increases with increasing the chirp. There is a noticeable increase in amplitude after $b=0.005$. Also the higher value of magnetic field enhances the effect of chirp on the output yield and our result here shows the maximum amplitude about $A_{\omega_x} \approx 0.35$ for $b=0.0099$ at $\omega_c / \omega_p = 0.6$ corresponding to magnetic field 322kG. This also infers that the output gain is closely related to the strength of magnetic field for different values of chirp parameter

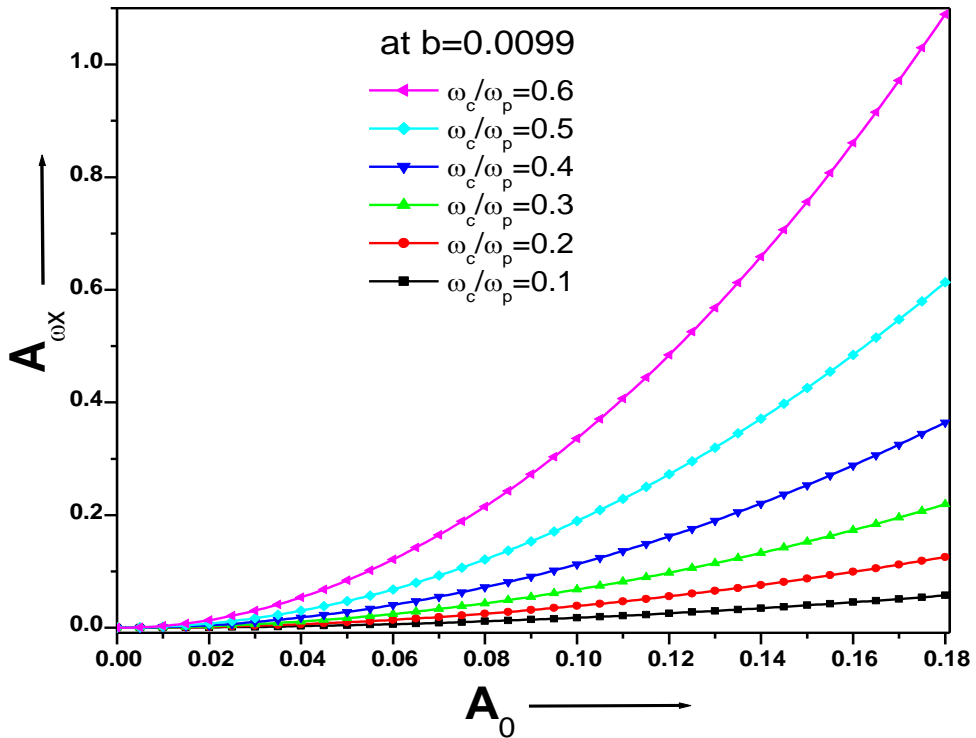


Fig.4.3.4. Plot of the normalised THz amplitude (A_{ω_x}) as a function of the normalised intensity of incident lasers (A_0) at $b=0.0099$ for different values of normalised cyclotron frequency (ω_c / ω_p).

Fig.4.3.4 shows the amplitude profile of terahertz wave (A_{ω_x}) as a function of the intensity of incident laser pulses ($A_0 = \sqrt{a_1 a_2}$) for distinct values of magnetic field

strength at fixed $b=0.0099$. A_{ω_X} and A_o are connected by a linear relationship in this graph. The increment in the incident beam intensity results the enhancement in the initial ionization of plasma and nonlinearity in the system due to the strength of ponderomotive force. As a result, greater will be the free electron density which produces more intense THz wave. Thus, strength of output wave can be controlled by overseeing the intensity of incident laser pulses.

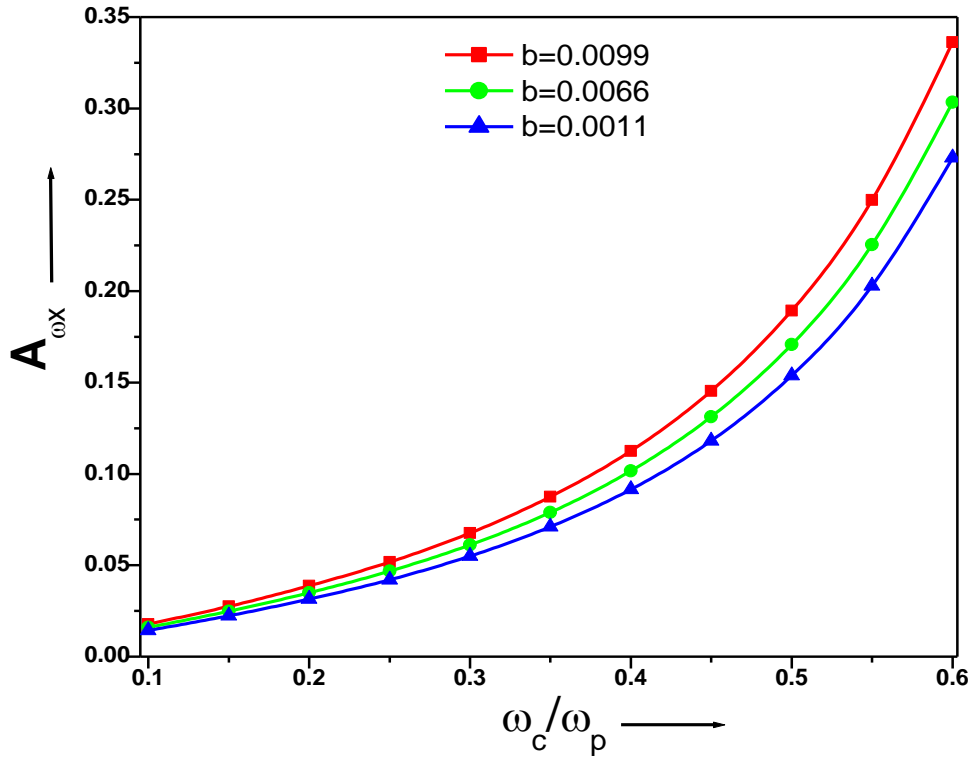


Fig.4.3.5. Plot of the normalised amplitude (A_{ω_X}) of THz wave with normalised cyclotron frequency (ω_c / ω_p) corresponding to static magnetic field 54 kG to 322 kG for different values of frequency chirp parameter (b).

Normalised THz amplitude (A_{ω_X}) as a function of normalised cyclotron frequency ω_c / ω_p is plotted in fig.4.3.5 with varying frequency chirp parameter (b). As seen from the graph the amplitude shows a sharp increase after $\omega_c = 0.3\omega_p$ for all values of chirp parameter. So the output of THz wave can be tuned by choosing suitable

values of chirp parameter and magnetic field strength. Thus it can be concluded from the graph that both applied magnetic field and frequency chirp together play a vital role in high intensity THz generation.

4.4. CONCLUSION

The first numerical method given in this chapter is developed for the investigation of the generation of THz radiation by beating of two chirped pulse lasers in plasma by introducing density ripples having spatial variation. The sensitiveness of THz field to the chirp characteristics of lasers is also noticed. The effect of collisions is neglected in the present model. We have numerically solved the equations for nonlinear current density and THz field. The resonance condition is satisfied with the help of density ripple of appropriate wave number. Also, the chirp keeps the interaction for longer period and thus the THz radiation of sufficiently high yield can be achieved. The optimized density ripple amplitude, chirp parameter and the intensity of laser pulses play a significant role in the enhancement of THz radiation. Results of this model provide a mathematical guideline for smooth and broadband THz emission which has a paramount importance in the THz time-domain spectroscopy [71-73].

In the second model, we numerically studied the sensitiveness of chirping of laser on THz generation by beating of the lasers in magnetized plasma. In this analysis we also found that THz spectra can be distorted by the onset of the spectral dip structures at $\omega/\omega_p \approx 1.36$ due to destructive interference of chirped laser pulses [Inset Fig-4.3.2] similar to Hamazaki *et al.*, [23]. In conclusion, the frequency chirping of incident lasers with a transverse magnetic field plays a crucial role to maintain the resonance condition during the interaction region. The increasing frequency of the laser pulse allows the electron to stay within the laser pulse longer and also increases the transverse momentum. As a result efficient gain in the output THz yield is observed. Also it becomes important to examine how the frequency chirp in the pump pulse affects the resultant THz spectra to properly understand the impacts of the propagation effects on the THz spectra. Therefore, our results provide a numerical guideline for broadband THz pulse generation using ultrashort pump pulse sources in plasmas.

CHAPTER-5

SELF-FOCUSING & NUMERICAL FORMALISM OF THz RADIATION FIELD IN PLASMA

5.1. INTRODUCTION

With the advent of laser technology, the laser-plasma interaction has been an active area of research on account of its various applications in the areas like self-focusing, harmonic generation, particle acceleration, terahertz (THz) generation and inertial confinement fusion etc. Out of these, rapid improvement and advancement in THz sources prove out to be a captivating field of interest due to its paramount applications in the fields of security, medicine, remote sensing, characterisation of different materials etc. To qualify a wave for a THz category, typically, a range of frequencies is 0.1-10 THz and now extending up to 40-50 THz [4-11]. Numerous techniques and methods have been employed for the generation of THz radiations in various platforms like in semiconductors, quantum cascade lasers, dielectric, electro-optic lasers [12-25] etc in order to achieve an intense, efficient and tunable THz radiation. Till date, one of the main techniques is filamentation [8, 10] (phenomena of periodic self-focusing and defocusing) for tabletop set to generate terahertz radiation. THz production can be realized due to the lasers beating in ripple density plasma, by a self focused pulse in plasma having ponderomotive, collisional, as well as relativistic nonlinearities. Jaffari *et al.* [84] have reported THz wave generation by non-linear coupling of two color Gaussian lasers. They have compared the non linear effects in multiply ionized plasma and a singly ionized one, and observed that the excitation is stronger in multiply ionized plasma. The presence of higher charge ion species not only enhances the cross focusing of beams but THz field amplitude too. THz radiations can be excited at the modulated frequency due to the modulated laser beam propagation in periodic structure plasma [55]. In this work, they have reported that the

missing process of resonance can be achieved due to density ripple and so, it satisfies the phase matching conditions and enhancement in power conversion efficiency can be achieved. Also, the excitation of THz waves can be realized as a result of self-focusing of an amplitude modulated pulse in rippled density plasma.

Nonlinear self-focusing is initiated by the nonlinear response of material to its refractive index which has a significant role in beam propagation (Fig.5.1). This will happen when the on-axis refractive index is increased. Beam tendency to spread balances the self-focusing. Every nonlinearity like ponderomotive, collisional, and relativistic makes a high-power laser beam become self-focused. Among many analytical methods, paraxial ray approximation (PRA) and Wentzel-Kramers-Brillouin (WKB) approximation are the best schemes for analyzing self-focusing. The main thrust is toward the development of efficient sources with minimum complexities—a true table-top setup.

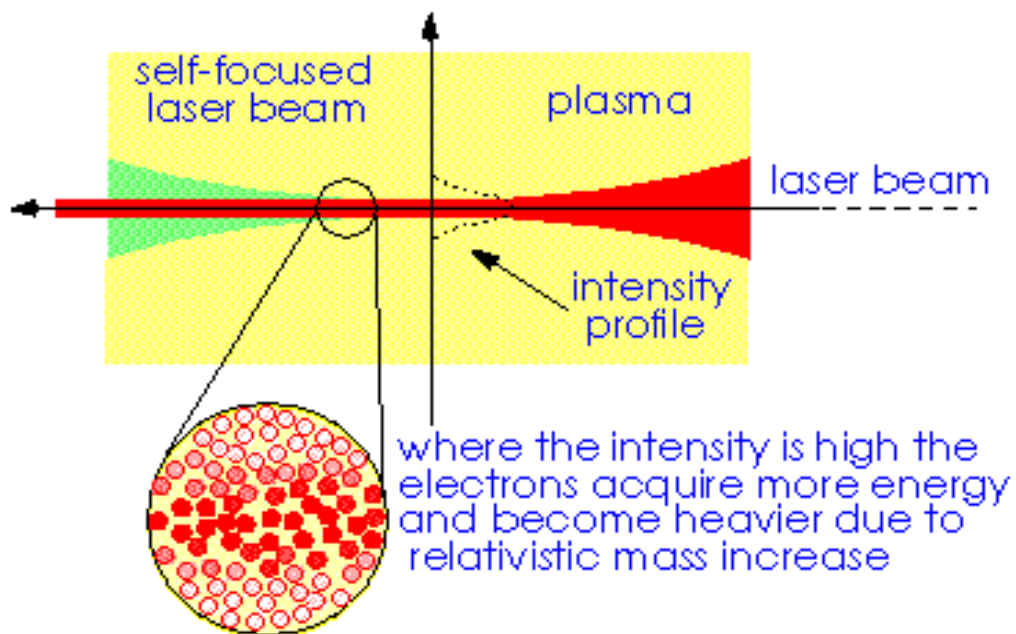


Fig.5.1 Self-focusing of laser beam

URL: <http://www.mpg.mpg.de/lpg/research/selffoc/selffoc1.frm.gif> Dated: 07/08/2020

Thus in this chapter, we proposed a scheme for excitation of THz waves which can be realized due to self-focusing of an amplitude modulated pulse in plasma. The process of

resonance can be satisfied by introducing the ripple of suitable wave number as a result improvement in power conversion efficiency can be achieved. The space periodic density variation of appropriate wave number can be obtained using different mechanism involving a machining beam, a pattern mask, transmission ring grating or using an assembly of circular Axicon grating to line focus the incident pulse [33, 34]. This chapter is organised as follows: our proposed model is given in section 5.2 along with all the numerical equations the sub-section 5.2.1, 5.2.2 and 5.2.3. In section 5.3, observations and analysis of the model is discussed, the last section i.e., 5.3 is devoted to the conclusion.

5.2 PROPOSED MODEL

5.2.1. SELF FOCUSING & THz GENERATION BY AMPLITUDE MODULATED PULSE

The electric field profile of super Gaussian laser is given as:

$$\vec{E}_a = \hat{x}E_0(r, z, t)e^{(i\omega_0 t - ik_0 z)} \quad (5.1)$$

$$\text{Here, } (\vec{E}_a \cdot \vec{E}_a^*)|_{z=0} = E_{00}^2 (1 + \mu \cos \Omega t)^2 e^{-2\left(\frac{r}{r_0}\right)^p} e^{-\left(\frac{t}{\tau}\right)^2}, \quad (5.2)$$

and also for $z > 0$, one may write,

$$|E_a|^2 = \frac{E_{00}^2}{f^2} (1 + \mu \cos \Omega(t - z/v_g))^2 e^{-2\left(\frac{r}{r_0 f}\right)^p} e^{-\left(\frac{t - z/v_g}{\tau_0}\right)^2}, \quad (5.3)$$

Here, Ω , μ , r_0 and p represents the modulation frequency, modulation index, initial pulse width and order of the incident laser pulse, respectively. The nonlinear interaction of incident laser pulse and plasma leads to a nonlinear force, this ponderomotive force can be obtained using following equation;

$$\vec{F}_p = -\frac{e^2}{4m_e \omega_0^2} \nabla (\vec{E}_a \cdot \vec{E}_a^*), \quad (5.4)$$

5.2.2. Ponderomotive Nonlinearity

Force obtained from Eq. (5.4) drives a finite intensity gradient on the electrons of the plasma and their redistribution along with variation of plasma density-distribution. As a results, the concentration of electrons get modified. The modified concentration of

electron obtained as [75-77]: $n = n_0 e^{[-\alpha(\vec{E}_a \cdot \vec{E}_a^*)]}$. Here, $\alpha = e^2 / 8m\omega_0^2 k_B T_0$. In case of ponderomotive nonlinearity plasmas' effective dielectric constant can be written as,

$$\varepsilon = \varepsilon_0 + \varphi(\vec{E}_a \cdot \vec{E}_a^*), \quad (5.5)$$

where, $\varepsilon_0 = 1 - \omega_p^2 / \omega_0^2$, $\omega_p^2 = 4\pi n_0^2 / m_e$ are dielectric constant and plasma frequency, respectively. The nonlinear term of equation (5.5) can be defined as,

$$\varphi(\vec{E}_a \cdot \vec{E}_a^*) = \frac{\omega_p^2}{\omega_0^2} [1 - \exp(-\alpha \vec{E}_a \cdot \vec{E}_a^*)], \quad (5.6a)$$

For $\vec{E}_a \cdot \vec{E}_a^* \ll 1$ since the mass of the electron is very small comparative to ion mass, i.e., $m \ll M$ thus φ shows a quadratic relation such as;

$$\varphi(\vec{E}_a \cdot \vec{E}_a^*) = \frac{\omega_p^2}{\omega_0^2} \alpha (\vec{E}_a \cdot \vec{E}_a^*), \quad (5.6b)$$

and hence the modified dielectric constant calculated by using equation (5.6b) in equation (5.5) as

$$\varepsilon = 1 - \frac{\omega_p^2}{\omega_0^2} + \frac{\omega_p^2}{\omega_0^2} (\alpha \vec{E}_a \cdot \vec{E}_a^*), \quad (5.7)$$

5.2.3. SELF-FOCUSING

On solving Maxwell's equations (3) & (4) in the absence of nonlinear source, we obtain

$$\nabla^2 \vec{E}_a - \vec{\nabla}(\vec{\nabla} \cdot \vec{E}_a) + \frac{\omega_0^2}{c^2} (\varepsilon \vec{E}_a) = 0, \quad (5.8)$$

Let the solution of the above equation is in the form;

$$\vec{E}_a(r, z, t) = \hat{x}A(r, z, t) \exp[i(\omega_0 t - k_0 z)], \quad (5.9)$$

Here $A(r, z, t)$ is complex amplitude. Substituting Eq. (5.9) into Eq. (5.8) and by assuming variation of A versus z to be slow, we get following equation;

$$\frac{\partial^2 A}{\partial r^2} + \frac{1}{r} \frac{\partial A}{\partial r} - 2ik_0 \frac{\partial A}{\partial z} - \frac{2i\omega_0 \varepsilon_0}{c^2} \frac{\partial A}{\partial t} - \frac{\varepsilon_2 r^2 \omega_0^2}{r_0^2 c^2} A = 0, \quad (5.10)$$

$$\text{here, } A(r, z, t) = A_0(r, z, t) \exp(-ik_0 S(r, z, t)), \quad (5.11)$$

$$\frac{\partial A_0^2}{\partial z} + A_0^2 \left(\frac{\partial^2 S}{\partial r^2} + \frac{1}{r} \frac{\partial S}{\partial r} \right) + \frac{\partial A_0^2}{\partial r} \frac{\partial S}{\partial r} + \frac{1}{v_g} \frac{\partial A_0^2}{\partial t} = 0, \quad (5.12)$$

$$\text{and } 2 \frac{\partial S}{\partial z} + \frac{2}{v_g} \frac{dS}{dt} + \left(\frac{\partial S}{\partial r} \right)^2 = \frac{1}{k_0^2 A_0} \left(\frac{\partial^2 A_0}{\partial r^2} + \frac{1}{r} \frac{\partial A_0}{\partial r} \right) - \frac{r^2}{r_0^2} \frac{\varepsilon_2(z)}{\varepsilon_0(z)}. \quad (5.13)$$

Here $v_g = k_0 c / \omega_0$ represents the group velocity of incident pulse in plasma. Now introducing a new set of variables (z, t) as $(z' = z, t' = t - z/v_g)$ and rewrite the Eq. (5.12) and (5.13) as

$$\frac{\partial A_0^2}{\partial z'} + \frac{\partial S}{\partial r} \frac{\partial A_0^2}{\partial r} + A_0^2 \left(\frac{\partial^2 S}{\partial r^2} + \frac{1}{r} \frac{\partial S}{\partial r} \right) = 0 \quad (5.14)$$

$$\text{and } 2 \frac{\partial S}{\partial z'} + \left(\frac{\partial S}{\partial r} \right)^2 = -\frac{r^2}{r_0^2} \frac{\varepsilon_2(z', t')}{\varepsilon_0(z', t')} + \frac{1}{k_0^2 A_0} \left(\frac{\partial^2 A_0}{\partial r^2} + \frac{1}{r} \frac{\partial A_0}{\partial r} \right) \quad (5.15)$$

using PRA and expanding eikonal up to r^2 as; $S(r, z', t') = S_0(z', t') + \beta S_2(z', t')$, here $\beta = r^2 / r_0^2$ with $S_2 = r_0^2 / 2f (\partial f / \partial z')$, we obtain the solution of Eq. (5.14) as follows:

$$A_0^2 = \frac{E_{00}^2}{f^2} (1 + \mu \cos \Omega t)^2 e^{-2 \left(\frac{r}{r_0 f} \right)^p} \quad (5.16)$$

Here, $t' = t - z/v_g$, $v_g = c \varepsilon^{1/2}$. Using the value of eikonal and Eq. (5.16) in Eq. (5.13) and comparing the coefficient of r^2 on both sides of the resulting equation, we get

$$\text{For Gaussian profile: } p = 2, \quad \frac{\partial^2 f}{\partial z'^2} + \frac{f}{r_0^2} \frac{\varepsilon_2}{\varepsilon_0} - \frac{4}{k_0^2 r_0^4 f^3} = 0, \quad (5.17)$$

$$\text{For super Gaussian profile: } p = 4, \quad \frac{\partial^2 f}{\partial z'^2} + \frac{f}{r_0^2} \frac{\varepsilon_2}{\varepsilon_0} + \frac{16}{k_0^2 r_0^4 f^3} = 0, \quad (5.18)$$

5.2.4. AMPLITUDE MODULATED WAVE ASSISTED THZ FIELD

We have considered a rippled density plasma channel where $n = n_0 + n_q$, as $n_q = n_q^0 e^{iqz}$ where n_0 is the electron plasma density without ripples (Fig.5.2). At modulation frequency the ponderomotive force on plasma electrons can be calculated as:

$$\vec{F}_p^\Omega = -\frac{e^2}{4m\omega_0^2} \vec{\nabla} \left[\frac{E_{00}^2}{f^2} (1 + \mu \cos \Omega t')^2 e^{-2\left(\frac{r}{r_0 f}\right)^p} \right] \quad (5.19)$$

The ponderomotive force in component form can be written as:

$$\left. \begin{aligned} F_{pr} &= \frac{e^2 E_{00}^2 \mu}{2m\omega_0^2} \left(\frac{p}{r}\right) \left(\frac{r}{r_0 f}\right)^p \frac{e^{i\Omega t'}}{f^2} e^{-t'^2/\tau_0^2} e^{-2\left(r/r_0 f\right)^p} \\ F_{pz} &= \frac{e^2 E_{00}^2 \mu}{4m\omega_0^2} \frac{\partial}{\partial z} \frac{e^{i\Omega t'}}{f^2} e^{-t'^2/\tau_0^2} e^{-2\left(r/r_0 f\right)^p} \end{aligned} \right] \quad (5.20)$$

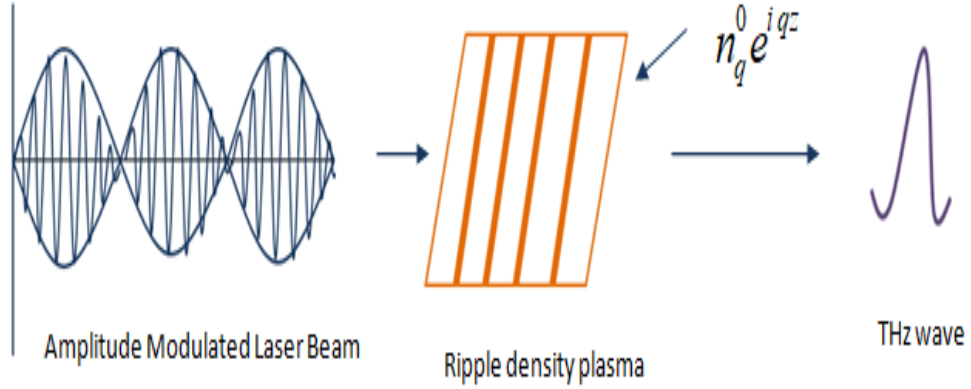


Fig.5.2. Schematic for THz generation via amplitude modulate wave in pre formed rippled density plasma

The oscillatory velocity acquired by plasma electrons due to this fore given as follows:

$$v_r^{NL} = -\frac{F_{pr}}{mi\Omega} = \frac{ie^2 E_{00}^2 \mu}{2m^2 \omega_0^2 \Omega f^2} \left(\frac{p}{r}\right) \left(\frac{r}{r_0 f}\right)^p e^{-i\Omega t'} e^{-t'^2/\tau_0^2} e^{-2\left(r/r_0 f\right)^p} \quad (5.21)$$

$$v_z^{NL} = -\frac{F_{pz}}{mi\Omega} = -\frac{\mu}{mi\Omega} \left[-\frac{e^2 E_{00}^2}{4m\omega_0^2} \frac{\partial}{\partial z} \frac{e^{-i\Omega t'}}{f^2} e^{-t'^2/\tau_0^2} e^{-2\left(r/r_0 f\right)^p} \right] \quad (5.22)$$

Hence, the nonlinear current density at modulated frequency is given as:

$$J_{\Omega r}^{NL} = -\left(\frac{\omega_p^2}{\omega_0^2}\right) \left(\frac{n_q}{n_0}\right) \frac{ieE_{00}^2 \mu}{16\pi m \Omega f^2} \left(\frac{p}{r}\right) \left(\frac{r}{r_0 f}\right)^p e^{-i\Omega t'} e^{-t'^2/\tau_0^2} e^{-2\left(r/r_0 f\right)^p} \quad (5.23a)$$

$$J_{\Omega z}^{NL} = + \left(\frac{\omega_p^2}{\omega_0^2} \right) \left(\frac{n_q}{n_0} \right) \frac{ieE_{00}^2 \mu}{32\pi mi\Omega} \frac{\partial}{\partial z} \left(\frac{e^{-i\Omega t}}{f^2} e^{-t^2/\tau_0^2} e^{-2(r/r_0 f)^p} \right) \quad (5.23b)$$

This nonlinear current give rise to THz wave at frequency Ω and wave number $q + \Omega/v_g$, and can be calculated using the following wave governing equation;

$$\nabla^2 \vec{E}_0 - \vec{\nabla}(\vec{\nabla} \cdot \vec{E}) + \frac{\Omega^2}{c^2} \varepsilon' \vec{E}_0 = -\frac{4\pi}{c^2} \frac{\partial \vec{J}_{\Omega}^{NL}}{\partial t} \quad (5.24a)$$

By rewriting above equation after neglecting the second term, we obtain:

$$\frac{\partial^2 \vec{E}}{\partial z^2} + \frac{\partial^2 \vec{E}}{\partial r^2} + \frac{1}{r} \frac{\partial \vec{E}}{\partial t^2} - \frac{\varepsilon'}{c^2} \frac{\partial \vec{E}}{\partial t^2} = -\frac{4\pi}{c^2} \frac{\partial \vec{J}_{\Omega}^{NL}}{\partial t} \quad (5.24b)$$

Eq (5.24b) has component along the \hat{r} and \hat{z} direction. The x - component of this equation is obtained using $E_x = E_r \cos\phi$ and taking E_r to be independent of ϕ

Hence, taking the r - component of Eq. (24b), we get,

$$\frac{\partial^2 E_r}{\partial z^2} + \frac{\partial^2 E_r}{\partial r^2} + \frac{1}{r} \frac{\partial \vec{E}_r}{\partial t^2} - \frac{\varepsilon'}{c^2} \frac{\partial^2 \vec{E}_r}{\partial t^2} = -\frac{4\pi}{c^2} \frac{\partial \vec{J}_{\Omega r}^{NL}}{\partial t} \quad (5.25)$$

$$\frac{\partial^2 E_r}{\partial z^2} + \frac{\partial^2 E_r}{\partial r^2} + \frac{1}{r} \frac{\partial \vec{E}_r}{\partial t^2} - \frac{\varepsilon'}{c^2} \frac{\partial \vec{E}_r}{\partial t^2} = -G e^{-i(\Omega t' - qz')} \quad (5.26)$$

$$\text{Here, } G = \left(\frac{\omega_p^2}{\omega_0^2} \right) \left(\frac{n_q^0}{n_0} \right) \frac{eE_{00}^2 \mu}{4mc^2 f^2} \left(\frac{p}{r} \right) \left(\frac{r}{r_0 f} \right)^p e^{-2\left(\frac{r}{r_0 f}\right)^p} e^{-t'^2/\tau_0^2} \left(\frac{2it'}{\tau_0^2 \Omega} - 1 \right) \quad (5.27)$$

and $\varepsilon' = (1 - \omega_p^2/\Omega^2)$. Having $k_T = q + \Omega/v_g$ for THz radiation frequency we can extract the dispersion relation Eq. (5.24b) as; $((\Omega^2 - \omega_p^2)/c^2) - k_T^2 = 0$ and so, we obtain density ripple wave number as,

$$q = -\omega_p^2 (\Omega^2 - \omega_p^2)^{-1/2} / c \quad (5.28)$$

At resonant condition the maximum THz radiation is observable for which $\Omega \gg \pm \omega_p$ is the necessary condition implies $q \rightarrow \infty$. Let the solution of Eq. (5.26) is;

$$E_r = A_r e^{-i(\Omega t' - k_T z')}, \text{ where } A_r = F(z')\psi(r, t'), \text{ implies, } E_r = F(z')\psi(r, t') e^{-i(\Omega t - k_T z')}.$$

Here $F(z')$ is the amplitude of THz radiation and $\psi(r, t') = (r/r_T)^{-p}$ and

$r_T^2 = (c^2 r_0^2 / \omega^2 \phi)^{1/2}$ is the beam width of THz. Now substituting the above value of E_r

in eq (5.26) and multiplying the resulting eq. by $\psi^*(r) \cdot r dr$ and integrating it over r from 0 to ∞ , the electric field can be calculated as

$$\begin{aligned} & \left(\frac{\partial^2 F}{\partial z^2} + 2ik_i \frac{\partial F}{\partial z} + F \left(\frac{k_i^2 c^2 - \Omega^2 - \omega_p^2}{c^2} \right) \right) \int_0^\infty \psi \psi^* r dr + (-p^2 F - 2pF) \int_0^\infty \frac{r^{p-1}}{(r_i f)^p} \psi \psi^* dr \\ & + \left(\frac{2p}{f} \frac{\partial f}{\partial z} \frac{\partial F}{\partial z} + \frac{2ik_i p F}{f} \frac{\partial f}{\partial z} + \frac{pF}{f} \frac{\partial^2 F}{\partial z^2} - \frac{pF(p+1)}{f^2} \left(\frac{\partial f}{\partial z} \right)^2 \right) \int_0^\infty \frac{\psi \psi^* r^{p+1}}{(r_i f)^p} dr + F \int_0^\infty \frac{\psi \psi^*}{r} dr, \quad (5.29) \\ & + (p^2 F) \int_0^\infty \frac{r^{2p-1}}{(r_i f)^{2p}} \psi \psi^* dr + \left(\frac{p^2 F}{f^2} \frac{\partial f}{\partial z} \right) \int_0^\infty \frac{r^{2p+1}}{(r_i f)^{2p}} \psi \psi^* dr = -\frac{4\pi}{c^2} L \int_0^\infty \frac{r^{p+1}}{r_i (r_i f)^p} e^{-r^p \left(\frac{2r_i p + r_0 p}{(r_0 r_i f)^p} \right)} dr \end{aligned}$$

Again simplifying above equation, we get

$$\begin{aligned} & \left(\frac{\partial^2 F}{\partial z^2} + 2ik_i \frac{\partial F}{\partial z} + F \left(\frac{k_i^2 c^2 - \Omega^2 - \omega_p^2}{c^2} \right) \right) \int_0^\infty \frac{r^3}{r_i^2} e^{-2\left(\frac{r}{r_i f}\right)^p} dr + (-p^2 F - 2pF) \int_0^\infty \frac{r}{r_i^2} \left(\frac{r}{r_i f} \right)^p e^{-2\left(\frac{r}{r_i f}\right)^p} dr \\ & + \left(\frac{2p}{f} \frac{\partial f}{\partial z} \frac{\partial F}{\partial z} + \frac{2ik_i p F}{f} \frac{\partial f}{\partial z} + \frac{pF}{f} \frac{\partial^2 F}{\partial z^2} - \frac{pF(p+1)}{f^2} \left(\frac{\partial f}{\partial z} \right)^2 \right) \int_0^\infty \frac{r^3}{r_i^2} \left(\frac{r}{r_i f} \right)^p e^{-2\left(\frac{r}{r_i f}\right)^p} dr + F \int_0^\infty \frac{r}{r_i^2} e^{-2\left(\frac{r}{r_i f}\right)^p} dr, \quad (5.30) \\ & + (p^2 F) \int_0^\infty \frac{r^{-1}}{r_i^2} \left(\frac{r}{r_i f} \right)^{2p} e^{-2\left(\frac{r}{r_i f}\right)^p} dr + \left(\frac{p^2 F}{f^2} \frac{\partial f}{\partial z} \right) \int_0^\infty \frac{r^3}{r_i^2} \left(\frac{r}{r_i f} \right)^{2p} e^{-2\left(\frac{r}{r_i f}\right)^p} dr = -\frac{4\pi}{c^2} L \int_0^\infty e^{-\left(\frac{r}{r_i f}\right)^p \left(\frac{2r_i^p + r_0^p}{r_i^p} \right)} dr \end{aligned}$$

Now solving Eq. (5.30) for both Gaussian and Super-Gaussian profile by choosing the value of $p = 2$ & 4 respectively, we obtain the final equations for THz field. We obtain the required results by solving above equations for a set of laser and plasma parameters.

5.3 ANALYSIS & OBSERVATIONS

The differential equations (17), (18) and (5.30) for beam width parameter of the incident laser pulse and THz amplitude analysed numerically for boundary conditions such as; $\partial f / \partial z = 0$ at $f = 1$. Fig.5.2. depicts the variation of beam width parameter to the normalised distance propagation. The solid line represents the Gaussian beam where the dotted line illustrates the super-Gaussian pulse propagation characteristics in ponderomotive regime. From the plot it is observed that the super Gaussian pulse propagate more without diffraction. As a result a more focused beam travel greater distance and helps to increase nonlinear current. Hence, on the account of this current efficient gain in output terahertz yield can be obtained.

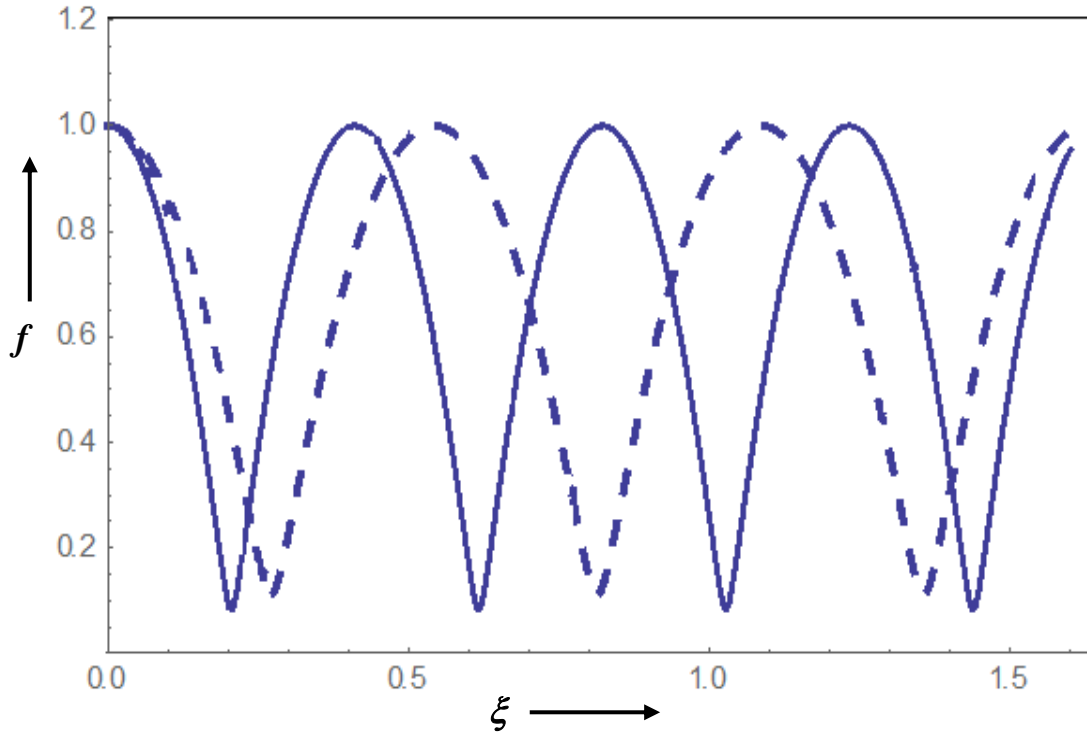


Fig.5.2. Plot of normalized propagation distance ξ versus beam with parameter f .

5.4 CONCLUSION

In the model anticipated in this chapter, we proposed a scheme to explore the effect of self focusing of super Gaussian amplitude modulated pulse on emitted terahertz radiation. The density ripple in the plasma plays vital role to achieve phase matching condition. We have solved the self focusing equation for ponderomotive nonlinearity by using PRA. Beam width parameters and THz field equation along with the resonance condition has been derived numerically. In the uniform plasma the in comparison to Gaussian pulse, the super Gaussian pulse propagate more Rayleigh length without any diffraction. Due to such behaviour of super-Gaussian pulse in plasma it seems a better candidate for particle acceleration and plasma channelling. Furthermore, it is also observed that the degree of self focusing can be tuned by changing the modulation index of the amplitude modulate incident laser pulse.

CHAPTER-6

SUMMARY & FUTURE SCOPE

6.1. SUMMARY

In the study presented in this thesis, we have explored the possibilities to enhance the efficiency of terahertz radiation along with its directionality and tunability. We have introduced variation of frequency along with laser and plasma characteristics to obtain a significant gain in the output yield. Also, we have optimized the laser and plasma parameters such as plasma density, polarization, frequency chirp, beam order, modulation index, beam width parameter, initial intensity and angle of incident laser etc. to obtain desired efficiency. Wave governing equation is derived along with the equation of ponderomotive force and nonlinear current density. Also, the role of externally applied static magnetic field and density ripple has been considered in different models. The conclusion of the results obtained from each model has already been discussed in the end of particular chapter. The results obtain from our model provide a mathematical guideline for smooth and broadband THz emission which has a paramount importance in the THz time-domain spectroscopy [71-73]. Therefore, our results show a great plausibility to provide a numerical guideline for broadband THz pulse generation using ultra short pump pulse sources in plasmas as well as developing a tunable THz source having power to use in medical applications. Thus THz source developed here will have wide-ranging potential applications, resulting in cross-disciplinary impact. Thus by attracting interdisciplinary researchers' attention and participation will greatly advance the THz science and technology, and would enable a broad range of new scientific investigations to be undertaken.

This would also extend to the users of accelerators. It has already been demonstrated experimentally that intense THz waves can also serve as a novel driving field for electron accelerators [85] to reduce the scale of today's particle accelerators, hopefully achieving pencil-sized high energy accelerators for versatile x-ray sources and medical treatment. Work presented in this thesis is expected to have significant

impacts on the THz high field community, condensed matter researchers and other multiple research communities who will take advantage of the capabilities of this new source of THz pulses. The proposed unprecedented THz source open up the following new opportunities:-

6.1.1. THz COMMUNITY

A novel THz source, establish diagnostic techniques for it and conduct cutting edge THz applications, thus advancing the field of THz science, particularly nonlinear THz-matter interactions.

6.1.2. PLASMA & HIGH ENERGY DENSITY PHYSICS

THz generation from relativistic laser-plasma interactions is a newly emerging application area of laser-driven plasma and high energy density physics. The extreme THz pulses offer a new long-wavelength pump light source capable of driving strong-field physics, opening up a new research branch of ultra intense THz-plasma interactions.

6.1.3. CONDENSED MATTER PHYSICS

THz applications in phase transition and spintronics are also research hotspots of material science, helping to address some of the relevant fundamental scientific problems involved. The extreme THz source can drive previously inaccessible transients in materials.

6.1.4. OTHER RESEARCH

For example, extremely energetic THz pulse can be used as a driver to accelerate electrons in accelerators, which has the longer term potential to reduce the size of high energy particle accelerators. Researchers from the fields of chemistry and biology are likely to use such a THz source as a unique and powerful research tool to investigate chemo-catalysis and hydration, respectively.

6.2. FUTURE SCOPE

In terms of future Scope, the advent of intense THz sources is opening up new opportunities in non linear light-matter interactions. One of the most profound features is that THz radiation can serve as a fascinating pump pulse [20], rather than a

non-ionizing probe in conventional applications like imaging and safety inspection. For experimental purpose, it is worth mentioning that, besides THz radiation, energetic particle (electron, ion and neutron) and high-flux radiation (attosecond pulse, x-ray and γ -ray) beams can also be produced concomitantly during laser-plasma interactions. These intrinsically synchronized “by-products” provide a great variety of optional ultrafast probes. By making full use of this advantageous feature of laser plasmas, we will develop multifunctional THz pump – THz / optical / x-ray probe systems, and conduct demonstrative applications in material science and strong-field physics.

As the THz photon energy is comparable to the characteristic energy of many fundamental systems, like excitons, phonons and magnons, intense THz pulses offer a unique tool to control transient states of matter, such as carrier dynamics, phononics and spintronics, just to name a few. Currently, GV/m-level THz fields are only achievable by using sub-wavelength-structured meta-materials to enhance the THz field in a localized μm -scale region [86]. Since the THz spot size is relatively large (typically $\sim\text{mm}$ in diameter), direct access to GV/m THz fields without the use of meta-materials will intrinsically enable clearer, higher signal-to-noise ratio detection of high-field THz effects. As it is expected that within the next decade, suitable lasers operating at $\sim 1\text{-}100\text{Hz}$ will be available both nationally and internationally, relativistic laser plasma-based THz sources could provide a unique, desirable and viable source for this.

Another interesting topic of applications is the propagation of powerful light pulses in optical media, which has sparked many intriguing physics and applications [87]. Relevant studies have long been limited to the optical region ($< \sim 1\ \mu\text{m}$), and extended to long wavelengths ($1.5\text{--}12\ \mu\text{m}$) only in recent years [88]. Due to the λ^2 scaling of the ponderomotive energy with the wavelength λ , the physical phenomena involved at long THz wavelengths could be significantly different from the routinely near-infrared laser case and thus of great interest for potentially new physics. Some THz nonlinear phenomena, such as saturable absorption and Kerr birefringence, have been observed from specific semiconductors and liquids of high nonlinearity [1], by using accelerator or crystal based THz sources. Here, the proposed extreme THz source

would enable us to study the nonlinear interaction of THz waves with gas and plasmas, extending the recently emerging mid-infrared strong-field physics [88, 89] to the new THz paradigm.

Broadband THz also has potential application in the field of high field communications. The realization of integrated, low-cost and efficient solutions for high-speed, on-chip communication requires terahertz-frequency waveguides and has great potential for information and communication technologies, including sixth-generation (6G) wireless communication, terahertz integrated circuits, and interconnects for intrachip and interchip communication. Generation and application of energetic, broadband terahertz pulses (bandwidth $\sim 0.1\text{--}50$ THz) is an active and contemporary area of research. Exploration of other simpler means of high energy, broadband terahertz generation is an active area of research [90-92].

References

- [1]. Hoffmann M C and Fülöp J A 2011 Intense ultrashort terahertz pulses: Generation and applications *J. Phys. D. Appl. Phys.* **44** 083001
- [2]. Siegel P H 2002 Terahertz technology *IEEE Trans. Microw. Theory Tech.* **50** 910
- [3]. Williams B. 2007 Terahertz quantum-cascade lasers. *Nature Photon* **1** 517–525
- [4]. Wilmink G J and Grundt J E 2011 Invited review article: Current state of research on biological effects of terahertz radiation *J. Infrared, Millimeter, Terahertz Waves* **32** 1074
- [5]. Leemans W. P. *et al.* 2003 Observation of Terahertz Emission from a Laser-Plasma Accelerated Electron Bunch Crossing a Plasma-Vacuum Boundary *Phys. Rev. Lett.* **91** (7) 74802
- [6]. Pickwell E and Wallace V P 2006 Biomedical applications of terahertz technology *J. Phys. D. Appl. Phys.* **39** R301
- [7]. Kawase M 2012 Application of Terahertz Waves to Food Science *Food Sci. Technol. Res.* **18** 601
- [8]. Pal V, Singh G, and Yadav R P 2015 Balanced Cluster Size Solution to Extend Lifetime of Wireless Sensor Networks *IEEE Internet Things J.* **2** (5) 399–401
- [9]. Clough B, Dai J, and Zhang X-C 2014 Laser Air Photonics: Covering the "Terahertz Gap" and Beyond *Chinese journal of physics* **52**(1) 416-430
- [10]. Mittleman D M 2013 Frontiers in terahertz sources and plasmonics," *Nat. Photonics* **7** (9), 666–669
- [11]. Dhillon S S *et al.* 2017 The 2017 terahertz science and technology roadmap *J. Phys. D. Appl. Phys.* **50** 043001
- [12]. Hirata A *et al.* 2006, 120-GHz-and millimetre-wave photonic wireless link for 1 Gbs data transmission *IEEE Trans. Microw. Theory Tech.* **54** 1937
- [13]. Krumbholz N *et al.* 2005, Omni directional terahertz mirrors: A key

- element for terahertz communication systems *Appl Phys Lett.* **88** 20295
- [14]. Brucherseifer M. *et al.* 2000, Label-free probing of the binding state of DNA by time domain terahertz sensing *Appl Phys Lett.* **77** 4049
- [15]. Davis A G *et al.* 2002, The development of terahertz sources and their applications *Phys. Med. Biol.* **47** 3679
- [16]. J. Faure *et al.* 2004 Modelling laser-based table-top THz sources: optical rectification, propagation and electro-optic sampling *Opt. Quantum Electron.* **36** 681
- [17]. E. Budiarto *et al.* 1996 High intensity terahertz pulses at 1-kHz repetition rate *IEEE J. Quantum Electron.* **32**, 1839
- [18]. Tonouchi M 2007 Cutting-edge terahertz technology *Nat. Photonics* **1** 97
- [19]. Kleine-Ostmann T and Nagatsuma T 2011 A review on terahertz communications research *J Infrared Milli Terahz Waves* **32** 143
- [20]. Kampfrath T, Tanaka K and Nelson K A 2013 Resonant and non-resonant control over matter and light by intense terahertz transients *Nat Photonics* **7** 680
- [21]. Vidal S, Degert J, Tondusson M, Freysz M and Oberl J 2014 Optimized terahertz generation via optical rectification in Zn Te crystals *Opt Soc. Am. B* **31** 149
- [22]. Lavrukhin D V *et al* 2019 Terahertz photoconductive emitter with dielectric-embedded high-aspect-ratio plasmonic grating for operation with low-power optical pumps *AIP Advances* **9** 015112
- [23]. Hamazaki J *et al.* 2016, Effects of chirp of pump pulses on broadband terahertz pulse spectra generated by optical rectification *J. Journ. Appl. Phys.* **55** 110305
- [24]. Frederike A *et al* 2017 Narrowband terahertz generation with chirped-and-delayed laser pulses in periodically poled lithium niobate *Opt. Letts.* **42** 11
- [25]. Kim K Y, Taylor A J, Glowina J H and Rodriguez G 2008 Coherent control of terahertz supercontinuum generation in ultrafast laser-gas

- interactions *Nat. Photonics* **2**(10) 605
- [26]. Wang W M, Sheng Z M, Wu H C, Chen M, Li C, Zhang J and Mima K 2008 Strong terahertz pulse generation by chirped laser pulses in tenuous gases *Opt. Exp.* **16** 16999
- [27]. Nagai M *et al* 2004 Generation and detection of terahertz radiation by electro-optical process in GaAs using 1.56 μ m fiber laser pulses *Appl. Phys. Lett.* **85** 3974
- [28]. Azima A *et al.* 2018, Direct measurement of the pulse duration and frequency chirp of seeded XUV free electron laser pulses *New J. Phys.* **20** 013010
- [29]. Hamster H, Sullivan A, Gordon S, White W and Falcone R W 1993 Sub picosecond, electromagnetic pulses from intense laser-plasma interaction *Phys. Rev. Lett.* **71** 2725
- [30]. Sheng Z M, Mima K, Zhang J and Sanuki H 2005 Emission of electromagnetic pulses from laser wakefields through linear mode conversion *Phys. Rev. Lett.* **94** 095003
- [31]. Liu C *et al* 2015 Effect of two-color laser pulse duration on intense terahertz generation at different laser intensities *Phys. Rev. A* **92** 063850
- [32]. Kwon K B *et al.* 2018, High-energy, short-duration bursts of coherent Terahertz radiation from an embedded plasma dipole *Nature, Scientific Reports* **8**, 145
- [33]. Tripathi D *et al.* 2010, Terahertz generation by an amplitude-modulated Gaussian laser beam in a rippled density plasma *Phys. Scr.* **82** 035504
- [34]. Mehta A *et al.* 2019, Generation of terahertz (THz) radiation by p-polarised laser beating in hot plasma with surface density ripple *Laser Phys. Lett.* **16** 045403
- [35]. Mehta A *et al.* 2019, Effect of frequency-chirped laser Pulses on terahertz generation in magnetized plasma *Laser Phys.* **29** 095405
- [36]. Hasanbeigi A, Mehdian H and Gomar P 2015 Enhancement of terahertz radiation power from a prebunched electron beam using

- helical wiggler and ion-channel guiding *Phys. Plasmas* **22** 123116
- [37]. Malik A K and Malik H K 2013 Tuning and focusing of terahertz radiation by dc magnetic field in a laser beating process *IEEE J. Quantum Electron.* **49** 232
- [38]. Bakhtiari F, Golmohammady S, Yousefi M, Kashani F D and Ghafary B 2015 Generation of terahertz radiation in collisional plasma by beating of two dark hollow laser beams *Laser Part. Beams* **33** 463
- [39]. Kumar M and Tripathi V K 2012 Resonant terahertz generation by optical mixing of two laser pulses in rippled density plasma *IEEE J. Quantum Electron.* **48** 1031
- [40]. Bhasin L and Tripathi V K 2009 Terahertz generation via optical rectification of x-mode laser in a rippled density magnetized plasma *Phys. Plasmas* **16** 103105
- [41]. Tyagi Y, Tripathi D, Walia K and Garg D 2018 Ion acoustic wave assisted laser beat wave terahertz generation in a plasma channel *Phys. Plasmas* **25** 043118
- [42]. Kumar M, Tripathi V K and Jeong Y U 2015 Laser driven terahertz generation in hot plasma with step density profile *Phys. Plasmas* **22** 063106
- [43]. Kumar M, Lee K, Hee Park S, Uk Jeong Y and Vinokurov N 2017 Terahertz radiation generation by nonlinear mixing of two lasers in a plasma with density hill *Phys. Plasmas* **24** 033104
- [44]. Kimura W D, Milchberg H M, Muggli P, X. Li and W. B. Mori W B 2011 Hollow plasma channel for positron plasma wakefield acceleration *Phy. Rev. Sp. Topics—Accelerators and Beams* **14**, 041301
- [45]. Kant N, Rajput J, Singh A 2018 Electron acceleration from rest to GeV energy by chirped axicon Gaussian laser pulse in vacuum in the presence of wiggler magnetic field *High En. Dens. Phys.* **26**, 16
- [46]. Akhmedzhanov R A, Ilyakov I E, Mironov V A, Suvorov E V, Fadeev D A, and Shishkin B V 2008 Generation of terahertz radiation by the axicon focusing of ionizing laser pulses *JETP Letts.* **88** 569–573

- [47]. Wei X, Liu C, Niu L, Zhang Z, Wang K, Yang Z and Liu J 2015 Generation of arbitrary order Bessel beams via 3D printed axicons at the terahertz frequency range *Appl. Optics* **54** (36) 10641
- [48]. Semenova V A, Kulya M S, Bespalov V G 2016 Spatial-temporal dynamics of broadband terahertz Bessel beams propagation *J. Phys.: Conf. Ser.* **735**, 012063
- [49]. Kulya M S, Semenova V A, Bespalov V G, Petrov N V 2018 On terahertz pulses broadband Gauss-Bessel beam free-space propagation *Sci. Reports* **8**, 1390
- [50]. A. M. Bystrov A M, Vvedenskii N V, Gildenburg V B 2005 Generation of terahertz radiation upon the optical breakdown of a gas *JETP Letters* **82**(12), 753
- [51]. Busch S, Town G E, Koch M 2014 *39th International Conference on Infrared, Millimeter, and Terahertz waves (IRMMW-THz)*, Tucson, **1-2**
- [52]. Sprangle P, Penano JR, Hafizi B, Kapetanacos CA 2004 Ultrashort laser pulses and electromagnetic pulse generation in air and on dielectric surfaces, *Phys. Rev. E* **69** 066415
- [53]. Houard A, Liu Y, Prade B, Tikhonchuk VT, Mysyrowicz A 2008 Strong enhancement of terahertz radiation from laser filaments in air by a static electric field. *Phys. Rev. Lett.* 2008 **100** 255006
- [54]. Malik P, Sharma SC, Sharma R 2017 Generating tunable THz radiation using rippled density plasma driven by density modulated relativistic electron beam *Phys. Plasmas* **24** 073101
- [55]. Kumar S, Singh R, Singh M, and Sharma R 2015 THz radiation by amplitude modulated self-focusing Gaussian laser beam in ripple density plasma *Laser Part. Beams* **33** (2) 257-263
- [56]. Singh R, Sharma R 2015 Terahertz radiation by self focusing amplitude-modulated Gaussian laser beam in magnetized ripple density plasma. *Laser Part. Beams* **33**(4) 741-747
- [57]. Mehta A, Rajput J, Kang K and Kant N 2020 Terahertz generation by beating of two chirped pulse lasers in spatially periodic density plasma *Laser Phys.* **30** 045402

- [58]. Kumar S, Singh RK, Sharma RP 2016 Strong terahertz generation by optical rectification of a super-Gaussian laser beam *EPL* **114** (5): 55003
- [59]. Singh M, Kumar S, Singh RK, Uma R, Sharma RP 2017 High-power terahertz emission in magnetized plasma via optical rectification of a super-Gaussian laser beam. *EPL* **119** (1): 15002
- [60]. Chen Z Y 2013 High field terahertz pulse generation from plasma wakefield driven by tailored laser pulses *Appl. Phys. Lett.*, **102** 241104
- [61]. Andreeva V A, Kosareva O G, Panov N A, Shipilo D E, Solyankin P M, Esaulkov M N, González De Alaiza Martínez P, Shkurinov A P, Makarov V A, Bergé L and Chin S L 2016 Ultrabroad terahertz spectrum generation from an air-based filament plasma *Phys. Rev. Lett.* **116** 063902
- [62]. Zhang Z, Yan L, Du Y, Huang W, Tang C and Huang Z 2017 Generation of high-power, tunable terahertz radiation from laser interaction with a relativistic electron beam *Phys. Rev. Accel. Beams* **20** 050701
- [63]. Liao G Q, Li Y T, Li C, Liu H, Zhang Y H, Jiang W M, Yuan X H, Nilsen J, Ozaki T, Wang W M, Sheng Z M, Neely D, McKenna P and Zhang J 2017 Intense terahertz radiation from relativistic laser-plasma interactions *Plasma Phys. Control. Fusion* **59** 014039
- [64]. S. Vij and Kant N 2019 Generation of terahertz radiation by beating of two color lasers in hot clustered plasma with step density profile *Plasma Res. Express* **1** 025012
- [65]. Mehta A and Kant N 2019 Terahertz radiation generation driven by the frequency chirped laser pulse in magneto-active plasma *Proc. SPIE* 10917 Terahertz, RF, Millimeter, and Submillimeter-Wave Technology and Applications XII, 109170R, March 2019
- [66]. Li C, Liao G-Q, Zhou M-L, Du F, Ma J-L, Li Y-T, Wang W-M, Sheng Z-M, Chen L-M and Zhang J 2016 Backward terahertz radiation from intense laser-solid interactions *Opt. Express* **24** 4010
- [67]. Hamster H, Sullivan A, Gordon S and Falcone R W 1994 Short-pulse

- terahertz radiation from high-intensity-laser-produced plasmas *Phys. Rev. E* **49** 671
- [68]. Bourdier A 1983 Oblique incidence of a strong electromagnetic wave on a cold inhomogeneous electron plasma. Relativistic effects *Phys. Fluids* **26** 1804
- [69]. Lichters R, Meyer-ter-Vehn J and Pukhov A 1996 Short-pulse laser harmonics from oscillating plasma surfaces driven at relativistic intensity *Phys. Plasmas* **3** 3425
- [70]. Wu H C, Sheng Z M and Zhang J 2008 Single-cycle powerful megawatt to gigawatt terahertz pulse radiated from a wavelength-scale plasma oscillator *Phys. Rev. E - Stat. Nonlinear, Soft Matter Phys.* **77** 046405
- [71]. Jones S P P *et al.* 2014, High-temperature electromagnons in the magnetically induced multiferroic cupric oxide driven by intersublattice exchange *Nat. Commun.* **5** 3787
- [72]. Kida N *et al.* 2008, Electric-Dipole Active Two-Magnon Excitation in ab Spiral Spin Phase of a Ferroelectric Magnet $\text{Gd}_{0.7}\text{Tb}_{0.3}\text{MnO}_3$ *Phys. Soc. Jpn.* **77** 123704
- [73]. Komatsu M *et al.* 2015, Terahertz spectral change associated with glass transition of poly- ϵ -caprolactone *J. Appl. Phys.* **117** 133102
- [74]. Wu H C, Sheng Z M, Zhang Q J, Cang Y and Zhang J 2005 Chirped pulse compression in non uniform plasma Bragg gratings *Appl. Phys. Lett.* **87** 201502
- [75]. Sodha M S ,Mishra S K and Mishra S 2009 Focusing of a dark hollow Gaussian electromagnetic beam in a magnetoplasma *J. Plasma Physics* **75**(6) 731–748
- [76]. Sodha, M. S., Ghatak, A. K., and Tripathi, V. K., (1974), Self-focusing of Laser Beams in Dielectrics, Plasmas and Semiconductors, Tata McGraw-Hill, New Delhi
- [77]. Sodha M S, Ghatak A K and Tripathi V K 1976 Self focusing of laser beams in plasmas and semiconductors *Progress in Optics*, E. Wolf, eds., North-Holland, Amsterdam **13** 169

- [78]. Ginzburg L 1970 *The Propagation of Electromagnetic Waves in Plasmas (2nd ed., Addison Wesley, Reading, Mass.)*
- [79]. Booth H A H, Self S A and SHERSBY-HARV R B R 1958 Containment of a fully ionized plasma by radio frequency fields, *J. Electr. and Control.* **4** 434
- [80]. Hora H , Pfirsch D and Schluter A 1967 Beschleunigung von inhomogenen Plasmen durch Laserlicht, *Z. Naturforsch.* **22a**, 278
- [81]. Hora H., 1969, Self-focusing of Laser Beams in a Plasma by Pondermotive Forces, *Z. Physik* **226**, 156. , Hora H 1972 Nonlinear Forces in Laser Produced Plasmas, in: *Laser Interactions and Related Plasma Phenomena Vol. 2*, eds. H. J. Schwarz and H. Hora (Plenum, New York) p. 341
- [82]. Born M and Wolf E 1970 *Principles of Optics (4th ed., Pergamon Press, London)*
- [83]. Boyd, R W 2008 *Nonlinear Optics (Third Edition) Academic Press USA*, pp. 1-3
- [84]. Jafari M J, Jafari Milani, MR, Rezaei S 2019 Terahertz radiation from multiion plasma irradiated by two cross focused Gaussian laser beam *Phys. Plasmas* **26**103107
- [85]. D. Zhang *et al.*, Segmented terahertz electron accelerator and manipulator (STEM) 2018 *Nat. Photonics* **12**, 336
- [86]. Lange C. *et al.* 2014 Extremely non perturbative nonlinearities in GaAs driven by atomically strong terahertz field in gold metamaterials *PRL* **113**, 227401
- [87]. Chin S L *et al.*, 2005 The propagation of powerful femtosecond laser pulses in optical media: physics, applications, and new challenges *Can. J. Phys.* **83**, 863
- [88]. Panagiotopoulos P *et al.* 2015 Super high power mid-infrared femtosecond light bullet *Nat. Photonics* **9**, 543
- [89]. Wolter B *et al.* 2015 Strong-field physics with Mid-IR fields *Phys. Rev. X* **5** 021034
- [90]. Dey I. *et al.*, 2017 Highly efficient broadband terahertz generation from

- ultrashort laser filamentation in liquids *Nat. Commun.***8**, 1184
- [91]. Li R. *et al.* 2019 Broadband and high-power terahertz radiation source based on extended interaction klystron *Sci. Reports* **9**, 4584
- [92]. Yang Y. *et al.* 2020 Terahertz topological photonics for on-chip communication *Nat. Photonics* **14**, 446–451

LIST OF PUBLICATIONS

The work in this thesis is in, part, based on the following publications:

✚ **JOURNAL ARTICLES**

CHAPTER 3

- [1]. **Alka Mehta**, Niti Kant and Shivani Vij, “Generation of terahertz (THz) radiation by p-polarised lasers beating in hot plasma with surface density ripple”, *Laser Physics Letters*, 16, 045403 (2019)

CHAPTER 4

- [2]. **Alka Mehta**, Jyoti Rajput and Niti Kant, “Effect of frequency-chirped laser pulses on terahertz radiation generation in magnetized plasma”, *Laser Physics*, **29**, 095405 (2019)
- [3]. **Alka Mehta**, Jyoti Rajput, K. Kang and Niti Kant, “Terahertz generation by beating of two chirped pulse lasers in spatially periodic density plasma”, *Laser Physics*, **30**, 045402, (2020)

CHAPTER 5

- [4]. **Alka Mehta**, Jyoti Rajput, Shivani Vij and Niti Kant, “Effect of self-focusing of amplitude modulated pulse on terahertz generation in plasma”, *Optics Express*, (Submitted)

✚ **CONFERENCE PROCEEDINGS**

- [5]. **Alka Mehta**, and Niti Kant, “Terahertz (THz) Radiation Generation Driven by The Frequency Chirped Laser Pulse in Magneto-Active Plasma”, *Proc. of SPIE* Vol. **10917** 109170R-2 (2019)
- [6]. **Alka Mehta**, Niti Kant, Vishal Thakur and Jyoti Rajput, 2020 “Numerical Study of Nonlinear Current Density Produced by Beating of Two Chirped Lasers in Plasma with Density-Ripple”, *Journal of Physics: Conference Series*, **1531**, 012037
- [7]. Sandeep Kumar, Niti Kant, Shivani Vij, **Alka Mehta** and Vishal Thakur, 2020 “Production of terahertz radiation by short pulse lasers”, *Journal of Physics: Conference Series*, 1531, 012011

Authors' Bio-Data

ALKA MEHTA

Nanakmatta, +919855788741 alka.officials@gmail.com
Uttarakhand

Ph.D. (Physics)
Lovely Professional University, Punjab



Thesis Title:

“High Power Laser Driven Terahertz Generation in Plasma”.

Supervisor Details:

Prof. Niti Kant
Department of Physics
Lovely Professional University,
Punjab:144411
India.

Basic Details & Interests:

The author was born at Nanakmatta, a small town of Uttarakhand (India), in 1990. In 2013, she received her B.Sc. Degree in PCM (Physics, Chemistry, Mathematics) from Kumaun University, Nainital. In 2015 she completed her M.Sc. in Physics from D.S.B. Campus of Kumaun University with specialization in Spectroscopy Physics under the supervision of the HOD of Physics Department; Dr. Sanjay Pant. Since August, 2016 she has been working at the Department of Physics, Lovely Professional University, Punjab for her Doctorate degree. Her research interests are terahertz radiation, particle acceleration, plasma physics & high harmonic generation. In her spare time, she like to spend time with family, nature, listning music, travelling & in reading books and articles.

Personal Dossier	
Father's Name	Mahesh Chandra Mehta
Permanent address	Alka readymade garments, Gurudwara road, Nanakmatta (262311), Uttarakhand.
Present address	Block-27, Department of Physics, Lovely Professional University, Phagwara (144411), Punjab.
ORCID id	https://orcid.org/0000-0002-9944-0238
Google Scholar id	alka.officials@gmail.com
Date of birth	25/05/1990
Language skills	Hindi, English (Full Proficiency) Punjabi, Sanskrit (Medium Proficiency)

Research Experience						
Name of Employer	Designation	Period	Basic salary	Nature of work	Project Title	Funding Agency
Lovely Professional University, Phagwara (144411), Punjab.	Research Associate (RA)	03/12/2019 to till date	47,000+ HRA	Analytical & Numerical Simulation	Efficient THz radiation during laser-plasma interaction	CSIR, New Delhi
Lovely Professional University, Phagwara (144411), Punjab.	Senior Research Fellow (SRF)	03/11/2018 to 02/12/2019	35,000+ HRA	Analytical & Numerical Simulation	Efficient THz radiation during laser-plasma interaction	CSIR, New Delhi

Academic Credentials				
Degree	University	Year	Percentage/CGPA	Division
Doctor of Philosophy (Ph.D.) in Physics	Lovely Professional University, Punjab.	2016 to 2020	9.25 CGPA	-
Master of Science (M.Sc.) in Physics	Kumaun University, Nainital, Uttarakhand	2013 to 2015	60.02%	First
Bachelor of Science (B.Sc.) in PCM	Kumaun University, Nainital, Uttarakhand	2011 to 2013	70.3%	First

Research Activity			
Short course	Dec 2 nd -5 th , 2015	Terahertz Techniques and Applications	Indian Laser Association at RRCAT, Indore.
Dissertation	July, 2015	Characteristics of 5- Amino Quinoline in different solvents and polymers.	A+ Grade, Kumaun University, Nainital, Uttarakhand.
Conference	Nov 18 th , 2017	One day Ph.D. symposium in Science and Technology.	Lovely Professional University, Punjab.

Technical skills	
Expertise	Solving coupled differential equations using MATHEMATICA Software
Operating Systems	Windows XP, Window7, 8, 8.1, 10, Android.
Software Knowledge	Mathematica, Origin Lab, Microsoft Office (Word, Excel, Power Point, Publisher), Mandeley, LaTeX , SPSS.
Tools Known	Spectrofluorometer, Spectrophotometer.

International Visit				
Country Visited	Duration of visit	Dates		Purpose of visit
		From	To	
USA	15 days	30/01/2019	16/02/2019	Presented paper at International Conference (SPIE)

Association with Professional Bodies	
Optical Society of America (OSA)	Early Career 5-years Membership
Optical Society Of India (OSI)	Life Membership
Plasma Science Society of India (PSSI)	Life Membership
Indian Laser Association (ILA)	Life Membership
American Physical Society (APS) - Physics	Student Membership
Indian Science Congress Association (ISCA)	Life Membership
Society of Photo-Optical Instrumentation Engineers (SPIE)	Student Membership

Additional Responsibilities
Taking responsibilities in organizing an International Conference RAFAS-2019 held at LPU
Took the responsibility of organizing poster session in a national Conference ISCA-106 th -2019 held at LPU
Guiding & Mentoring Undergraduate and Postgraduate project Students

Teaching Experience	
Teaching (01/12/2015 to 31/03/2016)	Teacher for Math and Physics to class 1st to 12th and Supervisor of sub junior section of Co-scholastic activities at Shri Guru Nanak Academy Residential School, Nanakmatta (Affiliated to CBSE, New Delhi), School Code- 09091, Affi. No. 3530084

Online Courses	
Learning How to Learn: Powerful mental tools to help you master tough subjects	University of California, San Diego
Cameras, Exposure, and Photography	Michigan State University
Chinese for Beginners	Peking University
Positive Psychology	The University of North Carolina at Chapel Hill

Extra-Curricular Activities	
Member of National Social Scheme (N.S.S.)	Holding the responsibility to make awareness among the people of Nation.
Member of Red Ribbon Club	Worked as active Volunteer in the College/Community level AIDS Awareness Campaign.

List of Publications	
[6].Alka Mehta, Niti Kant, Vishal Thakur and Jyoti Rajput 2020 “ <u>Numerical Study of Nonlinear Current Density Produced by Beating of Two Chirped Lasers in Plasma with Density-Ripple</u> ”, <i>Journal of Physics: Conference Series</i> , 1531, 012037 https://doi.org/10.1088/1742-6596/1531/1/012037	
[5].Sandeep Kumar, Niti Kant, Shivani Vij, Alka Mehta and Vishal Thakur, 2020 “ <u>Production of terahertz radiation by short pulse lasers</u> ”, <i>Journal of Physics: Conference Series</i> , 1531, 012011 https://doi.org/10.1088/1742-6596/1531/1/012011	
[4].Alka Mehta, Jyoti Rajput, K. Kang and Niti Kant, 2020 “ <u>Terahertz generation by beating of two chirped pulse lasers in spatially periodic density plasma</u> ”, <i>Laser Physics</i> , 30 , 045402 https://doi.org/10.1088/1555-6611/ab7238	

[3]. **Alka Mehta**, Jyoti Rajput and Niti Kant, 2019 “Effect of frequency-chirped laser pulses on terahertz radiation generation in magnetized plasma”, *Laser Physics*, **29**, 095405.

<https://doi.org/10.1088/1555-6611/ab344f>

[2]. **Alka Mehta** and Niti Kant, 2019 “Terahertz radiation generation driven by the frequency chirped laser pulse in magneto-active plasma”, *Proc. of SPIE Vol. 10917* 109170R-2.

<https://doi.org/10.1117/12.2505928>

[1]. **Alka Mehta**, Niti Kant and Shivani Vij, 2019 “Generation of terahertz (THz) radiation by p-polarised lasers beating in hot plasma with surface density ripple”, *Laser Physics Letters*, **16**, 045403. <https://doi.org/10.1088/1555-6611/ab3636>

Future Publications

[1]. **Alka Mehta**, Jyoti Rajput, Shivani Vij and Niti Kant, , “Effect of self-focusing of amplitude modulated pulse on terahertz generation in plasma”, *Optics Express* (Submitted)

Conferences/Seminars Presentation

[1]. **Alka Mehta** and Niti Kant, “Terahertz wave generation in ripple density plasma assisted by frequency chirped laser Pulses”, *12th International Conference on Plasma Science and Applications (ICPSA-2019)*, Poster presentation. Nov 11th-13th, 2019 at Department of Physics, Lucknow University, U.P., India.

[2]. **Alka Mehta**, Niti Kant, Vishal Thakur and Jyoti Rajput, “Numerical study of nonlinear current density produced by beating of two chirped lasers in plasma with density ripple”, *2nd International Conference on Recent Advances in Fundamental and Applied Sciences (RAFAS-2019)*, Oral presentation. Nov 5th-6th, 2019 at Lovely Professional University, Punjab, India.

[3]. **Alka Mehta** and Niti Kant, “Terahertz wave generation in plasma assisted by frequency chirped laser pulses”, *International conference on Photonics Metamaterials & Plasmonics (PMP-2019)*, Poster Presentation. Feb 14th-16th, 2019 at Department of Physics and material science & Engineering, Jaypee Institute of Information Technology, Noida, U.P. India.

[4]. **Alka Mehta** and Niti Kant, “Terahertz radiation generation driven by the frequency chirped laser pulse in magneto-active plasma”, *SPIE Photonics West ‘OPTO’-2019*. Oral Presentation. Feb 3-7, 2019 at San Francisco, California, U.S.A.

[5]. **Alka Mehta** and Niti Kant, “Generation of terahertz (THz) radiation by laser beating in magnetized plasma half-space with surface density ripple”, *106th Indian Science Congress*. Poster presentation. Jan 3-7, 2019 at LPU, Punjab.

[6]. Simranjeet Kaur, **Alka Mehta** and Niti Kant, “Terahertz (THz) radiation Generation in plasma by beating of two co-propagating q-Gaussian laser beams”, *Women Science Congress*. Poster presentation. Jan 5-6, 2019 at LPU, Punjab.

[7]. **Alka Mehta** and Niti Kant, “Terahertz (THz) generation by laser beating in ripple density magneto-plasma”, *33rd National Symposium on Plasma Science & Technology (PLASMA 2018)*. Poster presentation. Dec 4-7, 2018 at Delhi University, New Delhi.

References

<p>Prof. Niti Kant Department of Physics, Lovely Professional University, Phagwara, Punjab, India Email: nitikant@yahoo.com Contact no.: +91 98884 72261</p>	<p>Prof. Ramesh Chandra Department of Physics, Kumaun University, Nainital, Uttarakhand, India Email: rchandra.ntl@gmail.com Contact no.: +91 96906 81836</p>	<p>Prof. Dino Jaroszynski Department of Physics, Scottish University Physics Alliance, Scotland, UK Email: dino@phys.strath.ac.uk Contact no.: 01415483057</p>
---	--	--

Copy of Published work

Letter

Generation of terahertz (THz) radiation by p-polarised lasers beating in hot plasma with surface density ripple

Alka Mehta¹, Niti Kant¹ and Shivani Vij²¹ Department of Physics, Lovely Professional University, G.T. Road, Phagwara 144411, Punjab, India² Department of Applied Sciences, DAV Institute of Engineering and Technology, Jalandhar, 144008, IndiaE-mail: nitikant@yahoo.com

Received 19 December 2018

Accepted for publication 10 January 2019

Published 26 February 2019

**Abstract**

The present communication deals with a scheme to generate terahertz (THz) radiation by electromagnetic Gaussian beams beating in a hot collisionless plasma having a density ripple on its surface, parallel to the z -axis. These p-polarised laser beams propagate in the x - z plane, incident obliquely to the density ripple on the plasma surface, and exert a ponderomotive force on electrons. The plasma electrons start oscillating because the plasma neutrality disturbed by the nonlinearity arises due to the ponderomotive force. This oscillatory velocity beats with the density ripple; as a result, an irrotational current density \vec{J}^{NL} arises at the beating frequency $\omega_1 - \omega_2$ (with $\vec{\nabla} \times \vec{J}^{NL} \neq 0$). This nonlinear current density urges a wave whose frequency is in the THz range. Our results show that, for a set of laser and plasma parameters, the power of emitted THz radiation scales as the square of the density ripple amplitude, as well as the amplitude of the emitted THz wave, decreases with the THz frequency and increases with the incidence angle up to an optimum value. In our case, the maximum normalised amplitude of emitted THz radiation is reached up to 0.038 at laser intensity $\sim 7 \times 10^{14} \text{ W cm}^{-2}$, $\theta = 30^\circ$ and electron temperature $\sim 5 \text{ keV}$ with 30% density ripple.

Keywords: THz radiation, laser, hot plasma, density ripple, oblique incidence

(Some figures may appear in colour only in the online journal)

1. Introduction

The interaction of an intense laser beam with plasma offers various wide-ranging prospective applications of terahertz (THz) in science and technology. The potential outcomes of utilizing THz radiation in environmental monitoring, security, communications technology, food and material sciences, THz imaging and spectroscopy, remote identification of explosive and dangerous chemicals, etc are actively studied by various researchers [1–4]. Non-ionizing THz radiation can be broadly used in biological and medical applications. Radiation reflected and transmitted through biological objects carries

important information for analysis [5]. A promising technique for generating THz radiation is utilizing a short laser pulse [6]. In contrast with photoconductive antennas or optical rectification, laser coupling with the plasma gives an intense and broadband THz pulse. Researchers have both experimentally [7–10] and theoretically [11–19] proposed several techniques for efficient THz generation by considering plasma as a medium.

On the basis of a fluid model, coherent THz radiation was generated by the interaction of bunched relativistic electron beams with a helical wiggler pump [11]. By numerical analysis they showed that the presence of the ion channel can play

a vital role for the THz power enhancement and the maximum power can be tuned with ion-channel density. Malik *et al* [12] proposed a mechanism to tune the frequency and power of THz radiation. They applied an external DC magnetic field and fixed the focus of the emitted radiation by employing triangular lasers for the space-periodical beating in modulated plasma density. Bakhtiari *et al* [13] analytically investigated the effects of laser and plasma parameters on THz generation by beating two dark hollow laser beams in collisional plasma.

Kumar and Tripathi [14] put forward a numerical scheme of THz generation by optical mixing of two collinear laser pulses in rippled density plasma. The linearly polarised lasers propagate through plasma with a density ripple at an angle to the direction of propagation of the laser beam. As a result the phase matched THz wave generation rises for a density ripple of suitable wave number. By increasing the ripple angle the phase matching condition was also obtained, so that the required ripple wave number produced more resonant THz waves. A resonant THz generation was observed by Bhasin and Tripathi [15], by optical rectification of a picosecond laser in a rippled density magneto-plasma. They showed in their results that the magnetic field enhances the power of the emitted THz wave. Tyagi *et al* [16] recently investigated the generation of a THz radiation field inside a plasma channel assisted by an ion acoustic wave. The involvement of the ion acoustic wave is to provide proper phase matching for the momentum conservation. Kumar *et al* [17] suggested an analytical formalism of generating THz radiation in hot plasma with a step density profile. Resonant THz radiation was achieved due to coupling between Langmuir wave and electromagnetic wave. Recently they also proposed a mathematical model for efficient power conversion of radiated THz waves (about 0.15 GW) by nonlinear mixing of two p-polarised lasers in plasma with a density hill [18].

Our work presents a theoretical approach to deal with the generation of THz radiation by the interaction of lasers with the rippled density hot collisionless plasma. The nonlinear mixing of lasers plays an important role when the incident lasers travel at an angle normal to the plasma surface. The transverse intensity gradient of the electromagnetic wave contributes significantly to the plasma wave generation. The generated plasma wave interacts with the electromagnetic wave and leads to the generation of a radiation whose frequency lies in the THz range. Furthermore, the density ripple of a suitable wave number provides the phase matching, which further helps in the efficiency enhancement. Here, we choose hot plasma for the propagation of an electromagnetic wave because in cold plasma only damped oscillations exist. The paper is organised as follows: the theoretical considerations of linear and nonlinear current density in this work are presented in section 2. The THz radiation generation formalism is given in section 3. Observations are discussed in the fourth section and the last section is devoted to the conclusion of the present analysis.

2. Theoretical consideration for current density

Consider the propagation of two p-polarised laser beams, with two different frequencies (ω_1 and ω_2), in a hot plasma of

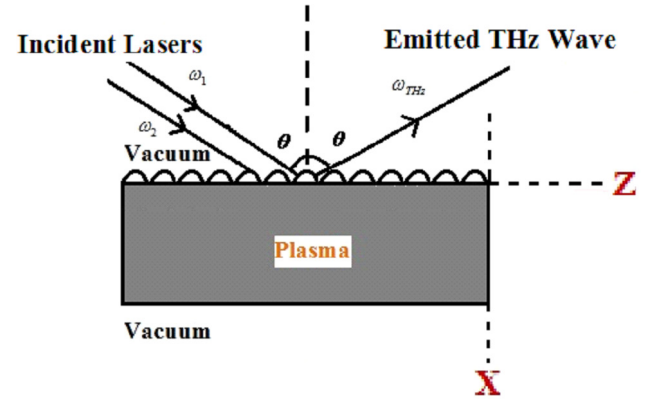


Figure 1. A schematic for THz wave generation in rippled density hot plasma.

electron temperature T_e with a density ripple on its surface. The plasma density ripple can be produced by using various schemes involving a machining beam, a patterned mask and transmission ring grating. By adjusting the period and the mask size, and by changing the groove structure, groove period and the duty cycle of such grating one can control the ripple parameters [15]. It should be noted that the frequency of incident lasers should be much greater than the plasma frequency (ω_p) for efficient THz generation because in this limit ions are treated as stationary. These lasers are incident obliquely at an angle θ (angle of incidence) on the plasma surface (at $x = 0$). The rippled density profile of the plasma electrons can be written as,

$$n = n_0 + n_q, \quad (1)$$

n_0 is the electron plasma density, $n_q (= n_0^0 e^{iqz})$ is the amplitude or periodicity of the density ripple, $q = 2\pi/\lambda$, is the ripple wave vector in the z -direction and λ is the wavelength of the ripple (figure 1). The electric and magnetic components associated with the laser field inside the plasma are given as,

$$\vec{E}_j = (\hat{z} \cos \theta - \hat{x} \sin \theta) A_j e^{-i(\omega_j t - k_j(z \sin \theta + x \cos \theta))} \quad (2)$$

$$\vec{B}_j = \frac{(\vec{k}_j \times \vec{E}_j)}{\omega_j}, \quad (3)$$

where $j = 1, 2$. $k_j = (\omega_j/c) \sqrt{1 - \omega_p^2/\omega_j^2}$, $\omega_p^2 = 4\pi n_0 e^2/m$. Under the influence of these fields, plasma electrons start oscillating. The oscillatory velocity of plasma electrons due to these fields is $\vec{v}_j = e\vec{E}_j/mi\omega_j$. Beating lasers couple nonlinearly at the difference frequency ($\omega_1 - \omega_2$) with the wave vector $(\vec{k}_1 - \vec{k}_2)$, which exerts a nonlinear ponderomotive force on the plasma electrons given as,

$$\vec{F}_{p(\omega_1 - \omega_2)} = -\frac{1}{2} [e(\vec{v}_j \times \vec{B}_j^* - \vec{v}_j^* \times \vec{B}_j) + m(\vec{v}_j \cdot \nabla \vec{v}_j)].$$

By substituting the values of \vec{B}_j and \vec{v}_j in the above expression, the second part on the right hand side becomes zero. Hence, the ponderomotive force comes out

$$\vec{F}_{p(\omega_1 - \omega_2)} = \frac{e^2(\vec{k}_1 - \vec{k}_2)\vec{E}_1 \cdot \vec{E}_2^*}{2mi\omega_1\omega_2}, \quad (4)$$

where the frequency $(\omega_1 - \omega_2)$ lies in the range of THz, e and m are the electronic charge and mass, respectively, and $*$ represents the complex conjugate. This nonlinear ponderomotive force disturbs the plasma neutrality; as a result, plasma electrons start oscillating in the x - z plane inside the plasma to produce a nonlinear velocity. The nonlinear velocity due to this ponderomotive force can be written as,

$$\vec{v}_{(\omega_1 - \omega_2)}^{NL} = -\frac{\vec{F}_p(\omega_1 - \omega_2)}{mi(\omega_1 - \omega_2)} = \frac{e^2}{2m^2\omega_1\omega_2} \frac{\vec{k}_1 - \vec{k}_2}{(\omega_1 - \omega_2)} \vec{E}_1 \cdot \vec{E}_2^*. \quad (5)$$

The divergence of this velocity is finite, i.e. $\vec{\nabla} \cdot \vec{v}_{(\omega_1 - \omega_2)}^{NL} \neq 0$, hence, it gives rise to the nonlinear density perturbation $n_{\omega_1 - \omega_2}^{NL}$ at $(\omega_1 - \omega_2)$ and $(\vec{k}_1 - \vec{k}_2)$. By solving the equation of continuity, $\partial n_{\omega_1 - \omega_2}^{NL} / \partial t + \vec{\nabla} \cdot (n_0 \vec{v}_{\omega_1 - \omega_2}^{NL}) = 0$, we obtain,

$$n_{\omega_1 - \omega_2}^{NL} = \frac{n_0(k_1 - k_2)(\hat{z} \sin \theta + \hat{x} \cos \theta)}{(\omega_1 - \omega_2)},$$

$$\vec{v}_{\omega_1 - \omega_2}^{NL} = \frac{\omega_p^2}{(\omega_1 - \omega_2)^2} \frac{(k_1 - k_2)^2}{8\pi m \omega_1 \omega_2} \vec{E}_1 \cdot \vec{E}_2^*. \quad (6)$$

This density perturbation produces a self-consistent space charge field $\vec{E}_s = -\vec{\nabla} \phi_S$, which also causes a density perturbation as, $n_{\omega_1 - \omega_2}^L = (k_1 - k_2)^2 \chi_e \phi_S / 4\pi e$. Here, $\chi_e = -\omega_p^2 / (\omega_1 - \omega_2)^2$ is the free electron plasma susceptibility. Now, using the Poisson equation, $\nabla^2 \phi_S = 4\pi e (n_{\omega_1 - \omega_2}^L + n_{\omega_1 - \omega_2}^{NL})$, we obtain the self-consistent space charge potential

$$\phi_S = -\frac{e\omega_p^2(\vec{E}_1 \cdot \vec{E}_2^*)}{2m\omega_1\omega_2((\omega_1 - \omega_2)^2 - \omega_p^2)}. \quad (7)$$

Hence, the net electron velocity due to the ponderomotive force and the self-consistent field is written as,

$$\vec{v}_{\omega_1 - \omega_2} = \vec{v}_{\omega_1 - \omega_2}^{NL} + \frac{e\vec{E}_s}{mi(\omega_1 - \omega_2)}$$

$$= \frac{e^2(\hat{x}k_x + \hat{z}k_z)}{2m^2\omega_1\omega_2} \frac{(\omega_1 - \omega_2)}{((\omega_1 - \omega_2)^2 - \omega_p^2)} \vec{E}_1 \cdot \vec{E}_2^*, \quad (8)$$

where $\vec{\nabla} = i(k_1 - k_2)(\hat{z} \sin \theta + \hat{x} \cos \theta)$. The net velocity $\vec{v}_{\omega_1 - \omega_2}$ is large, when $(\omega_1 - \omega_2)$ is close to ω_p . Velocity $\vec{v}_{\omega_1 - \omega_2}$ beats with the density ripple to produce a nonlinear current density at $(\omega_1 - \omega_2)$, \vec{k} ; where $\vec{k} = \vec{k}_1 - \vec{k}_2 + \vec{q}$, which is responsible for THz radiation generation. The nonlinear current density in the x - z plane can be written as,

$$\vec{J}_{(\omega_1 - \omega_2)}^{NL} = -\frac{e}{2} n_q \vec{v}_{\omega_1 - \omega_2}$$

$$= -\frac{e^3 n_q^0 e^{iqz} (\omega_1 - \omega_2)}{4m^2 \omega_1 \omega_2} \frac{(\hat{x}k_x + \hat{z}k_z)}{((\omega_1 - \omega_2)^2 - \omega_p^2)} (\vec{E}_1 \cdot \vec{E}_2^*). \quad (9)$$

If one includes collisions, $((\omega_1 - \omega_2)^2 - \omega_p^2)$ in equation (9) is replaced by $[(\omega_1 - \omega_2)(\omega_1 - \omega_2 + iv) - \omega_p^2]$, where v is the frequency of electron collision. Since this does not alter our results much, we are not taking it into consideration here. This nonlinear current density would excite the p-polarised

THz waves, and couples to the wave associated with the space charge field. Suppose that the self-consistent electric field of this composite wave is:

$$\vec{E}_{(\omega_1 - \omega_2)} = \vec{A}(x) e^{-i[(\omega_1 - \omega_2)t - k_z z]} \quad (10)$$

where $k_z = k_{1z} - k_{2z}$. The plasma electrons start oscillating under the influence of this self-consistent field. The drift velocity of plasma electrons at THz wave frequency ($\omega_{THz} = \omega_1 - \omega_2$) due to this self-consistent field can be derived by solving equation of motion and Poisson's equations simultaneously as;

$$\vec{v}_{\omega_1 - \omega_2}^L = \frac{e\vec{E}_{(\omega_1 - \omega_2)}}{mi(\omega_1 - \omega_2)} - \frac{v_{th}^2 \varepsilon_0}{n_0 i e (\omega_1 - \omega_2)} \vec{\nabla} (\vec{\nabla} \cdot \vec{E}_{(\omega_1 - \omega_2)}), \quad (11)$$

where, $v_{th} = (T_e/m)^{1/2}$ is the thermal velocity of electrons. Here, $v_{th} \ll \omega_{THz}/k$, so we ignore the kinetic effect. The linear current density due to the oscillatory motion of plasma electrons is,

$$\vec{J}_{(\omega_1 - \omega_2)}^L = -n_0 e \vec{v}_{(\omega_1 - \omega_2)}^L = -\frac{n_0 e^2 \vec{E}_{(\omega_1 - \omega_2)}}{mi(\omega_1 - \omega_2)}$$

$$+ \frac{v_{th}^2 \varepsilon_0}{i(\omega_1 - \omega_2)} \vec{\nabla} (\vec{\nabla} \cdot \vec{E}_{(\omega_1 - \omega_2)}). \quad (12)$$

3. Formalism of THz generation

The wave equation for THz generation, using Maxwell's equations can be written as:

$$\nabla^2 \vec{E} - \vec{\nabla} (\vec{\nabla} \cdot \vec{E}) \left(1 - \frac{v_{th}^2}{c^2}\right)$$

$$+ \frac{1}{c^2} ((\omega_1 - \omega_2)^2 - \omega_p^2) \vec{E} = -\frac{i(\omega_1 - \omega_2)}{c^2 \varepsilon_0} \vec{J}_{\omega_1 - \omega_2}^{NL}. \quad (13)$$

This equation provides two well-defined solutions in the absence of nonlinear sources: the first with $\vec{\nabla} \cdot \vec{E} = 0$, is an electromagnetic wave, and the second with $\vec{\nabla} \times \vec{E} = 0$, is a Langmuir wave, with corresponding dispersion relations $k_{mx} = ((\omega_1 - \omega_2)^2 - \omega_p^2 - k_z^2 c^2)^{1/2}/c$ and $k_{sx} = ((\omega_1 - \omega_2)^2 - \omega_p^2 - k_z^2 v_{th}^2)^{1/2}/v_{th}$, and are given in equations (14) and (15) respectively:

$$\vec{E}_m = A_m \left(\hat{x} - \frac{k_{mx}}{k_z} \hat{z} \right) e^{ik_{mx}x} e^{-i[(\omega_1 - \omega_2)t - k_z z]}, \quad (14)$$

$$\vec{E}_s = A_s \left(\hat{x} + \frac{k_z}{k_{sx}} \hat{z} \right) e^{ik_{sx}x} e^{-i[(\omega_1 - \omega_2)t - k_z z]}. \quad (15)$$

The isothermal approximation is inferred for the electron response in this deduction. One can make it valid in the adiabatic approximation by suitably multiplying the electron temperature by the ratio of specific heat at constant pressure and volume. In the presence of a nonlinear source, a particular

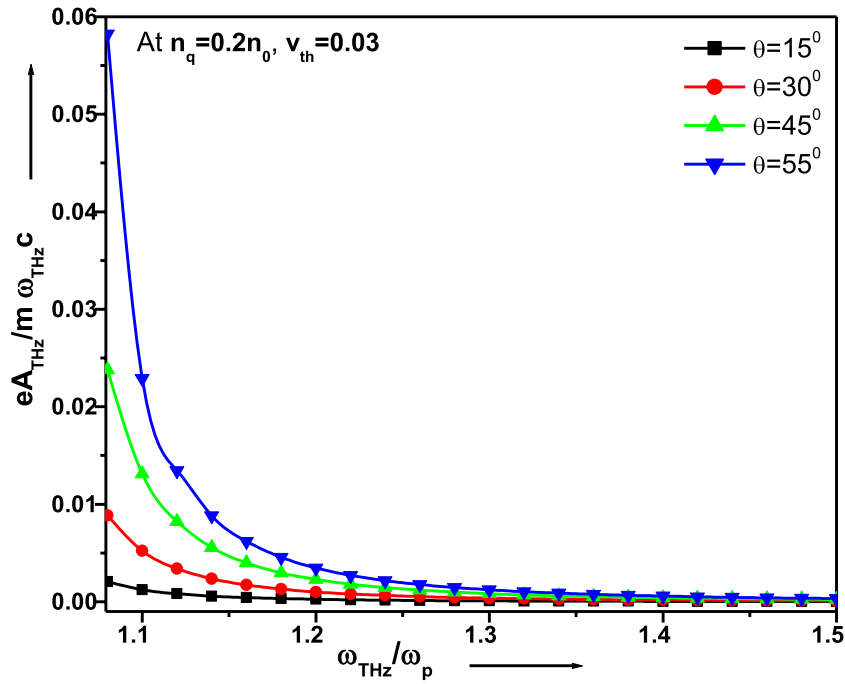


Figure 2. Variation of the normalised THz amplitude ($eA_{\text{THz}}/m\omega_{\text{THz}}c$) with the normalised THz frequency ($\omega_{\text{THz}}/\omega_p$) for different values of θ at $T_e = 0.5$ keV, $\omega_1 = 1.973 \times 10^{14}$, $\omega_2 = 1.783 \times 10^{14}$ and $n_q = 0.2n_0$.

solution is obtained from the wave equation (13) by putting $\vec{\nabla} \times \vec{E} = 0$:

$$\vec{E}_P = -\frac{i(\omega_1 - \omega_2)}{\varepsilon_0[(\omega_1 - \omega_2)^2 - \omega_p^2 - k^2 v_{th}^2]} \vec{J}_{\omega_1 - \omega_2}^{NL}. \quad (16)$$

Here, we have $\vec{\nabla} \times \vec{E}_P = 0$ and $\vec{\nabla} \times \vec{E}_s = 0$, therefore, no magnetic field is associated with both these components. Hence, the only electromagnetic wave field \vec{E}_m is responsible for the associated magnetic field \vec{H}_m . Therefore,

$$\vec{H}_m = \frac{\vec{k}_m \times \vec{E}_m}{\mu_0(\omega_1 - \omega_2)} = \hat{y} A_m \frac{k_{mx}^2 + k_z^2}{\mu_0 k_z (\omega_1 - \omega_2)} e^{ik_{mx}x} e^{-i[(\omega_1 - \omega_2)t - k_z z]}. \quad (17)$$

Only the outgoing part of an electromagnetic wave exists for $x < 0$ (in vacuum region), so that

$$\begin{aligned} \vec{E}_r &= A_r \left(\hat{x} + \frac{k_x}{k_z} \hat{z} \right) e^{-ik_x x} e^{-i[(\omega_1 - \omega_2)t - k_z z]}, \\ \vec{H}_r &= \hat{y} A_r \frac{k_x^2 + k_z^2}{\mu_0 k_z (\omega_1 - \omega_2)} e^{-ik_x x} e^{-i[(\omega_1 - \omega_2)t - k_z z]}. \end{aligned} \quad (18)$$

At $x = 0$, three boundary conditions can be obtained. For the first and second boundary conditions E_z and H_y must be continuous at $x = 0$, therefore, the first boundary condition ($E_{mz} + E_{sz} + E_{Pz} = E_{rz}$) and the second boundary condition ($H_{my} = H_{ry}$), simultaneously give:

$$A_s \frac{k_z^2}{k_{sx}} = A_r k_x + A_m k_{mx} + \frac{i(\omega_1 - \omega_2) k_z J_z^{NL}(\omega_1 - \omega_2)}{\varepsilon_0[(\omega_1 - \omega_2)^2 - \omega_p^2 - k^2 v_{th}^2]}, \quad (19)$$

$$A_m = A_r \frac{k_x^2 + k_z^2}{k_{mx}^2 + k_z^2}. \quad (20)$$

Now, taking the z -component of wave equation (13) and integrating it over x between the limits 0^- to 0^+ , to deduce the third boundary condition as;

$$\begin{aligned} A_r (k_x^2 + k_z^2)^2 &= A_m [k_{mx}^2 + k_z^2] - \frac{v_{th}^2}{c^2} (A_m k_z^2 + A_s k_z^2) \\ &+ \frac{i(\omega_1 - \omega_2) k_x k_z J_z^{NL}(\omega_1 - \omega_2) v_{th}^2 / c^2}{\varepsilon_0[(\omega_1 - \omega_2)^2 - \omega_p^2 - k^2 v_{th}^2]}. \end{aligned} \quad (21)$$

By solving equations (19)–(21) we get;

$$A_{\text{THz}} = \frac{i}{\varepsilon_0} \frac{k_x k_z (1 + k_{sx}/k_x)}{(k_x k_{sx} + k_z^2 + k_{mx} k_{sx})} \frac{(\omega_1 - \omega_2) J_z^{NL}(\omega_1 - \omega_2)}{[(\omega_1 - \omega_2)^2 - \omega_p^2 - k^2 v_{th}^2]}. \quad (22)$$

This is the expression for the amplitude of the reflected THz wave (here, A_r is replaced by A_{THz}).

4. Observations and discussion

Equation (22) is solved numerically for a set of suitable laser and plasma parameters. The values of the chosen parameters for computation are as follows: the normalised laser intensities, $a_1 = eA_0/m\omega_1 c = 0.22$, $a_2 = eA_0/m\omega_2 c = 0.24$ (A_0 is the amplitude of the incident laser beam corresponding to the laser intensity, $I \sim 7 \times 10^{14} \text{ W cm}^{-2}$), two different wavelengths, $\lambda_1 = 9.57 \mu\text{m}$, $\lambda_2 = 10.57 \mu\text{m}$ (for a CO₂ laser), $\omega_1 = 1.973 \times 10^{14}$, $\omega_2 = 1.783 \times 10^{14}$, electron thermal velocity $v_{th} = 0.03 c$ and $0.1 c - 0.18 c$, corresponding to electron temperature $T_e = 0.5$ keV, 5 keV ($0.2c$ corresponds to 20 keV) for $\theta = 15^\circ - 55^\circ$.

In figure 2, we have plotted the normalised THz amplitude $eA/m\omega_{\text{THz}}c$ with the normalised THz frequency $\omega_{\text{THz}}/\omega_p$ (where $\omega_{\text{THz}} = \omega_1 - \omega_2$) of the THz wave for different values of incidence angle θ . It can be observed from this figure that the amplitude decreases with increasing THz frequency. This amplitude is maximum when ω_{THz} is comparable with ω_p (due

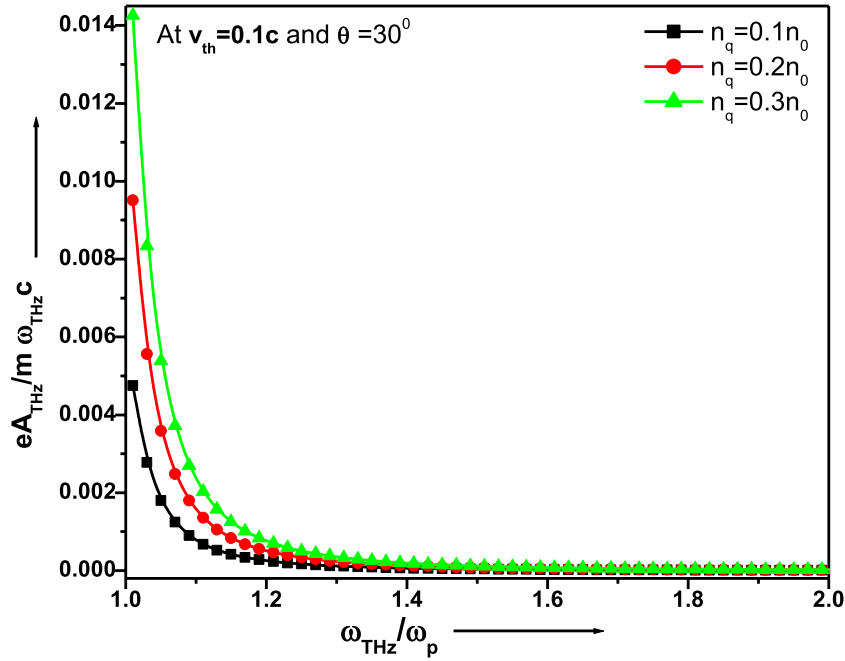


Figure 3. Variation of the normalised THz amplitude with the normalised THz frequency for different values of density ripple, at a constant angle of incidence $\theta = 30^\circ$ at $T_e = 5$ keV. The frequencies of incidence laser beams are the same as those in figure 2.

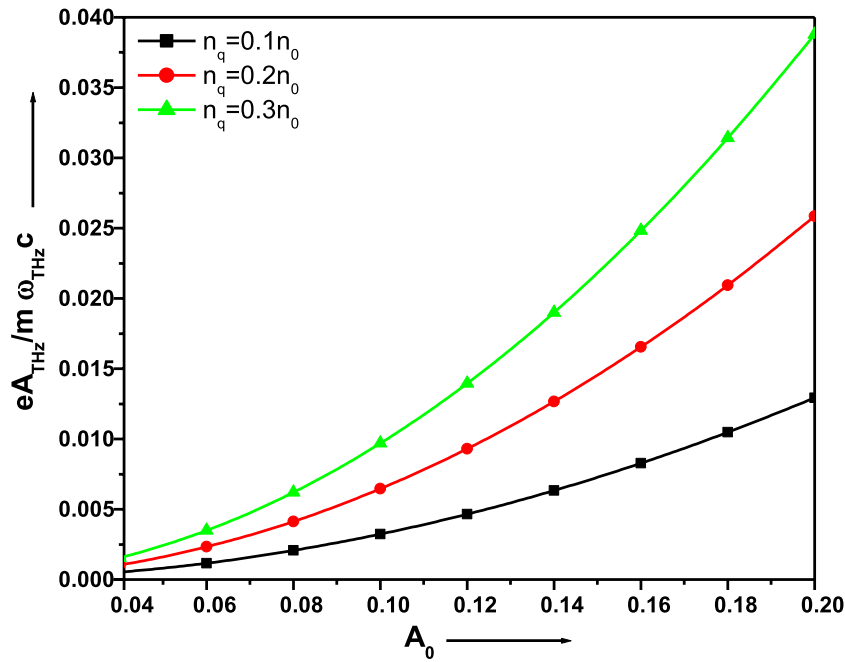


Figure 4. A spectrum of the normalised amplitude of the emitted THz wave versus the normalised amplitude of incident laser beams at $v_{th} = 0.1c$, corresponding to $T_e = 5$ keV, $\omega_{THz}/\omega_p = 1.08$, $n_q = 0.3n_0$ and $\theta = 30^\circ$. All other parameters are the same as those in figure 2.

to resonance). It is also observed that with increasing the value of θ from 15° to 55° , the normalised amplitude increases from 0.002 to 0.013 at $n_q = 0.2n_0$. We obtained the highest values at $n_q = 0.3n_0$ but it is difficult to create a 30% ripple experimentally, so we plotted our results corresponding to a 20% density ripple.

The variation of normalised THz amplitude is plotted with the increasing value of THz normalised frequency for different values of density ripple ($n_q = 0.1n_0, 0.2n_0, 0.3n_0$) shown in figure 3, at $\theta = 30^\circ$. The ripple helps THz generation in the

following two ways: first it makes the nonlinear current irrotational, and second by providing the phase matching (when the ripple wave vector \vec{q} equals $k_{THz} - \vec{k}_1 + \vec{k}_2$, where \vec{k}_1 and \vec{k}_2 are the laser wave vector and k_{THz} is the THz wave vector). Therefore, it is clear from this graph that the maximum momentum is transferred to the electrons at resonance conditions. On the other hand, the effect of the amplitude of density ripple n_q is to enhance the THz wave field. The higher the amplitude of the density ripple, the greater the number of electrons that take part in the excitation of radiation. Figure 3

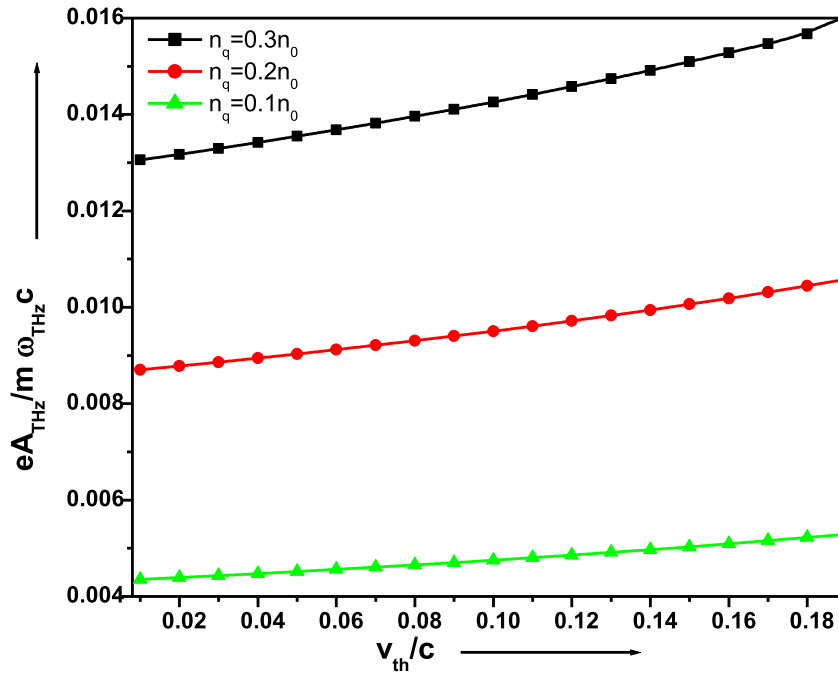


Figure 5. Variation of the normalised amplitude of THz yield ($eA_{\text{THz}}/m\omega_{\text{THz}}c$) with normalised velocity (v_{th}/c) for different values of density ripple at $\theta = 30^\circ$ and $\omega_n = 1.08$.

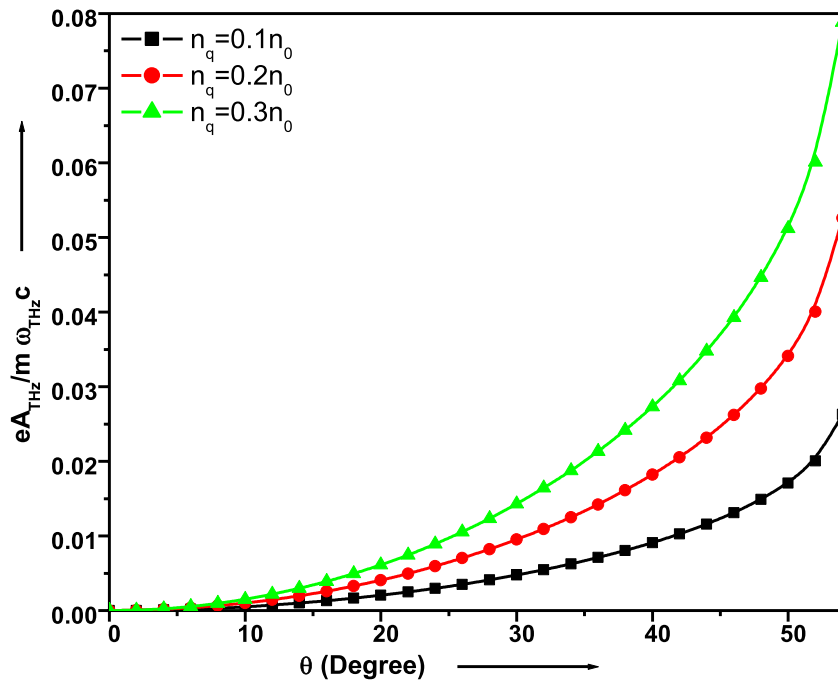


Figure 6. Variations of the normalised THz amplitude ($eA_{\text{THz}}/m\omega_{\text{THz}}c$) with the specular angle θ for different values of density ripple at $\omega_n = 1.08$.

also infers that the frequency distribution of the reflected THz wave is closely related to the incidence angle and coupling. Therefore, it could play an important role in the generation of THz waves of higher intensity.

For figure 4, we calculated the normalised amplitude for different intensity ranges and finally plotted the graph between the normalised amplitude of emitted THz waves and the amplitude of the incident laser (A_0) at $\theta = 30^\circ$, $n_q = 0.3n_0, 0.2n_0, 0.1n_0$ and $\omega_{\text{THz}}/\omega_p = 1.08$. This exhibits a

variation, which displays the linear relationship of THz amplitude with the intensity of incident lasers. The physical reason is that, with the enhancement of the laser intensity, the strength of the ponderomotive force, and hence the initial ionization of the plasma, increases. Thus, with the increase of free electron density, the nonlinearity increases. As THz generation is a nonlinear phenomenon, it enhances more and more. The highest value of the normalised amplitude corresponding to the incident laser beam intensity $\sim 7 \times 10^{14} \text{ W cm}^{-2}$ achieved is

0.038 in our scheme. We neglect the effect of collisions in our analysis. It can be seen [14] that in the presence of collisions, the term ω^2 is replaced by $\omega(\omega + iv)$ in equation (7). Since the imaginary term leads to resistivity and extracts energy from the electrons in collisions, consequently the efficiency decreases.

Figure 5 shows the variation of the normalised amplitude of the THz wave with normalised velocity for different values of ripple density $n_q = 0.1, 0.2$ and 0.3 at $\theta = 30^\circ$, together with numerical calculations. It is clear from figure 5 that initially at $n_q = 0.1n_0$, the THz wave of small amplitude is generated; it starts increasing up to 0.16, as the ripple increases to 30%. Similar results were observed by Kumar *et al* [17]. We observe that the normalised THz amplitude peaks at around 0.016 at thermal velocity $\sim 0.19c$ correspond to the electron temperature ~ 20 keV. This is a very high electron temperature, therefore, in our analysis the thermal velocity is valid up to $0.19c$, beyond which it will not be valid. Figure 6 shows the variation of the normalised amplitude of the THz wave with the specular angle at different values of ripple density. The THz wave amplitude increases linearly with the density ripple and specular angle from 0 to 55° , and shows a maximum at 55° .

5. Conclusion

The generation of THz radiation via nonlinear mixing of two laser pulses in hot plasma is a fetching alternative. We have mathematically investigated the laser beat wave excitation of the terahertz radiation in hot collisionless plasma with a density ripple on its surface. In the presence of a Gaussian laser beam, the plasma gets depleted from the high field region to the low field region on account of the ponderomotive force. From the above analysis it can be concluded that the efficiency and the amplitude of the reflected THz field are sensitive not only to the density ripple but to the angle of incidence and the frequency of the beating lasers. It increases with the plasma density and angle of incidence θ . The frequency of the emission of the resonant signal is tunable with the ripple density amplitude [20]. Here, we ignored the kinetic damping, which is justified when $v_{th} \ll \omega_{THz}/k_{THz}$. We have also not considered the Landau damping of the electrostatic part of the ω_{THz} frequency wave associated with the electromagnetic THz wave. For the THz frequency substantially greater than the maximum plasma frequency ($(\omega_{THz} - \omega_p)$ greater than the Landau damping rate), this effect may not alter the results significantly. Also, we have neglected the effect of beam size, so the THz emission occurs if, and only if, $\theta \neq 0$. On the other hand, at $\theta = 0$ the nonlinear current density has no transverse component; as a result, electromagnetic radiation does not take place [21, 22]. Therefore, the fact that the laser spot size must be bigger than the THz wavelength is the necessary condition for validation of the present scheme. On account of nonlinear coupling between the electromagnetic wave and plasma wave, the power associated with the plasma wave and generated THz yield are also accordingly modified. Wu *et al* [23] examined a strong THz emission from a non-uniform

plasma slab in contrast to a uniform slab, and the numerically evaluated conversion efficiency is in fairly good agreement with their particle-in-cell simulation results. This shows a great plausibility for developing a tunable THz source with the power for use in medical applications.

Acknowledgment

This work was supported by a financial grant from CSIR, New Delhi, India, under Project No. 03(1438)/18/EMR-II.

References

- [1] Siegel P H 2002 Terahertz technology *IEEE Trans. Microwave Theory Technol.* **50** 910
- [2] Dhillon S S *et al* 2017 The 2017 terahertz science and technology roadmap *J. Phys. D: Appl. Phys.* **50** 043001
- [3] Wilkink G J and Grundt J E 2011 Invited review article: current state of research on biological effects of terahertz radiation *J. Infrared Millim. Terahertz Waves* **32** 1074
- [4] Kawase M 2012 Application of terahertz waves to food science *Food Sci. Technol. Res.* **18** 601
- [5] Pickwell E and Wallace V P 2006 Biomedical applications of terahertz technology *J. Phys. D: Appl. Phys.* **39** R301
- [6] Hoffmann M C and Fülöp J A 2011 Intense ultrashort terahertz pulses: generation and applications *J. Phys. D: Appl. Phys.* **44** 083001
- [7] Andreeva V A *et al* 2016 Ultrabroad terahertz spectrum generation from an air-based filament plasma *Phys. Rev. Lett.* **116** 063902
- [8] Zhang Z, Yan L, Du Y, Huang W, Tang C and Huang Z 2017 Generation of high-power, tunable terahertz radiation from laser interaction with a relativistic electron beam *Phys. Rev. Accel. Beams* **20** 050701
- [9] Liao G Q *et al* 2017 Intense terahertz radiation from relativistic laser-plasma interactions *Plasma Phys. Control. Fusion* **59** 014039
- [10] Li C, Liao G-Q, Zhou M-L, Du F, Ma J-L, Li Y-T, Wang W-M, Sheng Z-M, Chen L-M and Zhang J 2016 Backward terahertz radiation from intense laser-solid interactions *Opt. Express* **24** 4010
- [11] Hasanbeigi A, Mehdian H and Gomar P 2015 Enhancement of terahertz radiation power from a prebunched electron beam using helical wiggler and ion-channel guiding *Phys. Plasmas* **22** 123116
- [12] Malik A K and Malik H K 2013 Tuning and focusing of terahertz radiation by dc magnetic field in a laser beating process *IEEE J. Quantum Electron.* **49** 232
- [13] Bakhtiari F, Golmohammady S, Yousefi M, Kashani F D and Ghafary B 2015 Generation of terahertz radiation in collisional plasma by beating of two dark hollow laser beams *Laser Part. Beams* **33** 463
- [14] Kumar M and Tripathi V K 2012 Resonant terahertz generation by optical mixing of two laser pulses in rippled density plasma *IEEE J. Quantum Electron.* **48** 1031
- [15] Bhasin L and Tripathi V K 2009 Terahertz generation via optical rectification of x-mode laser in a rippled density magnetized plasma *Phys. Plasmas* **16** 103105
- [16] Tyagi Y, Tripathi D, Walia K and Garg D 2018 Ion acoustic wave assisted laser beat wave terahertz generation in a plasma channel *Phys. Plasmas* **25** 043118
- [17] Kumar M, Tripathi V K and Jeong Y U 2015 Laser driven terahertz generation in hot plasma with step density profile *Phys. Plasmas* **22** 063106

- [18] Kumar M, Lee K, Hee Park S, Uk Jeong Y and Vinokurov N 2017 Terahertz radiation generation by nonlinear mixing of two lasers in a plasma with density hill *Phys. Plasmas* **24** 033104
- [19] Bulanov S S, MacChi A, Maksimchuk A, Matsuoka T, Nees J and Pegoraro F 2007 Electromagnetic pulse reflection at self-generated plasma mirrors: laser pulse shaping and high order harmonic generation *Phys. Plasmas* **14** 093105
- [20] Hamster H, Sullivan A, Gordon S and Falcone R W 1994 Short-pulse terahertz radiation from high-intensity-laser-produced plasmas *Phys. Rev. E* **49** 671
- [21] Bourdier A 1983 Oblique incidence of a strong electromagnetic wave on a cold inhomogeneous electron plasma. Relativistic effects *Phys. Fluids* **26** 1804
- [22] Lichters R, Meyer-ter-Vehn J and Pukhov A 1996 Short-pulse laser harmonics from oscillating plasma surfaces driven at relativistic intensity *Phys. Plasmas* **3** 3425
- [23] Wu H C, Sheng Z M and Zhang J 2008 Single-cycle powerful megawatt to gigawatt terahertz pulse radiated from a wavelength-scale plasma oscillator *Phys. Rev. E* **77** 046405

PROCEEDINGS OF SPIE

[SPIDigitalLibrary.org/conference-proceedings-of-spie](https://spiedigitallibrary.org/conference-proceedings-of-spie)

Terahertz radiation generation driven by the frequency chirped laser pulse in magneto-active plasma

Alka Mehta, Niti Kant

Alka Mehta, Niti Kant, "Terahertz radiation generation driven by the frequency chirped laser pulse in magneto-active plasma," Proc. SPIE 10917, Terahertz, RF, Millimeter, and Submillimeter-Wave Technology and Applications XII, 109170R (1 March 2019); doi: 10.1117/12.2505928

SPIE.

Event: SPIE OPTO, 2019, San Francisco, California, United States

Terahertz radiation generation driven by the frequency chirped laser pulse in magneto-active plasma

Alka Mehta* and Niti Kant

*Department of Physics, Lovely Professional University,
G.T. Road, Phagwara 144411, Punjab, India*

ABSTRACT

This mathematical model deals with the nonlinear response of a magneto-active plasma to the interaction of frequency chirped laser pulses. The beating lasers produce a nonlinear ponderomotive force due to their oscillatory motion. This force drives a nonlinear current, which is responsible for the THz-wave generation at beat frequency. The influence of the external magnetic field on the optimization process of THz field amplitude is investigated numerically. A linear frequency chirp increases the duration of nonlinear interaction of laser pulse with plasma electrons and hence, enforces the resonance for longer duration. The presence of magnetic field further improves the resonance condition. Our numerical simulations reveal that there is a significant enhancement in the THz field strength for optimized value of chirp parameter and magnetic field.

Keywords: Terahertz wave generation, Frequency chirped laser, Magneto-active plasma.

1. INTRODUCTION

Terahertz (THz) generation phenomenon emerges out as a versatile tool during the recent decade due to its association with the versatile wide range of applications like material characterization, medical diagnosis, structural imaging etc [1-2]. Specially, optically generated THz pulses, produced from difference-frequency generation (DFG), are remarkably reliable for the above mentioned applications as they are far efficient and highly tunable. Although, THz frequency pulses achieved from accelerator-based sources are restricted by the peak intensity and bandwidth. That is why, after the invention of highly intense tabletop lasers, the accelerator-based systems have captured awareness in this field. It is to be noted that THz frequency radiation can also be realized from tenuous gases irradiated by ultrashort lasers [3]. It has been reported that the longitudinal intonation in formed plasmas and the self-consistent currents produced due to laser-based ionization of gases are mainly accountable for THz radiation.

*Email: alka.officials@gmail.com

The principal challenges in the development of THz branch are establishing high conversion efficiencies and their scaling up to higher energies. Efforts have been continuously made for the betterment of THz radiation quality and efficiency. One of the same is introduction of frequency chirp and external magnetic field. Frederike et al. [4] have realized the generation of THz generation in periodically poled lithium niobate (PPLN) due to frequency chirped laser pulses, which are slightly delayed. They have reported a narrowband THz radiation with internal conversion efficiencies up to 0.13% with a multi-cycle THz energy of 40μJ. They reported that chirp and delay pumping of PPLN is a promising scheme for narrowband THz generation at m level. On the same lines, in order to realize effective THz generation, Kim et al. [5] have reported generation of THz super-continuum radiation with a remarkable efficiency of $> 10^{-4}$ and bandwidth in excess of 75 THz.

Similarly, Wang et al. [3] have studied THz mechanism from gas targets irradiated by short laser pulses. They analysed that chirped laser pulses helps in generating strong THz pulses with amplitudes scaling linearly with laser amplitude. The external magnetic field also plays an important role in enhancing THz efficiency. Singh et al. [6] have studied the THz generation by optical rectification of Gaussian and Hyperbolic shapes of laser in magnetized plasma. They reported that applied axial magnetic field enhanced the yield of THz power via cyclotron resonance. Varshney et al. [7] have observed strong THz radiation by ordinary mode laser-beating in a rippled density magnetized plasma. They reported that applied magnetic field plays two crucial roles here. On the first end, it controls the phase velocity as well as group velocity of lasers and on the other side; it also controls the polarization of generated THz wave. Shivani et al. [8] recently investigated THz radiation using vertically aligned array of Carbon nanotube. They applied wiggler magnetic field to enhance the efficiency of THz radiation of nanoantenna which provides the necessary momentum to the generated THz radiation. They also explore the impact of radius and length of nanotubes on the efficiency of THz generation.

In the present manuscript, we are interested to give a theoretical model for efficient THz radiation generation in magneto-plasma due to frequency chirped laser pulses. Here, the plasma is magnetized with static magnetic field applied externally. The paper is organised as follows: the theoretical considerations of ponderomotive force and nonlinear current density along with the THz radiation generation formalism in this work are presented in Sec. 2. Observations are discussed in the 3rd section and the last section is devoted to the conclusion of present analysis.

2. THEORETICAL CONSIDERATIONS

2.1 Ponderomotive force

Consider a plasma of density n_0 with static magnetic field $\vec{B}_s = B_s \hat{y}$. Two laser beams of frequencies ω_1 and ω_2 propagate through the plasma with electric field, $\vec{E}_j = A_j e^{-i(\omega_j t - k_j z)}$ where, $j = 1, 2$, $k_j \approx (\omega_j / c)$.

Let us consider a positive chirp frequency $\omega_1 = \omega_0[1 + b\omega_0(t - z/c)]$, where b is the frequency chirp parameter, c is the velocity of light, and frequency $(\omega_1 - \omega_2 = \omega_r)$ lies in the range of THz. Thus the electric field of these two waves can be represented as,

$$\vec{E}_1 = A_1 e^{-i\omega_1(t-z/c)} \quad (1)$$

$$\vec{E}_2 = A_2 e^{-i(\omega_1 - \omega_r)(t-z/c)} \quad (2)$$

The lasers impart an oscillatory velocity to the plasma electrons, $\vec{v}_1 = e\vec{E}_1 / m i \omega_0 (1 + 2b\omega_0(t - z/c))$ and $\vec{v}_2 = e\vec{E}_2 / m i \omega_0 [(1 + 2b\omega_0(t - z/c)) - \omega_r / \omega_0]$ along with the nonlinear terahertz ponderomotive force as,

$$\vec{F}_{\omega_r}^p = -\frac{m}{2} [\nabla(\vec{v}_1 \cdot \vec{v}_2^*)] - \hat{z} i k_r e^2 \vec{E}_1 \cdot \vec{E}_2^* \left[\left(1 + 2b\omega_0\left(t - \frac{z}{c}\right)\right)^2 - \frac{\omega_r \left(1 + 2b\omega_0\left(t - \frac{z}{c}\right)\right)}{\omega_0} + 2 \frac{i b \omega_r}{c k_r} \left\{1 - \frac{2\omega_0}{\omega_r} \left(1 + 2b\omega_0\left(t - \frac{z}{c}\right)\right)\right\} \right] \quad (3)$$

$$\vec{F}_{\omega_r}^p = \frac{\left[\left(1 + 2b\omega_0\left(t - \frac{z}{c}\right)\right)^2 - \frac{\omega_r \left(1 + 2b\omega_0\left(t - \frac{z}{c}\right)\right)}{\omega_0} + 2 \frac{i b \omega_r}{c k_r} \left\{1 - \frac{2\omega_0}{\omega_r} \left(1 + 2b\omega_0\left(t - \frac{z}{c}\right)\right)\right\} \right]}{2m\omega_0^2 \left(1 + 2b\omega_0\left(t - \frac{z}{c}\right)\right)^2 \left[\left(1 + 2b\omega_0\left(t - \frac{z}{c}\right)\right) - \frac{\omega_r}{\omega_0}\right]^2}$$

where, $-e$ and m are the electronic charge and mass respectively and $*$ represents the complex conjugate.

2.2 Nonlinear current density:

The response of electrons to this ponderomotive force upon solving the equation of motion,

$$\frac{\partial \vec{v}_{\omega_r}^{NL}}{\partial t} = -\frac{\vec{F}_{\omega_r}^p}{m} - \vec{v}_{\omega_r}^{NL} \times \omega_c \hat{y}$$

turns out to be

$$\vec{v}_{x\omega_r}^{NL} = \frac{\omega_c \vec{F}_{\omega_r}^p}{m(\omega_r^2 - \omega_c^2)} \quad \text{and} \quad \vec{v}_{z\omega_r}^{NL} = \frac{i\omega_r \vec{F}_{\omega_r}^p}{m(\omega_r^2 - \omega_c^2)} \quad (4)$$

We choose $\omega_1, \omega_2 \gg \omega_p, \omega_c$ where, $\omega_p = \sqrt{4\pi n_0 e^2 / m}$ is the plasma frequency and $\omega_c = eB_s / m$ is the cyclotron frequency. The nonlinear current density can be calculated by solving the equation $\vec{J}_{\omega_r}^{NL} = -en_0 \vec{v}_{\omega_r}^{NL}$ as,

$$\vec{J}_{\omega_r}^{NL} = -\frac{en_0 \vec{F}_{\omega_r}^p (\omega_c \hat{x} + i\omega_r \hat{z})}{m(\omega_r^2 - \omega_c^2)} \quad (5)$$

This nonlinear current drives a wave whose frequency lies in THz range.

2.3 Terahertz wave generation formalism:

The wave equation for the propagation of THz wave, with the inclusion of nonlinear current density given as,

$$\nabla^2 \vec{E} - \vec{\nabla}(\vec{\nabla} \cdot \vec{E}) + \frac{\omega_T^2}{c^2} \vec{\epsilon} \vec{E} = -\frac{i\omega_T}{c^2 \epsilon_0} \vec{J}_{\omega_T}^{NL} \quad (6)$$

Here $\vec{\epsilon}$ is the plasma permittivity tensor at ω_T . Taking fast phase variations in \vec{E} as $\vec{E} = \vec{A} e^{-i(\omega_T t - kz)}$, where, x and z components of equation (6) can be deduced. Hence, the normalised amplitude of the THz wave is

$$\vec{A}_{\omega_T} = \frac{ien_0 \omega_T (\omega_c \hat{x} + i\omega_T \hat{z})}{c^2 m \epsilon_0 (\omega_T^2 - \omega_c^2) \left(\frac{\omega^2 \vec{\epsilon}}{c^2} - k_T^2 \right)} \vec{F}_{\omega_T}^p \quad (7)$$

For an optimised set of parameters equation (7) yields the amplitude of the generated THz wave.

3. NUMERICAL RESULTS AND DISCUSSION

Equation (7) is solved numerically for a set of suitable laser and plasma parameters. The values of the chosen parameters for computation are as follows: the normalised laser intensities, $a_1 = eA_0 / m\omega_1 c = 0.22$, $a_2 = eA_0 / m\omega_2 c = 0.24$ (A_0 is the amplitude of incident laser beam corresponding to laser intensity, $\sim 7 \times 10^{14} \text{ W/cm}^2$), for CO₂ laser at incident laser beam frequency $\omega_0 = 1.973 \times 10^{14}$.

In figure 2, we have plotted normalised THz amplitude $eA_{THz} / m\omega c$ with normalised THz frequency ω_{THz} / ω_p (where $\omega_{THz} = \omega_1 - \omega_2$) of THz wave for different values of chirp parameter. It can be observed from this figure that the amplitude decreases with increasing THz frequency. This amplitude is maximum when ω_{THz} is comparable with ω_p (due to resonance). It also observed that with increasing the value of b from 0.0007–0.0015 the normalised amplitude increases from 0.0004–0.0016 at $B_s = 10 \text{ kG}$. Also the variation of normalised THz amplitude is plotted with the normalised frequency for different value of magnetic field and chirp parameters shown in Figure 3. The external magnetic field helps THz generation by providing the phase matching. So, it is clear from this graph that the maximum momentum is transfer to the electrons at resonance condition and the normalised THz amplitude yield increases from 0.015 to 0.055.

On the other hand, the frequency chirp enhance the THz wave field. Since, higher the value of chirp parameter, longer the time laser pulses intersects with plasma so that higher the number of electrons take part in the excitation of radiation.

Therefore, it could play an important role in the generation of THz wave of higher intensity. The physical reason is that, in the presence of external magnetic field and a positive chirp, the initial ionization of the plasma increases. Thus with the increase of free electron density, the nonlinearity increases. As THz generation is a nonlinear phenomenon, it enhances more and more. The highest value of the normalised amplitude corresponding to incident laser beam intensity $\sim 7 \times 10^{14} \text{ W/cm}^2$ achieved is 0.055 in our scheme. We neglect the effect of collisions in our analysis. It can be seen [14] that in the presence of collisions, the term ω^2 is replaced by $\omega(\omega + i\nu)$ in equation (5). Since the imaginary term leads to resistivity and extracts energy from the electrons in collisions, consequently the efficiency decreases.

4. CONCLUSION

The generation of THz radiation via nonlinear mixing of two laser pulses in plasma using frequency chirped laser pulses is a fetching alternative. We have mathematically investigated the laser beat wave excitation of the terahertz radiation in collision less magnetised plasma. In the presence of a Gaussian laser beam on account of the ponderomotive force, the plasma gets depleted from the high field region to the low field region. From the above analysis it can be concluded that, the efficiency and the amplitude of THz field are sensitive not only to the applied external magnetic field but to the frequency chirped laser pulses. It increases with increasing the value of static magnetic field and chirp parameter. Here, we ignored the kinetic damping which is justified when $v_{th} \ll \omega_T / k_T$. Our result shows a great plausibility of developing a tunable THz source having power to use in medical applications.

ACKNOWLEDGEMENT

This work was supported by a financial grant from CSIR, New Delhi, India, under Project No. 03(1438)/18/EMR-II.

REFERENCES

- [1] Kampfrath, T., Tanaka, K., and Nelson, K., A., "Resonant and non-resonant control over matter and light by intense terahertz transients" Nat Photonics 7, 680 (2013).
- [2] Vidal, S., Degert, J., Tondusson, M., Freysz, M., and Oberl, J., "Optimized terahertz generation via optical rectification in Zn Te crystals" Opt Soc. Am. B 31, 149 (2014).
- [3] Wang, W. M., Sheng, Z. M., Wu, H. C., Chen, M. Li C., Zhang, J., and Mima, K., "Strong terahertz pulse generation by chirped laser pulses in tenuous gases" Opt. Exp. 16, 16999 (2008).
- [4] A. Frederike, A., et al., "Narrowband terahertz generation with chirped-and-delayed laser pulses in periodically poled lithium niobate" Opt. Letts. 42, 11 (2017).
- [5] Kim, K., Y., Taylor, A. J., Glowina, J. H., and Rodriguez, G., "Coherent control of terahertz supercontinuum generation in ultrafast laser-gas interactions" Nat. Photonics 2(10), 605 (2008).

[6] Singh, R. K., Singh, M., Rajouria, S. K., and Sharma, R. P. "High power terahertz radiation generation by optical rectification of a shaped pulse laser in axially magnetized plasma", *Phys. Plasmas* 24, 1313 (2017).

[7] Varshney, P., Sajal, V., Singh, K. P., Kumar, R., and Sharma, N. K., "Strong terahertz radiation generation by beating of extraordinary mode lasers in a rippled density magnetized plasma" *Laser Part. Beams* 31, 337 (2013).

[8] Vij, S., Kant, N., and Thakur, V., "Resonant Enhancement of THz Radiation Through Vertically Aligned Carbon Nanotubes Array by Applying Wiggler Magnetic Field" *Plasmonics*, <https://doi.org/10.1007/s11468-018-0892-2>, (2019).

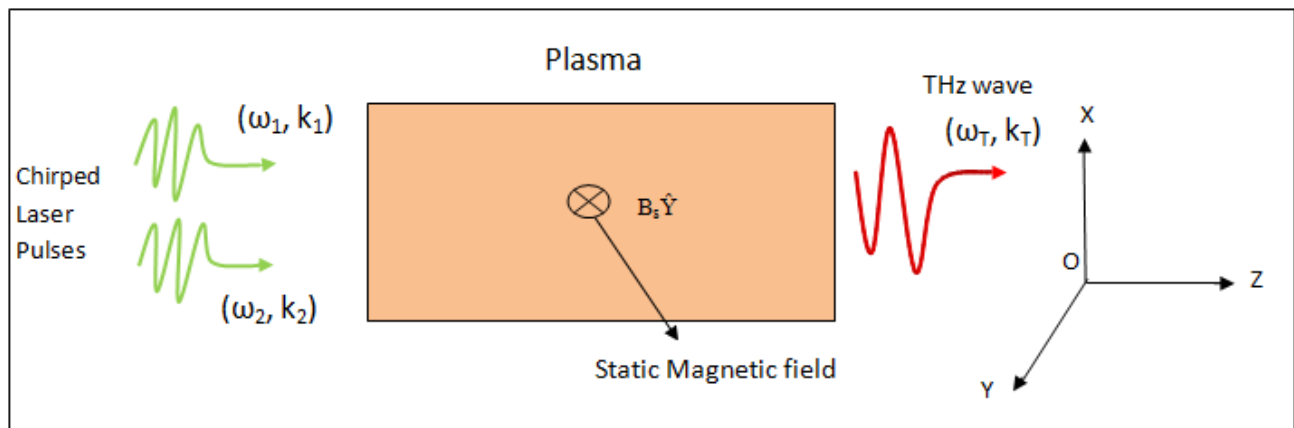


Fig:1. Schematic diagram of THz generation using frequency chirped laser pulses.

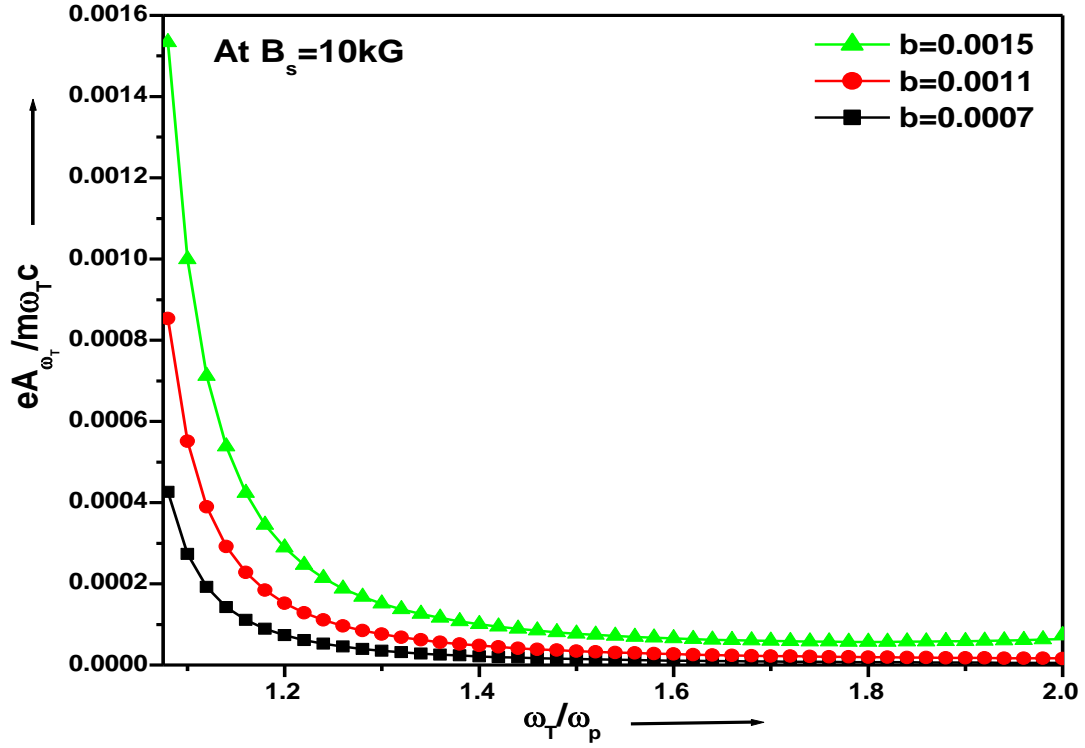


Fig:2 Variation of normalised terahertz amplitude ($eA_{THz} / m\omega_{THz}c$) with normalised THz frequency (ω_{THz} / ω_p) for different values of chirp parameter (b) at $\omega_0 = 1.973 \times 10^{14}$ and $B_s = 10\text{kG}$.

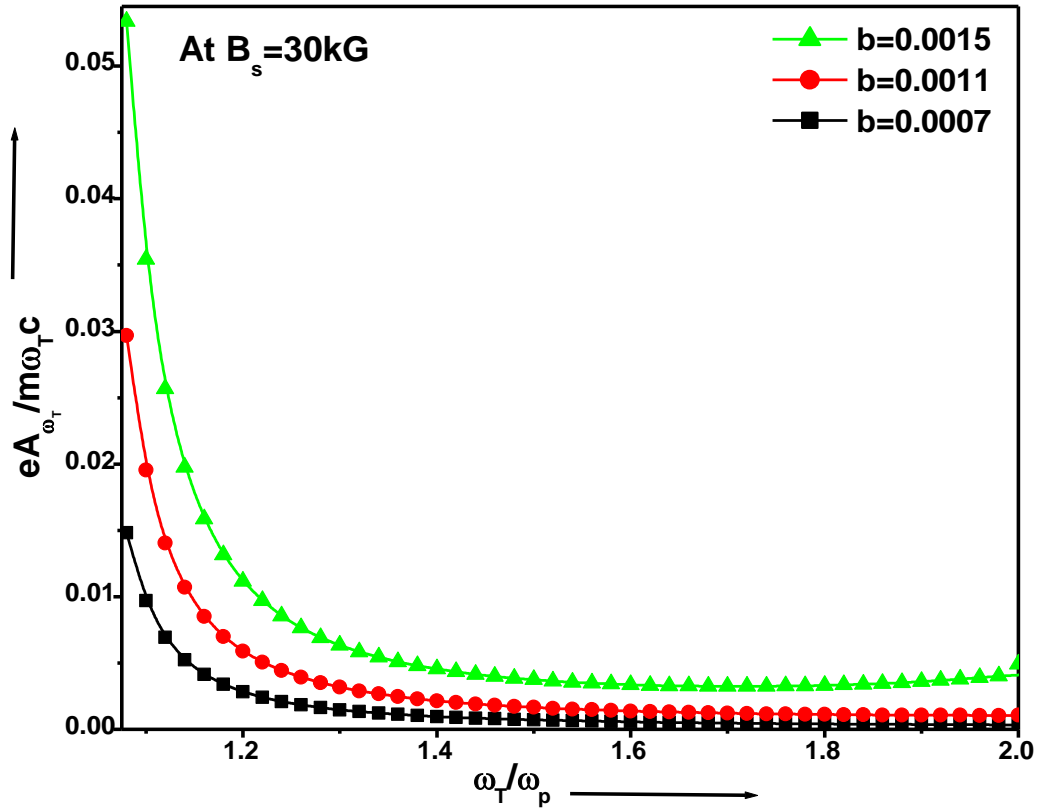


Fig:3 Variation of normalised terahertz amplitude ($eA_{THz} / m\omega_{THz}c$) with normalised THz frequency (ω_{THz} / ω_p) at $B_s = 30kG$
 other parameters are same as that of fig.2.

PAPER

Effect of frequency-chirped laser pulses on terahertz radiation generation in magnetized plasma

To cite this article: Alka Mehta *et al* 2019 *Laser Phys.* **29** 095405

View the [article online](#) for updates and enhancements.

Effect of frequency-chirped laser pulses on terahertz radiation generation in magnetized plasma

Alka Mehta, Jyoti Rajput and Niti Kant

Department of Physics, Lovely Professional University, G.T. Road, Phagwara 144411, Punjab, India

E-mail: nitikant@yahoo.com

Received 19 July 2019

Accepted for publication 19 July 2019

Published 16 August 2019



Abstract

The effect of frequency chirp on the generated terahertz (THz) wave by the interaction between intense laser pulses and under dense plasma in the presence of transverse magnetic field is investigated theoretically in the present model. An expression for the electron Lorentz factor coupling cyclotron motion nonlinearity is derived for static magnetic field perpendicular to the laser propagation axis. The beating lasers produce a nonlinear ponderomotive force due to their oscillatory motion. This force drives a nonlinear current, at beat frequency, which produces the THz radiation. The influence of the external magnetic field on the optimization process of THz field amplitude is investigated numerically. A linear frequency chirp increases the duration of nonlinear interaction of laser pulse with plasma electrons and hence, enforces the interaction for longer duration. The presence of magnetic field further provides the additional momentum to the THz photon to obtain a significant gain in output yield. Our numerical simulations reveal that there is a significant enhancement in the THz field strength for optimized value of the chirp parameter and magnetic field.

Keywords: terahertz (THz) radiation generation, frequency chirp, transverse magnetized field, laser-plasma interaction, nonlinearity

(Some figures may appear in colour only in the online journal)

1. Introduction

For the past two decades, the terahertz (THz) portion of the electromagnetic spectrum has emerged as a resourceful tool owing to its versatile and wide range of applications in different aspects of science and technology [1–5]. In particular, the production of optically generated THz pulses from difference-frequency generation (DFG), is recognized as a promising regime for these applications due to its high tunability and efficiency. DFG technique utilizes two relatively long (>1 ns) laser pulses separated in frequency, depending on the desired signal frequency. Furthermore, a range of solid-state materials such as lithium tantalite, lithium niobate, gallium arsenide and zinc telluride have been employed in order to produce THz radiation by nonlinear phenomenon [6]. The breakdown and damage threshold of these optical crystals, due to short pulse laser, limits the reliability of these materials

for THz generation. Hence, the alternative to avoid this issue is to employ a nonlinear medium, which can endure high-peak ultrashort laser power. In this context, several schemes and models have been proposed and realized [7–11]. Plasma emerges as a potential alternative medium for the same technique and can withstand high power due to ultrashort laser pulses. At first, Hamster *et al* [12] demonstrated that the main source of THz radiation is the self-consistent current driven by ponderomotive force of a short pulse laser in plasma. Plasma waves driven by the ponderomotive force of the laser have been extensively employed for frequency upconversion, particle and photon acceleration, etc. For these applications, the typical plasma oscillation frequency lies in the terahertz (THz) scale. Sheng *et al* [13] have revealed that THz waves (GV/m) can be produced around the plasma oscillation frequency due to linear mode conversion of the laser wake field. However, THz frequency pulses produced due to accelerator-based

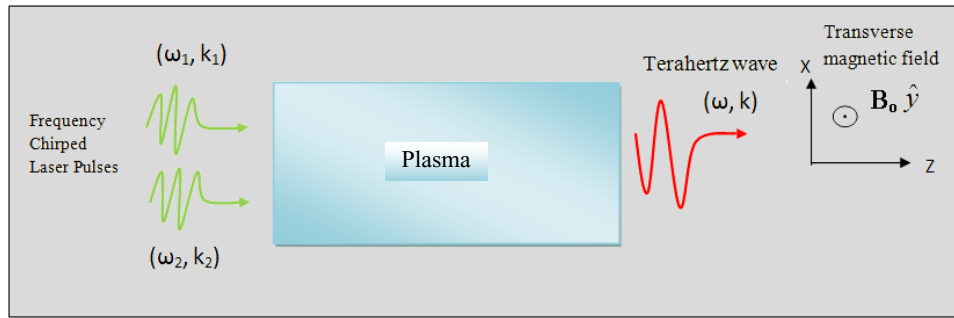


Figure 1. Schematic diagram of frequency-chirp-driven THz generation.

sources are limited by the bandwidth and laser peak intensity. Liu *et al* [14] have simulated THz generation in the two-color laser field based on the transient photocurrent model along with the physical mechanisms of THz generation at low and high laser intensities via THz spectrum investigation.

The primary challenges in the progress of THz generation to date are ascertaining high conversion efficiencies with their scaling to achieve higher energies. Various schemes and methods have been devised for the improvement in the quality as well as efficiency of THz radiation. One of which is the application of external magnetic field and suitable frequency chirp. Hamazaki *et al* [15] have investigated the influence of frequency chirp on THz pulse spectra generated due to optical rectification. They observed that to ensure the smooth and single-peaked THz spectra, pre-compensation for the dispersion of GaP is required. Also, the excessive amount of frequency chirp causes distortions in the THz spectra. Frederike *et al* [16] have experimentally generated THz wave employing periodically poled lithium niobate (PPLN) using dual frequency chirped, moderately delayed laser pulses from Ti: sapphire laser. As a result, internal conversion efficiencies up to 0.13% with a multi-cycle THz energy of 40 μJ have been reported. They further concluded that frequency chirp with delayed pumping of PPLN is crucial to establish narrowband THz ($\sim\text{mJ}$ level) for future applications. Along similar lines, a noteworthy efficiency of $>10^{-4}$ and a remarkable bandwidth in excess of 75 THz have been realized by Kim *et al* [17], in which they have explained the THz generation mechanism due to transient nonlinear electron current produced by two-color photo-ionization in gases. Wang *et al* [18] have analyzed that chirped laser pulses facilitate the generation of strong THz pulses having amplitudes varying linearly with laser amplitude. These THz pulses have amplitude 10–100 times greater than that from the well-known two-color laser scheme, hence, facilitating one to achieve THz field up to 10 MV cm^{-1} with initial laser intensity of about $10^{16} \text{ W cm}^{-2}$.

The present investigation deals with the influence of frequency chirp on the generated THz wave due to interaction between intense laser pulses and under dense plasma in the presence of transverse magnetic field. For achieving a significant enhancement in THz efficiency and field strength, the frequency-chirped laser and magnetic field parameters are optimized. The external magnetic field also plays a crucial role in enhancing the efficiency of THz wave. Tunable and coherent THz radiation through electrostatic to electromagnetic field conversion due to an ionization front can be

produced in a uniform electrostatic field. The paper is organized as follows. Section 2 formulates the problem for THz wave excitation due to frequency-chirped laser in a magneto-plasma with expressions of ponderomotive force and nonlinear current density. A brief discussion of the results is given in section 3 and finally, the conclusion is presented in the last section.

2. Numerical analysis for Ponderomotive force and nonlinear current density

To validate the theory behind the generation of THz radiation caused by the beating of two laser pulses in plasma, we provide the analytical calculations. We consider plasma of electron density n_0 . The electric field for laser pulses is assumed to be polarized in x -direction as $\vec{E}_j = \hat{x}A_j e^{-i(\omega_j t - k_j z)}$, where, $j = 1, 2$, $k_j \approx (\omega_j/c)$, external magnetic field is applied perpendicular to it, i.e. in the y -direction as $\vec{B}_S = B_0 \hat{y}$. Two lasers of slightly different frequencies ω_1 and ω_2 propagate through the plasma. Let us suppose the frequency of the incident laser is positively chirped (figure 1) and given as; $\omega_1 = [\omega_0 + b\omega_0^2 (t - z/c)]$, where ω_0 is the frequency of the incident laser beam in the absence of chirp, b is the frequency chirp parameter, c is the velocity of light, and the frequency ω_2 is chosen as the difference, $\omega_1 - \omega_2 = \omega$, which lies in the THz range. One can generate highly efficient chirped laser pulse by using two counter-propagating laser-induced plasma Bragg gratings [19]. To control femtosecond laser pulses, the plasma grating can be a novel solution because it has a much higher damage threshold than ordinary dielectric/metal optical elements. Thus, the electric field of these two waves can be represented as,

$$\left. \begin{aligned} \vec{E}_1 &= \hat{x}A_1 e^{-i(\omega_1 t - \omega_1 z/c)} \\ \vec{E}_2 &= \hat{x}A_2 e^{-i(\omega_2 t - \omega_2 z/c)} \end{aligned} \right\} \quad (1)$$

and the magnetic field of incident lasers inside the plasma can be expressed as,

$$\vec{B}_j = \frac{c(\vec{k}_j \times \vec{E}_j)}{\omega_j}, \quad (2)$$

where, $j = 1, 2$. The lasers impart an oscillatory velocity to the plasma electrons, $\vec{v}_1 = e\vec{E}_1/mi\omega_0[1 + b\omega_0(2t - z/c)]$ and $\vec{v}_2 = e\vec{E}_2/mi\omega_0[1 + b\omega_0(2t - z/c) - \omega/\omega_0]$ along with the nonlinear terahertz ponderomotive force as,

$$\vec{F}_\omega^p = -\frac{e}{2c} \left(\vec{v}_1 \times \vec{B}_2^* + \vec{v}_2^* \times \vec{B}_1 \right) - \frac{m}{2} \vec{\nabla} (\vec{v}_1 \cdot \vec{v}_2^*),$$

$$\vec{F}_\omega^p = \hat{z} \frac{e^2 \omega (\vec{E}_1 \cdot \vec{E}_2^*) [(1+b\omega_0(2t-z/c))(1+b\omega_0(2t-z/c)-\omega/\omega_0) + ib\omega_0(1+b\omega_0(2t-z/c)-\omega/2\omega_0)]/\omega}{m i \omega_0^2 c (1+b\omega_0(2t-z/c))^2 (1+b\omega_0(2t-z/c)-\omega/\omega_0)^2}, \quad (3)$$

where, $-e$ and m are the electronic charge and mass, respectively, and $*$ represents the complex conjugate. In the presence of external magnetic field, the electrons start moving in a circle due to the Lorentz force. This circular motion is superimposed with the electric field of laser pulse, which results in a cycloid of angular frequency ω_c . The response of electrons to the ponderomotive force along with the cyclotron motion can be obtained by solving the equation of motion, $\partial \vec{v}_\omega^{nl} / \partial t = -\vec{F}_\omega^p / m - \vec{v}_\omega^{nl} \times \vec{\omega}_c$ as,

$$\vec{v}_\omega^{nl} = \frac{\omega_c F_\omega^p \hat{x} - i \omega F_\omega^p \hat{z}}{m(\omega^2 - \omega_c^2)}. \quad (4)$$

We choose $\omega_1, \omega_2 \gg \omega_p, \omega_c$ where, $\omega_p = \sqrt{4\pi n_0 e^2 / m}$ is the plasma frequency and $\omega_c = eB_0 / mc$ is the cyclotron frequency. The nonlinear current density can be calculated by solving the equation, $\vec{J}_\omega^{NL} = -en_0 \vec{v}_\omega^{nl} / 2 = -\omega_p^2 (\omega_c \hat{x} - i\omega \hat{z}) F_\omega^p / 8\pi e (\omega^2 - \omega_c^2)$.

This nonlinear current drives a wave whose frequency lies in THz range. Now, using Maxwell's III and IV equations the wave equation governing the propagation of THz wave, with the inclusion of nonlinear current density is given as,

$$-\nabla^2 \vec{E}_\omega + \vec{\nabla} (\vec{\nabla} \cdot \vec{E}_\omega) = \frac{\omega^2}{c^2} \vec{\epsilon} \cdot \vec{E}_\omega + \frac{4i\pi\omega}{c^2} \vec{J}_\omega^{nl}, \quad (5)$$

where, $\vec{\epsilon}$ is the permittivity tensor at the THz frequency, and one may write the solution of the above equation as $\vec{E}_\omega = \vec{A}_\omega(x) e^{-i(\omega t - kx)}$, and taking the divergence of equation (5), the z component,

$$E_{\omega z} = -\frac{\epsilon_{zx}}{\epsilon_{xx}} E_{\omega x} - \frac{4\pi}{\omega k_z \epsilon_{zz}} \frac{\partial J_{\omega z}^{nl}}{\partial z}, \quad (6)$$

where $\epsilon_{xx} = \epsilon_{zz} = 1 - \omega_p^2 / (\omega^2 - \omega_c^2)$ and $\epsilon_{xz} = -\epsilon_{zx} = -i\omega_c \omega_p^2 / \omega (\omega^2 - \omega_c^2)$. Now, we put the value of $E_{\omega z}$ from equation (6) into the wave equation and obtain the equation governing $E_{\omega x}$ of the THz wave:

$$-k^2 E_{\omega x} + \frac{\omega^2}{c^2} \left(\epsilon_{xx} + \frac{\epsilon_{zx}^2}{\epsilon_{zz}} \right) E_{\omega x} = -\frac{4\pi i \omega}{c^2} \left(J_{\omega x}^{nl} + \frac{\epsilon_{xz}}{\epsilon_{zz}} J_{\omega z}^{nl} \right). \quad (7)$$

Solving equation (7) by substituting the values of nonlinear current density, we obtain the final amplitude of THz wave:

$$A_{\omega x} = -\frac{a_1 a_2 m c \omega^2 \omega_p^2 (\omega_c + i\omega \epsilon_{xz} / \epsilon_{zz}) [i\omega G + b\omega_0 (1 + b\omega_0 (2t - z/c) - \omega / 2\omega_0)]}{2i\omega e G^2 (\omega^2 - \omega_c^2) [k^2 c^2 - \omega^2 (\epsilon_{xx} + \epsilon_{zx}^2 / \epsilon_{zz})]}. \quad (8)$$

Here, $a_1 = eA_1 / m\omega_0 c$, $a_2 = eA_2^* / m\omega_0 c$ and $G = (1 + b\omega_0 (2t - z/c)) (1 + b\omega_0 (2t - z/c) - \omega / \omega_0)$.

3. Results and discussion

As the static magnetic field also introduces an additional motion to the electrons, this gives an extra nonlinear current term, which can be seen from current density equation. In a non-relativistic regime, the presence of chirped laser beams shows that for a suitable choice of the pulse intensity and external magnetic field strength, a significant gain in THz amplitude has been observed for optimized value of chirp parameter.

A suitable set of laser and plasma parameters is chosen for computations such as femtosecond laser pulses having wavelength 800 nm (Ti-Sapphire Laser) and angular frequency $\omega_0 = 2.3545 \times 10^{15}$ rad s⁻¹. Here, $\omega_p = 3\pi$ THz, corresponding to electron density $n_0 = 2.8 \times 10^{16}$ cm⁻³. For our numerical simulation we consider the normalized amplitude of incident lasers as $a_1 = a_2 = eA_0 / m\omega_0 c = 0.1$, where A_0 is the amplitude of the incident laser beam corresponding to the laser intensity $I \approx 3 \times 10^{14}$ W cm⁻².

The graph between the normalized THz amplitude ($A_{\omega x}$) versus the normalized frequency of terahertz wave (ω / ω_p) plotted in figure 2 for different values of magnetic field (54–322 kG), corresponds to the normalized value of cyclotron frequency, $\omega_c / \omega_p = 0.1$ – 0.6 , at a fixed value of frequency chirp parameter $b = 0.0099$. From this graph, it can be analyzed that the THz amplitude decreases with increasing THz frequency and amplitude is maximum when the ratio of the frequency of THz to the plasma wave tends to unity. The physical reason behind this is that at this particular point, $\omega / \omega_p \sim 1.07$ is in proximity to the normalized value of upper hybrid frequency ω_{UH} / ω_p ; in the present analysis $\omega_{UH} = \sqrt{\omega_c^2 + \omega_p^2} = 1.077\omega_p$. This is the upper hybrid resonance condition. So, when the beating frequency is close to the upper hybrid frequency, an efficient increase in terahertz amplitude is observed, as the region near resonance frequency excites the THz radiation by achieving the resonance condition. The resonance condition in collisionless unmagnetized plasma is $\omega = \omega_p$. Also, the applied magnetic field provides the additional transverse component of nonlinear current density, which results in a significant gain

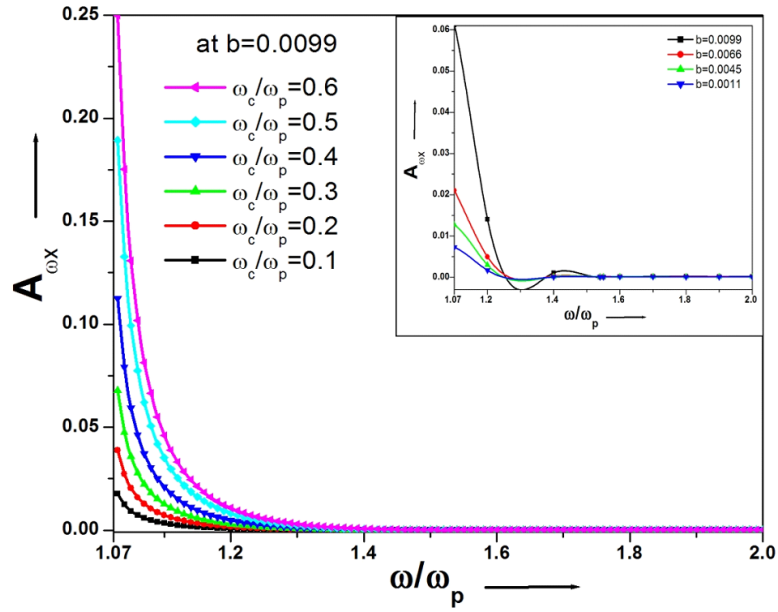


Figure 2. Plot of the normalized amplitude of THz wave (A_{ω_x}) with normalized frequency (ω/ω_p) for different values of normalized cyclotron frequency at $a_1 = a_2 = 0.1$. Inset graph: plot similar to figure, for different values of chirp parameter in the absence of magnetic field.

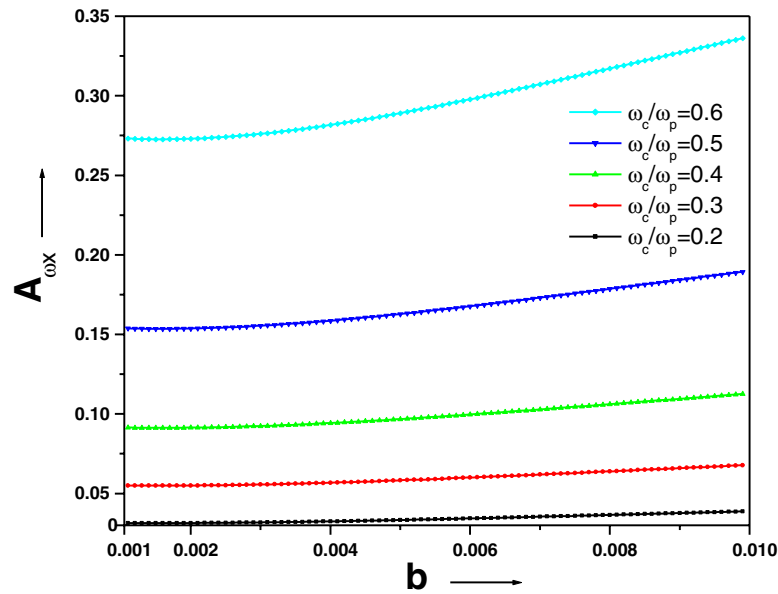


Figure 3. Plot of the normalized THz amplitude (A_{ω_x}) as a function of the frequency chirp parameter (b). Rest of the parameters are the same as those in figure 2.

in amplitude of THz wave. The inset figure of figure 2 is plotted for different values of chirp parameter in the absence of magnetic field; other parameters are the same as in figure 2. We observe a dip in the normalized THz amplitude at $(\omega/\omega_p) \sim 1.36$ due to destructive interference. As we apply the external magnetic field, this dip disappears due to resonance.

Figure 3 displays the variation of normalized THz amplitude (A_{ω_x}) with frequency chirp parameter (b) for varying electron cyclotron frequency $\omega_c/\omega_p = 0.1-0.6$, which corresponds to magnetic field strength 54–322 kG. It is clear from the graph that the amplitude of THz wave gradually increases with increasing the chirp. There is a noticeable increase in

amplitude after $b = 0.005$. Also, the higher value of magnetic field enhances the effect of chirp on the output yield and our result here shows a maximum amplitude of about $A_{\omega_x} \approx 0.35$ for $b = 0.0099$ at $\omega_c/\omega_p = 0.6$, corresponding to magnetic field 322 kG. This also infers that the output gain is closely related to the strength of the magnetic field for different values of chirp parameter.

Figure 4 shows the amplitude profile of terahertz wave (A_{ω_x}) as a function of the intensity of incident laser pulses ($A_o = \sqrt{a_1 a_2}$) for distinct values of magnetic field strength at fixed $b = 0.0099$. A_{ω_x} and A_o are connected by a linear relationship in this graph. The increment in the incident

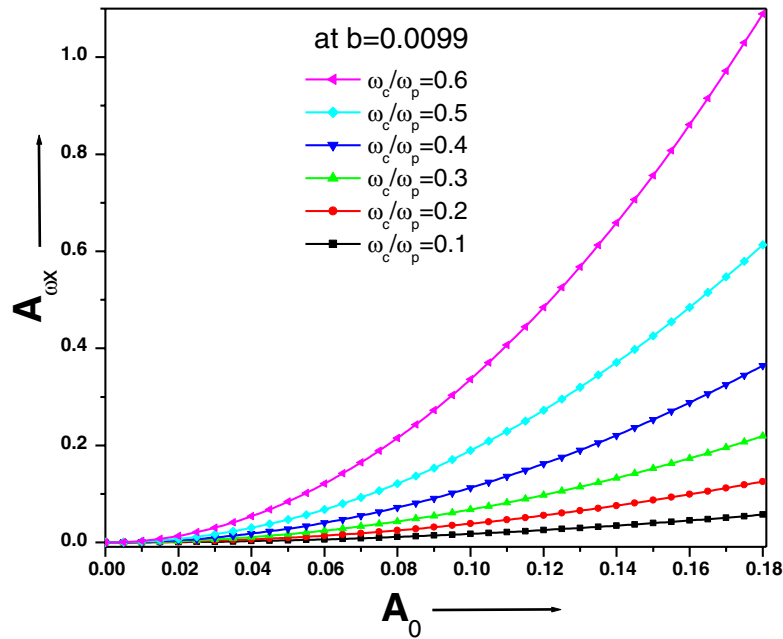


Figure 4. Plot of the normalized THz amplitude (A_{ω_x}) as a function of the normalized intensity of incident lasers (A_0) at $b = 0.0099$ for different values of normalized cyclotron frequency (ω_c/ω_p).

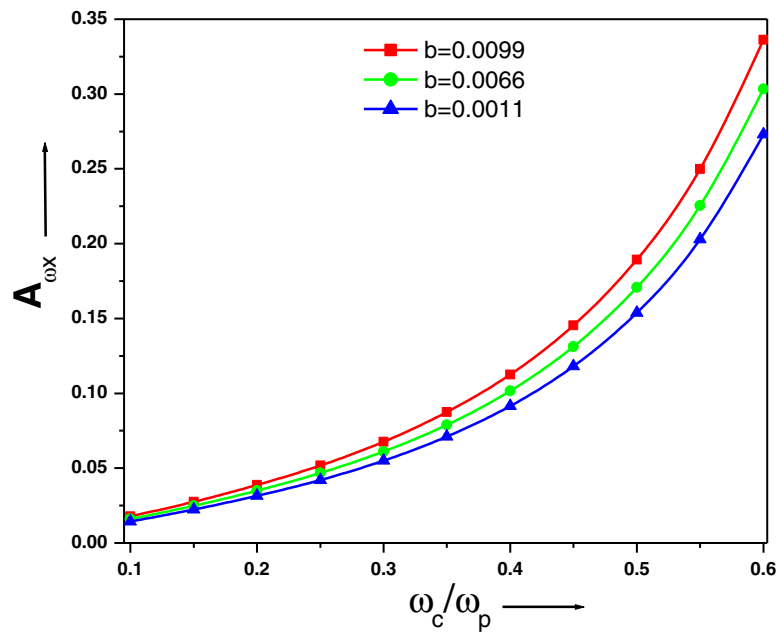


Figure 5. Plot of the normalized amplitude (A_{ω_x}) of THz wave with normalized cyclotron frequency (ω_c/ω_p) corresponding to static magnetic field from 54–322 kG for different values of frequency chirp parameter (b).

beam intensity results in the enhancement in the initial ionization of the plasma and nonlinearity in the system due to the strength of ponderomotive force. As a result, the free electron density will be greater, which produces more intense THz wave. Thus, the strength of the output wave can be controlled by overseeing the intensity of incident laser pulses. Normalized THz amplitude (A_{ω_x}) as a function of normalized cyclotron frequency ω_c/ω_p is plotted in figure 5

with varying frequency chirp parameter (b). As can be seen from the graph, the amplitude shows a sharp increase after $\omega_c = 0.3\omega_p$ for all values of chirp parameter. So, the output of THz wave can be tuned by choosing suitable values of chirp parameter and magnetic field strength. Thus, it can be concluded from the graph that applied magnetic field and frequency chirp together play a vital role in high-intensity THz generation.

4. Conclusion

In the present paper, we numerically studied the sensitivity of the chirping of laser on THz generation by the beating of the lasers in plasma. We consider the effects of chirp on THz yield. In our analysis, we also found that THz spectra can be distorted by the onset of the spectral dip structures around $\omega/\omega_p \approx 1.36$ due to destructive interference of chirped laser pulses (inset figure 2) similar to Hamazaki *et al* [15]. Here, we neglected the effect of collisions in the current scheme. In conclusion, the frequency chirping of incident lasers with a transverse magnetic field plays a crucial role in maintaining the resonance condition in the interaction region. The increasing frequency of the laser pulse allows the electron to stay within the laser pulse longer and also increases the transverse momentum. As a result, efficient gain in the output THz yield is observed.

Also, it becomes important to examine how the frequency chirp in the pump pulse affects the resultant THz spectra, to properly understand the impact of the propagation effects on the THz spectra. Therefore, our results provide a numerical guideline for broadband THz pulse generation using ultra-short pump pulse sources in plasmas.

Acknowledgment

This work was supported by a financial grant from CSIR, New Delhi, India, under Project No. 03(1438)/18/EMR-II.

References

- [1] Kampfrath T, Tanaka K and Nelson K A 2013 Resonant and non-resonant control over matter and light by intense terahertz transients *Nat. Photon.* **7** 680
- [2] Vidal S, Degert J, Tondusson M, Freysz M and Oberl J 2014 Optimized terahertz generation via optical rectification in Zn Te crystals *Opt. Soc. Am. B* **31** 149
- [3] Tonouchi M 2007 Cutting-edge terahertz technology *Nat. Photon.* **1** 97
- [4] Kleine-Ostmann T and Nagatsuma T 2011 A review on terahertz communications research *J. Infrared Millim. Terahertz Waves* **32** 143
- [5] Lavrukhin D V *et al* 2019 Terahertz photoconductive emitter with dielectric-embedded high-aspect-ratio plasmonic grating for operation with low-power optical pumps *AIP Adv.* **9** 015112
- [6] Nagai M *et al* 2004 Generation and detection of terahertz radiation by electro-optical process in GaAs using 1.56 μm fiber laser pulses *Appl. Phys. Lett.* **85** 3974
- [7] Hamster H, Sullivan A, Gordon S, White W and Falcone R W 1993 Sub picosecond, electromagnetic pulses from intense laser-plasma interaction *Phys. Rev. Lett.* **71** 2725
- [8] Chen Z Y 2013 High field terahertz pulse generation from plasma wakefield driven by tailored laser pulses *Appl. Phys. Lett.* **102** 241104
- [9] Mehta A and Kant N 2019 Terahertz radiation generation driven by the frequency chirped laser pulse in magneto-active plasma *Proc. SPIE* **10917** 109170R
- [10] Vij S, Kant N and Thakur V 2019 Resonant enhancement of THz radiation through vertically aligned carbon nanotubes array by applying wiggler magnetic field *Plasmonics* **2019** 1–6
- [11] Mehta A, Kant N and Vij S 2019 Generation of terahertz (THz) radiation by p-polarised laser beating in hot plasma with surface density ripple *Laser Phys. Lett.* **16** 045403
- [12] Hamster H, Sullivan A, Gordon S and Falcone R 1994 Short-pulse terahertz radiation from high-intensity-laser-produced plasmas *Phys. Rev. E* **49** 671
- [13] Sheng Z M, Mima K, Zhang J and Sanuki H 2005 Emission of electro-magnetic pulses from laser wakefields through linear mode conversion *Phys. Rev. Lett.* **94** 095003
- [14] Liu C *et al* 2015 Effect of two-color laser pulse duration on intense terahertz generation at different laser intensities *Phys. Rev. A* **92** 063850
- [15] Hamazaki J, Furusawa K, Sekine N, Kasamats A and Hosako I 2016 Effects of chirp of pump pulses on broadband terahertz pulse spectra generated by optical rectification *Jpn. J. Appl. Phys.* **55** 110305
- [16] Frederike A *et al* 2017 Narrowband terahertz generation with chirped-and-delayed laser pulses in periodically poled lithium niobate *Opt. Lett.* **42** 11
- [17] Kim K Y, Taylor A J, Glownia J H and Rodriguez G 2008 Coherent control of terahertz supercontinuum generation in ultrafast laser-gas interactions *Nat. Photon.* **2** 605
- [18] Wang W M, Sheng Z M, Wu H C, Chen M, Li C, Zhang J and Mima K 2008 Strong terahertz pulse generation by chirped laser pulses in tenuous gases *Opt. Express* **16** 16999
- [19] Wu H C, Sheng Z M, Zhang Q J, Cang Y and Zhang J 2005 Chirped pulse compression in nonuniform plasma Bragg gratings *Appl. Phys. Lett.* **87** 201502

Terahertz generation by beating of two chirped pulse lasers in spatially periodic density plasma

Alka Mehta¹, Jyoti Rajput¹, K Kang² and Niti Kant¹

¹ Department of Physics, Lovely Professional University, G.T. Road, Phagwara 144411, Punjab, India

² Department of Physics and Photon Science, Gwangju Institute of Science and Technology, Gwangju 500-712, Republic of Korea

E-mail: nitikant@yahoo.com

Received 13 December 2019

Accepted for publication 27 January 2020

Published 27 February 2020



CrossMark

Abstract

The present paper reports on the combined influence of the chirp characteristics of pump pulses and spatially periodic density (density ripple) plasma, on terahertz (THz) radiation generation, by beating of two chirped pulses. The beating lasers exert a nonlinear ponderomotive force along the z -direction. A self-consistent field is generated due to the nonlinear oscillations of plasma electrons; as a result of these linear and nonlinear forces the plasma electrons attain an oscillatory velocity that couples with the density ripple to generate a stronger transient transverse current, driving THz radiation. The importance of chirp parameter, amplitude and periodicity of density structure are discussed for emitted THz radiation. Our numerical simulations disclose that the variation of the chirp frequency parameter and ripple amplitude have considerable roles in improving the nonlinear oscillating current. By optimizing the chirp parameter and amplitude of the density ripple, a notable change in the magnitude of the terahertz field amplitude is found. The present paper may be useful for broadband THz pulses, for use in plasma diagnostics and time-domain spectroscopy.

Keywords: terahertz radiation, density ripple, plasma, frequency chirp, ponderomotive force

(Some figures may appear in colour only in the online journal)

Introduction

The terahertz (THz) region in the electromagnetic spectrum lies between the microwaves and the infra-red region, narrowing the gap between electronics and optics. Previously, complications in efficiently producing and controlling THz waves served as an obstruction for the region. However, due to continuous development in this area, THz radiation is a matter of recent interest. THz radiations are utilised in many fields such as remote sensing, communication technology [1, 2], environmental monitoring, and biological imaging etc [3, 4]. Due to the unique abilities of THz radiation, a variety of ideas have emerged for several applications including security telecommunications, industrial non-destructive testing, health, etc. Recently, an experiment was conducted at the Free-electron LASer in Hamburg (FLASH) at Deutsches

Elektronen-Synchrotron (DESY), utilizing THz radiation. Azima *et al* [5] employed a single-shot THz streak-camera to measure the duration and spectral phase of the intense XUV pulses. However, for THz applications in the case of photo-conductive antennas and semiconductors, etc, low conversion efficiency and the material breakdown efficiency serve as major shortcomings.

In order to overcome these concerns, plasma acts as an appropriate medium which overcomes the material damage related problems in the case of THz generation. Several techniques have been proposed experimentally [6–8] and theoretically [9–14] for efficient THz generation by employing plasma as a medium. Kwon *et al* [15] have reported highly energetic, short duration bursts of coherent THz radiation from an embedded plasma dipole. Plasma dipole oscillations are produced due to the trapping of electrons in the potential

wells generated due to the ponderomotive force arising from two laser pulses (moderately detuned), due to which a quasi-monochromatic radiation is produced. Recently, Tripathi *et al* [16] have investigated THz radiation generation due to an amplitude modulated laser beam in the presence of a density ripple. They concluded that the THz amplitude varies linearly with the modulation index and square of laser amplitude and inversely varies with electron collision frequency. The density ripple provides the phase-matching condition and gives rise to high power efficiency. A scheme to generate terahertz (THz) radiation by electromagnetic Gaussian beams beating in a hot collisionless density rippled plasma has also been investigated [17]. It was concluded that the power of the emitted THz radiation is proportional to the square of the density ripple amplitude. The THz wave amplitude decreases with the THz frequency and increases with the incidence angle up to an optimum value.

Recently, Mehta *et al* [18] investigated the effect of frequency-chirped laser pulses on terahertz radiation generation in magnetised plasma. A suitable frequency chirp enhances the laser and electron interaction duration and an applied magnetic field further imparts a significant momentum to THz photons. Hence, the combined effect of the frequency chirp and applied magnetic field results in a significant enhancement in the THz field strength.

To understand the theory behind the origin of the THz field caused by the beating of two lasers in a nonlinear medium (plasma for the present scheme), we provide the analytical calculations below. In this paper, we develop an analytical formalism for THz generation from chirped lasers beating in rippled density plasma. The density ripple is applied on the chirped laser pulses in order to adjust and control the yield of the THz wave. The density ripple plays a vital role in establishing the phase-matching condition. The resonance condition results in a resonant excitation of THz radiation [16]. The THz amplitude enhances considerably in the presence of density ripple. Further, the application of frequency chirp extends the laser–plasma interaction time and thus facilitates the resonance condition for longer duration, which can be useful in the broadband THz radiation generation. Recently, Hamazaki *et al* [19] have experimentally investigated the impact of the frequency chirp of the laser pump pulse in broadband THz pulse generation by optical rectification in gallium phosphate by measuring the time domain spectroscopy signals. They also reported the significance of accurate control over the frequency chirp of the laser pulse for producing the broadband THz pulses by optical rectification.

The mechanism of THz generation is as follows: we consider two Gaussian lasers with electric fields $\vec{E}_1(\vec{k}_1, \omega_1)$ and $\vec{E}_2(\vec{k}_2, \omega_2)$, polarised along \hat{y} , propagating in the \hat{z} direction (figure 1). The lasers have a linear frequency chirp and the frequencies $\omega_1 = \omega_0(1 + b\omega_0(t - z/c))$ and $\omega_2 = \omega_0(1 + b\omega_0(t - z/c) - \omega_T/\omega_0)$ can be chosen, as the difference $(\omega_1 - \omega_2 = \omega_T)$ lies in THz range.

Numerical analysis for current density

The theory of generation of THz radiation due to the beating of two chirped laser pulses in plasma is explained and the analytical calculations are presented below. We consider plasma of electron density n_0 . The electric field profile of laser pulses (with two slightly different frequencies ω_1 and ω_2) is considered as $\vec{E}_j = \hat{y}A_j e^{i(k_j z - \omega_j t)}$, here, $j = 1, 2$. The laser imparts oscillatory velocity to the plasma electrons: $\vec{v}_j = e\vec{E}_j/mi\omega_0\alpha_j$, where $\alpha_1 = 1 + b\omega_0(2t - z/c)$ and $\alpha_2 = \alpha_1 - ((\omega_1 - \omega_2)/\omega_0)$. A nonlinear ponderomotive force exerted due to the variation of amplitude of the laser's field beating at $(\omega_1 - \omega_2)$ is written as:

$$\vec{F}_p = \hat{z}e^2 \frac{\alpha_1\beta_1 + \beta_2}{2mi\omega_0c\alpha_1\alpha_2} (\vec{E}_1 \cdot \vec{E}_2^*), \quad (1)$$

where $\beta_1 = [ck_1/\omega_1 - ck_2/\omega_2 - 2ib/\alpha_1\alpha_2]$, $\beta_2 = (\omega_1 - \omega_2)/\omega_0 [c(k_1 - k_2)/(\omega_1 - \omega_2) + ck_2/\omega_2 + ib/\alpha_1\alpha_2]$ and e , m , c and $*$ represent the electronic charge, mass, speed of light in a vacuum and complex conjugate respectively. Here it is clear that the variables $\alpha_1, \alpha_2, \beta_1$ and β_2 are the function of chirp parameter b . Due to the nonlinear motion of plasma electrons a linear (n_ω^l) and nonlinear (n_ω^{nl}) density perturbation is also observed which can be calculated by solving the equation of motion such as: $n_\omega^{nl} = n_0(k_1 - k_2)F_p/m(\omega_1 - \omega_2)^2$ and $n_\omega^l = (k_1 - k_2)^2 \chi_e \phi_s / 4\pi e$, where $\chi_e = -\omega_p^2/(\omega_1 - \omega_2)^2$ is the free electron plasma susceptibility. The refractive index (μ) of a material is related to the susceptibility by the relation $\chi_e = \mu^2 - 1$, and for plasma medium in the present case, $\mu = \epsilon^{1/2} = (1 - \omega_p^2/\omega_T^2)^{1/2}$. Here, ϵ is the permittivity of the medium and we choose $\omega_1, \omega_2 \gg \omega_p$, where $\omega_p = (4\pi n_0 e^2/m)^{1/2}$ is the plasma frequency. Now by employing Poisson's equation, $\nabla^2 \phi = 4\pi e(n_\omega^{nl} + n_\omega^l)$, the electrostatic potential ϕ of this self-consistent space charge field can be written as $\phi = -4\pi e n_\omega^{nl} / (1 + \chi_e)(k_1 - k_2)^2$. Thus, the nonlinear velocity under the influence of the ponderomotive force along with the self-consistent field is:

$$\vec{v}_\omega^{nl} = -\frac{\vec{F}_p + e\vec{\nabla}\phi}{mi(\omega_1 - \omega_2)} = -\frac{\vec{F}_p}{mi(\omega_1 - \omega_2)} \left(1 - \frac{i\omega_p^2}{(\omega_1 - \omega_2)^2 - \omega_p^2} \right). \quad (2)$$

Here, we introduce a density perturbation $n = n_0 + n_q e^{iqz}$, where n_q represents the ripple amplitude and q is the density ripple wave number. This nonlinear velocity beats with the density ripple to drive a nonlinear current density along the propagation direction:

$$\vec{J}_\omega^{NL} = -\frac{e}{2} n_q e^{iqz} \vec{v}_\omega^{nl} = -\hat{z} \frac{e\omega_p^2 n_q e^{iqz} (\vec{E}_1 \cdot \vec{E}_2^*) (\alpha_1\beta_1 + \beta_2) ((\omega_1 - \omega_2)^2 - \omega_p^2 (1+i))}{16\pi n_0 \omega_0 m c \alpha_1 \alpha_2 (\omega_1 - \omega_2) ((\omega_1 - \omega_2)^2 - \omega_p^2)}. \quad (3)$$

This non-linear current further couples to the wave associated to the self-consistent space charge field and drives a THz wave. Employing Maxwell's III and IV equations, we have

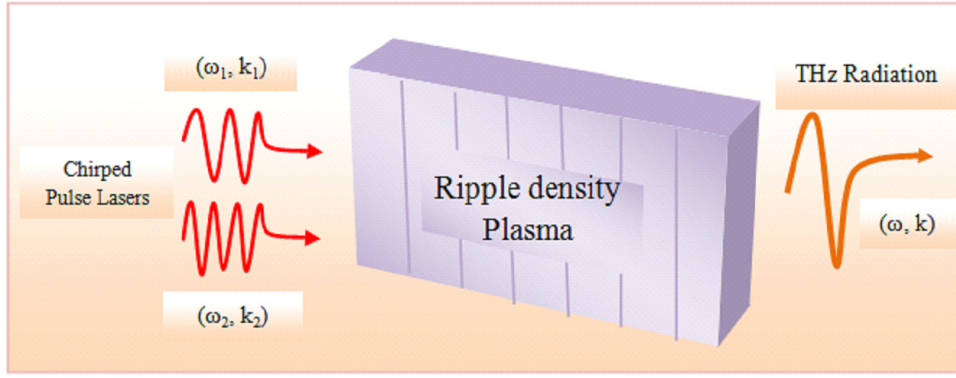


Figure 1. Schematic of THz generation via frequency chirped laser pulses in rippled density plasma.

derived the wave equation depending on the non-linear current density term. This wave equation can be given as

$$\nabla^2 \vec{E}_\omega - \vec{\nabla}(\vec{\nabla} \cdot \vec{E}) - \frac{\omega_T^2}{c^2} \left(1 - \frac{\omega_p^2}{\omega_T^2}\right) \vec{E}_\omega = -\frac{4\pi i \omega_T}{c^2} \vec{J}_\omega^{NL}. \quad (4)$$

The exact phase-matching condition and resonant excitation of THz generation can be achieved by introducing a suitable value of density ripple wave number \vec{q} . Hence $\vec{k}_T = \vec{k}_1 - \vec{k}_2 + \vec{q}$, and $k_T^2 - \omega_T^2 \epsilon / c^2 = 0$, where \vec{k}_T is the THz wave vector and $q \approx \omega / c (\sqrt{\epsilon} - 1)$. The electric field of THz varies as $\vec{E}_\omega = \hat{y} A_\omega(z, t) e^{-i(\omega_T t - k_T z)}$. By assuming the fast variation of the THz field in order to neglect the higher order derivatives and using the phase matching condition, the z -component of the above equation gives the required THz field, $\partial E_{\omega z} / \partial z = 2\pi \omega J_{\omega z}^{NL} / c^2 k$. Now by including the value of the nonlinear current from equation (3), we obtain the final equation for the field of THz radiation:

$$\frac{\partial}{\partial z} \left(\frac{E_{\omega z}}{E_1} \right) = -\frac{en_q \omega_p^2 E_2^* (\alpha_1 \beta_1 + \beta_2) (\omega_T^2 - \omega_p^2 (1+i))}{8n_0 m \omega_0 c^3 k_T (\omega_T^2 - \omega_p^2)}, \quad (5)$$

where $E_{\omega z} / E_1$ is the normalised field of the THz wave. The efficiency of the generated THz radiation is the ratio of the energy per unit area of the THz wave to the energy per unit area of the pump lasers, i.e. $\eta = W_{THz} / W_{pump}$, where the average electromagnetic energy stored per unit volume is given by the formula

$$W_{Ei} = \frac{\epsilon}{8\pi} \frac{\partial}{\partial \omega_i} \left[\omega_i \left(1 - \frac{\omega_p^2}{\omega_i^2}\right) \right] \langle |E_i|^2 \rangle. \quad (6)$$

Thus using equation (6), one can obtain the efficiency of the generated THz radiation. The features of THz electric field's amplitude have been studied by solving equation (5) for an optimised set of laser and plasma parameters.

Results and discussion

The proper matching of the ripple wave number with the beat wave number provides the maximum transfer of energy and momentum under the resonance condition. In the present scheme, we consider a non-relativistic regime to see the

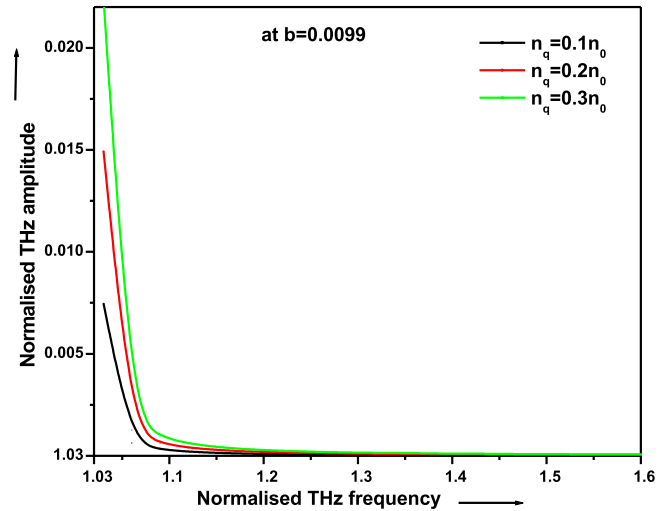


Figure 2. Variation of normalised THz amplitude as function of normalised THz frequency for different values of density ripple at fixed value of chirp parameter $b = 0.0099$.

combined effect of chirp characteristics and density ripple on the THz emission due to frequency chirped pulse lasers. Since the chirp parameter b is inversely proportional to group delay dispersion (GDD), the increase of b naturally implies the decrease of GDD. Obviously, the decreased GDD means less chirp. For a suitable choice of the pulse intensity, density ripple amplitude and chirp parameter, a significant gain in THz amplitude is observed. The following set of laser and plasma parameters are considered throughout the paper: incident laser pulse of intensity $I \approx 3 \times 10^{14} \text{ W cm}^{-2}$ (femtosecond laser), angular frequency $\omega_0 = 2.355 \times 10^{15} \text{ rad s}^{-1}$, and plasma frequency $\omega_p = 3\pi \text{ THz}$, corresponding to electron density $n_0 = 2.8 \times 10^{16} \text{ cm}^{-3}$. The variation of normalised THz amplitude as a function of normalised frequency of the THz wave for different values of density ripple amplitude ($n_q = 0.1n_0, 0.2n_0, 0.3n_0$), at fixed value of frequency chirp parameter $b = 0.0099$, is plotted in figure 2. From this graph, it is analysed that the higher values of the THz amplitude are obtained near the resonance condition $\omega \approx \omega_p$ and decrease as ω departs from ω_p . We therefore analysed from figure 2 that there is an enhancement in the THz amplitude by increasing the value of n_q , and the effect of n_q on THz amplitude remains significant near the resonance condition.

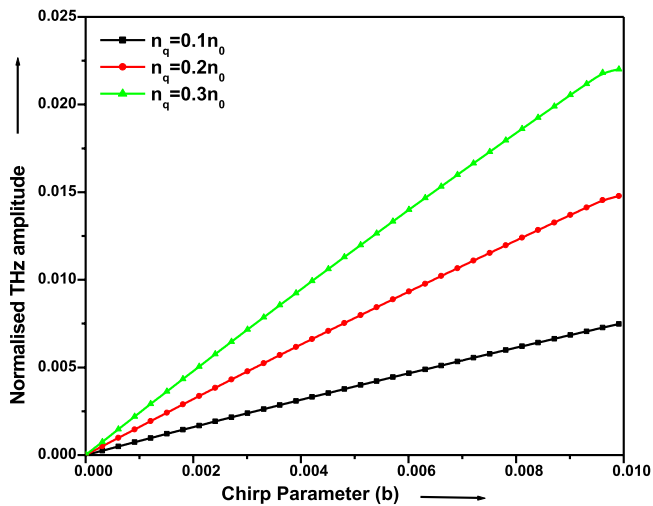


Figure 3. Plot of normalised THz amplitude versus frequency chirp parameter (b). The remaining parameters are similar to those in figure 2.

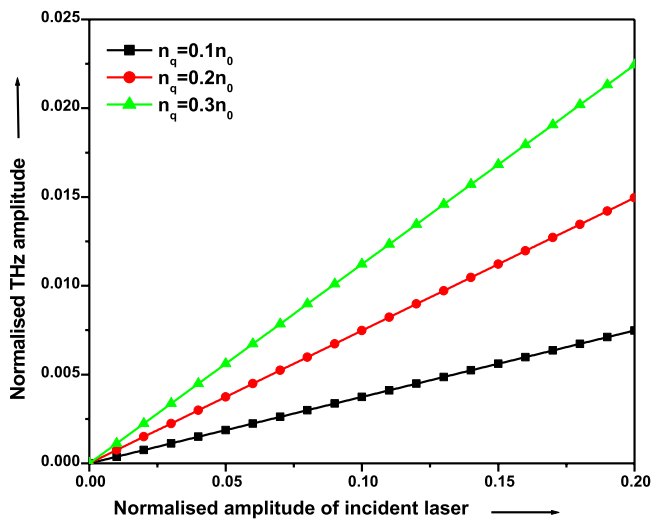


Figure 4. Spectrum of normalised THz amplitude corresponding to incident laser amplitude at $b = 0.0099$ for different values of ripple density.

Figure 3 displays the variation of normalised THz amplitude with frequency chirp parameter (b) ranges 0.000 03 to 0.0099, for varying density ripple amplitude (n_q). It is clear from the graph the amplitude of the THz wave gradually increases with an increase in the value of the chirp parameter. As seen from the graph, the amplitude shows a sharp increase until $b = 0.0099$. The present scheme is only valid for a chirp parameter of a maximum of 0.0099; beyond this value a negligible chirp appears and it is difficult to see the chirp effect. We therefore choose it as the optimised value of the chirp parameter for present scheme. It is further observed, from the above figure, that the THz field amplitude varies with the chirp parameter. Higher values of density ripple also enhance the effect of the chirp on the output yield. This also infers that the output gain is closely related to the amplitude of ripples for different values of chirp parameter. So, the output of the

THz wave can be tuned by choosing suitable values of chirp parameter and density ripple of a suitable wave number. It can thus be concluded from the graph that both ripple and frequency chirp together play a vital role in high intensity THz generation.

Figure 4 shows the spectrum of normalised THz corresponding to the amplitude of incident lasers for distinct values of density ripple at fixed $b = 0.0099$. It can be concluded from the graph that the amplitude of the laser and THz wave are connected by a linear relationship. The increment in the incident pulse intensity results in the enhancement in the initial ionization of plasma and nonlinearity in the system due to the strength of the ponderomotive force. As a result, the free electron density will be greater, which produces a more intense THz wave. The strength of output wave can therefore be controlled by overseeing the intensity of the incident laser pulses.

Conclusion

A numerical method is developed for the investigation of the generation of THz radiation by the beating of two chirped pulse lasers in plasma, by introducing density ripples having spatial variation. The sensitiveness of the THz field to the chirp characteristics of lasers is also noticed. The effect of collisions is neglected in the present model. We have numerically solved the equations for the nonlinear current density and THz field. The resonance condition is satisfied with the help of density ripple of an appropriate wave number. The chirp also continues the interaction for a longer period and thus THz radiation of a sufficiently high yield can be achieved. The optimised density ripple amplitude, chirp parameter and the intensity of laser pulses play significant roles in the enhancement of THz radiation. Our results provide a mathematical guideline for smooth and broadband THz emission, which are of paramount importance in plasma diagnostics and THz time-domain spectroscopy [20–22].

Acknowledgment

This work was supported by a financial grant from CSIR, New Delhi, India, under Project No. 03(1438)/18/EMR-II.

References

- [1] Hirata A *et al* 2006 120 GHz-and millimeter-wave photonic wireless link for 1 Gb/s data transmission *IEEE Trans. Microw. Theory Tech.* **54** 1937
- [2] Krumbholz N *et al* 2005 Omnidirectional terahertz mirrors: a key element for terahertz communication systems *Appl. Phys. Lett.* **88** 20295
- [3] Brucherseifer M *et al* 2000 Label-free probing of the binding state of DNA by time domain terahertz sensing *Appl. Phys. Lett.* **77** 4049
- [4] Davis A G *et al* 2002 The development of terahertz sources and their applications *Phys. Med. Biol.* **47** 3679

- [5] Azima A *et al* 2018 Direct measurement of the pulse duration and frequency chirp of seeded XUV free electron laser pulses *New J. Phys.* **20** 013010
- [6] Andreeva V A *et al* 2016 Ultrabroad terahertz spectrum generation from an air-based filament plasma *Phys. Rev. Lett.* **116** 063902
- [7] Zhang Z *et al* 2017 Generation of high-power, tunable terahertz radiation from laser interaction with a relativistic electron beam *Phys. Rev. Accel. Beams* **20** 050701
- [8] Liao G Q *et al* 2017 Intense terahertz radiation from relativistic laser-plasma interactions *Plasma Phys. Control. Fusion* **59** 014039
- [9] Vij S and Kant N 2019 Generation of terahertz radiation by beating of two color lasers in hot clustered plasma with step density profile *Plasma Res. Express* **1** 025012
- [10] Vij S, Kant N and Thakur V 2019 Resonant enhancement of THz radiation through vertically aligned carbon nanotubes array by applying wiggler magnetic field *Plasmonics* (<https://doi.org/10.1007/s11468-018-0892-2>)
- [11] Bakhtiari F *et al* 2015 Generation of terahertz radiation in collisional plasma by beating of two dark hollow laser beams *Laser Part. Beams* **33** 463
- [12] Kumar M and Tripathi V K 2012 Resonant terahertz generation by optical mixing of two laser pulses in rippled density plasma *IEEE J. Quantum Electron.* **48** 1031
- [13] Bhasin L and Tripathi V K 2009 Terahertz generation via optical rectification of x-mode laser in a rippled density magnetized plasma *Phys. Plasmas* **16** 103105
- [14] Mehta A and Kant N 2019 Terahertz radiation generation driven by the frequency chirped laser pulse in magnetoactive plasma *Proc. SPIE* **10917** 109170R
- [15] Kwon K B *et al* 2018 High-energy, short-duration bursts of coherent terahertz radiation from an embedded plasma dipole *Sci. Rep.* **8** 145
- [16] Tripathi D *et al* 2010 Terahertz generation by an amplitude-modulated Gaussian laser beam in a rippled density plasma *Phys. Scr.* **82** 035504
- [17] Mehta A *et al* 2019 Generation of terahertz (THz) radiation by p-polarised laser beating in hot plasma with surface density ripple *Laser Phys. Lett.* **16** 045403
- [18] Mehta A *et al* 2019 Effect of frequency-chirped laser pulses on terahertz generation in magnetized plasma *Laser Phys.* **29** 095405
- [19] Hamazaki J *et al* 2016 Effects of chirp of pump pulses on broadband terahertz pulse spectra generated by optical rectification *Japan. J. Appl. Phys.* **55** 110305
- [20] Jones S P P *et al* 2014 High-temperature electromagnons in the magnetically induced multiferroic cupric oxide driven by intersublattice exchange *Nat. Commun.* **5** 3787
- [21] Kida N *et al* 2008 Electric-dipole active two-magnon excitation in ab spiral spin phase of a ferroelectric magnet $\text{Gd}_{0.7}\text{Tb}_{0.3}\text{MnO}_3$ *Phys. Soc. Japan* **77** 123704
- [22] Komatsu M *et al* 2015 Terahertz spectral change associated with glass transition of poly- ϵ -caprolactone *J. Appl. Phys.* **117** 133102